Dielectric Relaxation and Solvation Dynamics of Water in Complex Chemical and Biological Systems

Nilashis Nandi†

Department of Chemistry, Faculty of Science, Nagoya University, Furo-cho, Chikusa-ku, Nagoya, 464-01, Japan

Kankan Bhattacharyya

Department of Physical Chemistry, Indian Association for the Cultivation of Science, Jadavpur, Calcutta, 700032, India

Biman Bagchi*

Solid State and Structural Chemistry Unit, Indian Institute of Science, Bangalore, 560012, India

Received February 23, 1999 (Revised Manuscript Received April 11, 2000)

Contents

I. Introduction

Because of its unique properties, water drives many natural and biological processes. While a detailed understanding of its precise role is still being unravelled, it is clear that the existence of water shells around biomolecules play a crucial role. This is why water is considered to be the lubricant of life. The biologically active chemical species is often located at an interface or confined within a small region, a few nanometers in size. The polarity, viscosity, and pH in these microenvironments are in many cases vastly different from those in bulk water. The proximity of the reactants and the substantially altered local properties of such confined environments exert profound influence on the reactivity and dynamics of the confined species. As a result, chemistry in aqueous biomolecular systems and in orga-

* Corresponding author. Fax: 91-80-360-1310 and 91-80-360-1683. E-mail: bbagchi@sscu.iisc.ernet.in.
† Present address: Max Planck Institut fur Kolloid-und Grenzflachenforschung, Am Muhlenberg 2, Haus 1, D 14476, Golm, Potsdam, Germany.

10.1021/cr980127v CCC: $35.00
Published on Web 05/12/2000

Nilashis Nandi received his Ph.D. from Tagore's University at Santiniketan. He did post-doctoral research with Prof. Biman Bagchi at the Indian Institute of Science, Bangalore. Subsequently, he carried out further research in the laboratory of Prof. Iwao Ohmine at the Nagoya University, Nagoya, as a J.S.P.S. fellow. He is currently a Humboldt fellow in the laboratory of Prof. Dieter Vollhardt at the Max Plank Institute for Colloid and Interface Science at Golm. His research interest lies in the field of theoretical biophysical chemistry.

Kankan Bhattacharyya carried out Ph.D. research at Indian Association for the cultivation of Science (IACS) and obtained his Ph.D. degree in 1984. He was a post-doctoral research associate at the Radiation Laboratory, University of Notre Dame, and at Columbia University. He joined the faculty of IACS in 1987 and became a professor in 1998. His research interests includes ultrafast laser spectroscopy and organized assemblies.

nized molecular assemblies differs markedly from that in a homogeneous fluid medium.[1−30] Nature uses this difference extremely efficiently to carry out various chemical processes.[5−9,31−35]

An aqueous solution of a biomolecule is a multicomponent system that is homogeneous on a length scale larger than the size of the biomolecule but heterogeneous on the length scale of water molecules. In all the species present, namely, the biomolecule, the water molecules in the hydration shell and the water molecules in bulk are highly correlated. Each of them affect the structure and dynamics of others. Consequently, the relaxation processes of aqueous biomolecular solutions are often drastically different from those in pure water. The complex relaxation processes of aqueous biomolecules are important not only as interesting physical problems but also for their profound biological implications. This provides the main impetus for studying the structure and dynamics of aqueous biomolecular systems.[1−13,34−48]

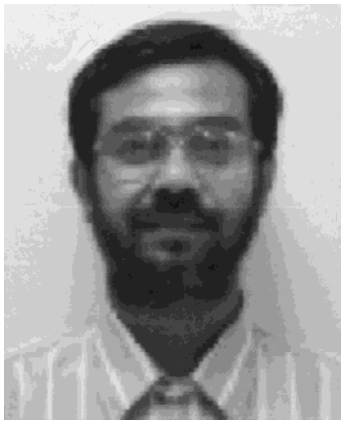

Biman Bagchi carried out his Ph.D. research at Brown University, Providence, RI, with Professor Julian H. Gibbs and obtained his Ph.D. degree in 1981. He was a research associate at the Janes Franck Institute, University of Chicago (1981–1983), and at the University of Maryland (1983–1984). He joined the faculty of the Indian Institute of Science, Bangalore, in the fall of 1984. He is a Fellow of the Indian Academies of Science. His research interests include molecular relaxation and transport processes in liquids and organized assemblies, time-dependent statistical mechanics, polymers, and biomolecules.

Self-organized molecular assemblies, in general, refer to molecular aggregates held together by weak molecular interactions. They include aggregates such as micelles and vesicles in water, reverse micelles and microemulsions in hydrocarbons, supramolecules involving cage-like hosts (e.g., cyclodextrins or calixarenes), microporous solids (e.g., zeolites), semirigid materials (e.g., polymers, hydrogels, etc.), and so on. The most important feature of any organized assembly is the confinement of a spectroscopic probe, often along with many solvent molecules in a small region. Such confinement results in significant changes in the local dielectric constant and viscosity and imposes considerable constraint on the free movement of the probe and the confined solvent molecules. The above features are clearly similar to the ones present in biopolymers. Consequently, these organized assemblies serve as simple models of more complex biological systems.[19−25] It is indeed remarkable that the dynamics of water molecules in many organized molecular assemblies show features that closely resemble the relaxation of biological systems in aqueous solutions. The organized assemblies are however less complex than the biological systems they mimic. In this review, we attempt to develop a unified picture of the dynamical properties of water in different complex, natural, and biological systems.

With this end in view, we have organized the present review as follows. Before we discuss the relaxation dynamics in biomolecular solutions and organized media, we briefly outline the present status of the dielectric relaxation and solvation dynamics studies in *pure* water in section II. The structures of the biomolecules, the organized assemblies, and their hydration zones are of utmost importance in understanding the relaxation processes occurring in these complex systems. We give a brief description of the structure of these systems in section III. In section IV, we discuss the dielectric relaxation studies in aqueous biomolecular systems and in organized assemblies. In section V, we review the studies on

solvation dynamics in such systems. In the concluding section, we outline the possible future directions of the subject.

At the outset it should be emphasized that, because of the inherent complexity of the biological systems, the study of aqueous biomolecular systems is still in its infancy as far as the microscopic understanding of the measurable properties are concerned. Thus, one is forced to use terms and concepts such as local dielectric constant or polarity, width of the hydration shell, etc. The proper significance of these terms and concepts should be viewed only from the perspective in which they are used. The water molecules in the immediate vicinity of a biomolecule are traditionally called "bound water".[1,49,50] They differ appreciably from bulk water molecules. As pointed out by Kuntz and Kauzmann many years ago, even the operational definition of water of hydration is doubtful.[1] Water molecules near a biomolecule can be rigidly bound and strongly localized or can have a similar degree of disorder as that of a bulk water molecule. There are several reasons for the difficulty in quantifying the concepts. First and foremost among them is the heterogeneity that operates at a molecular level in such systems. Second, the interaction between water and the biomolecule is not only strong but also anisotropic. Thus, the discussions of the dynamics of these systems at present are at best semiquantitative. Even a continuum model description is sometimes extremely difficult. Despite these difficulties, recent studies in this area have significantly improved our understanding of the relaxation properties of the complex biological systems.

Because of the fundamental importance of the subject and intense recent activity in this area, many excellent monographs and reviews have already summarized different aspects of the complex biomolecular systems and organized assemblies.[1−7,13−17,19−26] Several of them surveyed the studies of hydration of biomolecules by dielectric spectroscopy.[1,3,4,49−54] The binding of organic probes with cyclodextrins and other hosts in aqueous medium arises as a result of the hydrophobic effect. Different aspects of hydrophobic binding have also been reviewed recently by several authors.[8,14−17] We discuss some of these advancements in section IV.A.4. Many solvated biomolecule and organized assemblies involve an interface between two drastically different media. The properties of the molecules at various interfaces have been studied recently using a number of new experimental and theoretical techniques as discussed in many recent reviews.[25−30] The topic of the present review, namely, the dynamics of water in restricted environments, has not been reviewed so far.

II. Dielectric Relaxation and Solvation Dynamics in Pure Water

In this section, we briefly outline the recent theoretical and experimental studies on dielectric relaxation and solvation dynamics in pure water.

A. Dielectric Relaxation of Pure Water

The dielectric relaxation experiments measure the collective polarization of all the polar molecules present in a given system. The dielectric relaxation time usually provides a measure of the time taken by a system to reach the final (equilibrium) polarization after an external field is suddenly switched on (or off). The response of a system consists of two parts: electronic and orientational. The electronic polarization is nearly instantaneous. However, the orientational polarization is much slower and occurs at a time scale that ranges from a few microseconds (μs) for a large macromolecular chain to a few picoseconds (ps) for the reorientation of a small -OH group. The dielectric relaxation spectrum of pure water has been investigated in considerable detail by different experimental techniques as well as by molecular dynamics simulations.[55−68] Molecular theories of dielectric relaxation provide microscopic understanding of the relaxation phenomena.[57−62,69−73] Dielectric relaxation measures the phenomenological coefficient $\epsilon(\omega)$, which is then connected to the total dipole moment time correlation function, $\langle \vec{M}(t)\vec{M}(0)\rangle$, where $\vec{M}(t)$ is the *total* dipole moment of the whole system. That is, $\vec{M}(t)$ is the sum of all the individual molecular moments, $\vec{\mu}_i(t)$:

$$\vec{M}(t) = \sum_{i=1}^{N} \vec{\mu}_i(t) \tag{2.1}$$

In eq 2.1, μ_i is the total dipole moment of the ith molecule: permanent plus induced dipole moment. The normalized time-dependent dipole moment correlation function is defined as

$$\phi(t) = \frac{\langle \vec{M}(t)\vec{M}(0)\rangle}{\langle M^2(0)\rangle} \tag{2.2}$$

For a spherical system, the frequency (ω)-dependent dielectric function is related to the normalized time-dependent dipole moment correlation function by the following *exact* relation:[72]

$$\frac{[\epsilon(\omega) - 1]}{[\epsilon(\omega) + 2]} = \frac{4\pi\langle \vec{M}(0)\vec{M}(0)\rangle}{9k_B TV} \times [1 - i\omega \int_0^\infty \exp(-i\omega t)\phi(t)\, dt] \tag{2.3}$$

where k_B denotes the Boltzmann constant, T is the temperature, and N is the number of molecules present in volume (V) of the whole sphere. Water molecules are highly correlated in their liquid state. The degree of dipolar correlation may be expressed by a correlation factor (g_c), which is defined as

$$g_c = \frac{\langle M^2\rangle}{N\mu^2} \tag{2.4}$$

Thus, the g_c factor can be considered as an empirical measure of dipolar correlation; g_c is equal to unity for a completely random system. We shall use g_c as a fitting parameter to reproduce the known dielectric constant of water, which is 78.6 at 298 K. We find that a value of g_c equals 0.25 for liquid water at 298

K, which indicates a considerable degree of orientational ordering in water.[74]

The above expression (eq 2.3) for dielectric dispersion is exactly valid for a spherical system. When working with a spherical system, one needs to take the large system limit by increasing the radius of the sphere while keeping the intrinsic properties, such as the densities of the species, constant. The calculations of dielectric relaxation in aqueous biological solutions considered in this review are all carried out with this spherical system.

The complex dielectric function ($\epsilon(\omega)$) may be decomposed into real and imaginary parts as

$$\epsilon(\omega) = \epsilon' - i\epsilon'' \tag{2.5}$$

At room temperature the real part, ϵ' (permittivity factor), of pure water is nearly 80 at a few megahertz and about 1 at 10 000 GHz. The imaginary part (ϵ'') corresponds to absorption (dielectric loss) and exhibits distinct peaks at certain characteristic frequency (ν_m).[61] The dielectric relaxation time (τ_D) is equal to the reciprocal of ν_m.[60,61]

The dielectric spectra of pure water in the Debye relaxation region (that is, in the low-frequency region) has been traditionally characterized by two relaxations with time constants 8.2 and 1.02 ps, respectively.[55,56,63] The former one constitutes more than 90% of the total relaxation. More recent studies indicate a faster value of the second time constant (0.2 ps)[64] that is presumably due to high-frequency modes in water.

The high-frequency part of $\epsilon(\omega)$ is complex as many high-frequency vibrational modes contribute to the dielectric spectra of water beyond the Debye relaxation regime. This spectral region has been extensively investigated by far-infrared (far-IR) spectroscopy and simulations.[55,65,66,75−78] Different intermolecular vibration, libration, and other high-frequency modes of water contribute to the far-IR spectrum. In the far-IR spectrum of water, the broad shoulder around 200 cm^{-1} is due to the intermolecular O···O vibrational mode of the O−H···O units in the hydrogen bond network and is due to dipole-induced dipole interaction. The librational motion of water gives rise to the 650 cm^{-1} band. Among all the vibrational modes of water, these two modes (at 200 cm^{-1} and 650 cm^{-1}) play the most important role in the solvation dynamics. The frequency-dependent dielectric function, $\epsilon(z)$, (where $z = i\omega$) can be described by[65,79,80]

$$\epsilon(z) = \sum_{i=1}^{n} \frac{\Delta\epsilon_i}{1 + z\tau_i^D} + \sum_{j=1}^{m} \Delta w_j (1 - z\Phi_j(z)) \tag{2.6}$$

which includes n Debye relaxation processes and m vibrational modes, $\Delta\epsilon_i$ is the weight of the ith Debye relaxation with relaxation time constant τ_i^D, and Δw_j is the weight of the jth vibrational mode with vibrational moment correlation function Φ_z. The functional form of $\Phi_j(z)$ is calculated from the model

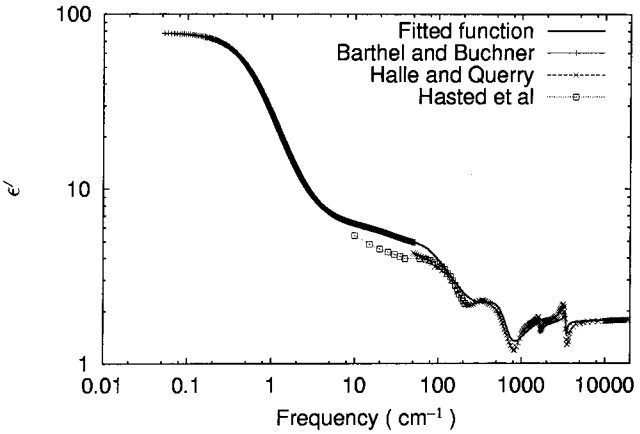

Figure 1. Real part of the complex permittivity (ϵ') of pure water at room temperature. The line indicated by fitted function is obtained from eqs 2.6 and 2.7 to fit the experimental data of Barthel and Buchner,[63] Hale and Querry,[77] and Hasted and co-workers.[55,56,75,76] The experimental works referred to above are also shown in the plot.

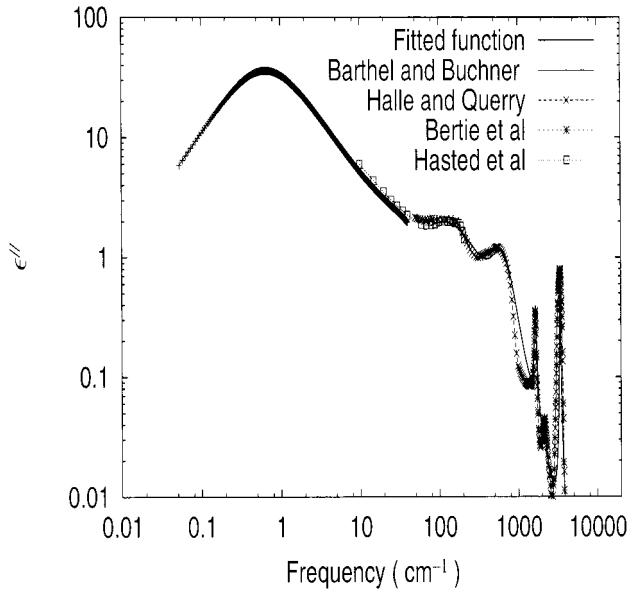

Figure 2. Imaginary part of the complex permittivity (ϵ'') of pure water at room temperature. The line indicated by fitted function is obtained from eqs 2.6 and 2.7 to fit the experimental data of Barthel and Buchner,[63] Hale and Querry,[77] Bertie and co-workers,[78] and Hasted and co-workers.[55,56,75,76] The experimental works referred above are also shown in the plot.

of a damped harmonic oscillator and is given by

$$\Phi_j(t) = \exp(-\gamma_j t)\left[\cos(\Omega_j^0 t) + \frac{\gamma_j}{\Omega_j^0}\sin(\Omega_j^0 t)\right] \tag{2.7}$$

where, γ_j and Ω_j^0 characterize the line shapes of the far-IR spectra of water. The real and imaginary parts of the frequency-dependent dielectric function of pure water are shown in Figures 1 and 2, respectively.

B. Solvation Dynamics in Pure Water

Solvation dynamics refers to the reorganization of the polar solvent dipoles around a charged probe suddenly created in a medium. For such a study, one chooses a probe molecule that is nonpolar or weakly

polar in the ground state but is highly polar in the electronically excited state. As long as the solute probe is in the ground state, the solvent dipoles remain randomly oriented around the solute. When the probe solute is excited by an ultrashort pulse, the solvent dipoles initially (i.e., at $t = 0$) remain randomly oriented about the instantaneously created solute charge distribution, and the potential energy of the solute, $E(0)$, is high. With an increase in time, the solvent dipoles gradually reorient and the energy of the system decreases. Thus, if $E(0)$, $E(t)$, and $E(\infty)$ denote the energies of the fluorescence solute at times 0, t, and ∞ with $0 < t < \infty$, $E(0) > E(t) > E(\infty)$. If one records the emission energy of the excited solute as a function of time, it is observed that with an increase in time the emission maximum shifts to lower energy, i.e., longer wavelength. This phenomenon is called time-dependent fluorescence Stokes shift (TDFSS). The solvation dynamics is monitored by the decay of solvation time correlation function ($S(t)$) defined as

$$S(t) = \frac{E(t) - E(0)}{E(0) - E(\infty)} \tag{2.8}$$

Solvation dynamics of a very large number of solvents has been reported in the past decade.[81] Among all the liquids, water exhibits the fastest dynamics reported so far.[82,83] The initial part of the solvent response of water is extremely fast (few tens of femtoseconds) and constitutes more than 60% of the total solvation. The subsequent relaxation occurs in the picosecond time scale.[83] In water, the decay of the solvation time correlation function, $S(t)$, can be fitted to an expression of the following form:[80]

$$S(t) = A_G \exp(-t^2/\tau_G^2) + B \cos(\alpha t) \exp(-t/\tau_1) + C \exp(-t/\tau_2) + D \exp(-t/\tau_3) \tag{2.9}$$

where A_G, C, and D are the relative weights of the initial Gaussian and the subsequent exponential decay processes and τ_G, τ_2, and τ_3 are the corresponding relaxation time constants. The second term in eq 2.9 ($B \cos(\alpha t) \exp(-t/\tau_1)$) takes into account the oscillatory features of the $S(t)$ observed beyond the Gaussian decay in theoretical calculations and simulations.[80,82−85] The early simulation studies predicted a very fast inertial component with a Gaussian time constant of less than 10 fs.[82] Fleming et al.[83] experimentally detected a Gaussian component of time constant of less than 50 fs and a slower biexponential decay with time constants of 126 and 880 fs, respectively. Several other experimental[86−90] and simulation studies[91−98] on solvation dynamics of large dye molecules as well as electrons in water demonstrated that the initial part of solvation in water occurs with a time constant of a few tens of femtoseconds.

Several theories have been developed to treat solvation dynamics in water. These theories use the experimental dielectric data to provide a quantitative description of the ultrafast solvation water.[69,79,99−108] The results of theoretical studies are shown in Figure 3. All these theoretical analyses suggest that the ultrafast Gaussian component may arise from the 200 cm^{-1} intermolecular vibrational mode. Two other major conclusions are that it is the long wavelength polarization mode that drives the initial solvation and that solvation could be faster if the polarizability of water is neglected. The librational mode at 685 cm^{-1} is important only at very short times.

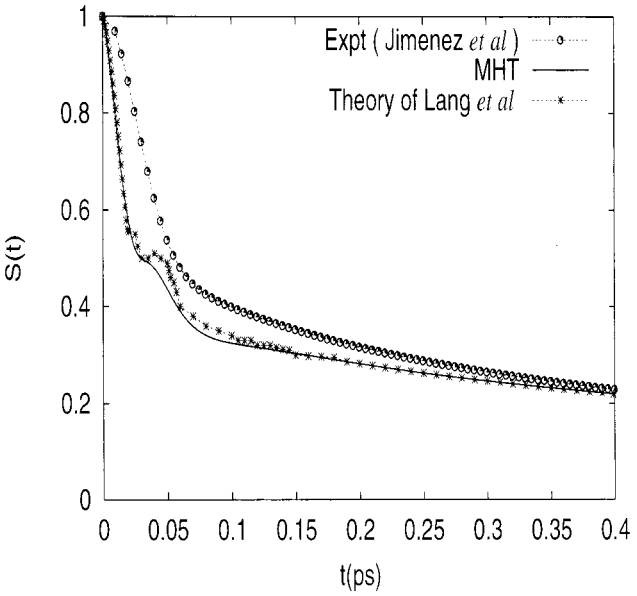

Figure 3. Experimentally obtained solvation time correlation function for the solvation of a coumarin dye in water.[83] The theoretically obtained time correlation functions for the solvation of an eosin dye as obtained from the molecular hydrodynamic theory (MHT)[80] and the continuum model theory of Lang et al.[84] are also shown in the same plot. The solute is assumed as an ionic probe of the same size of an eosin dye in MHT while the theory of Lang et al. used the charge densities (in a vacuum) for the ground and excited state of the chromophore.

It is seen from Figure 3 that the molecular hydrodynamic theory (MHT) does a somewhat better job in describing the solvation time correlation function than the continuum model of Lang et al.[84] This is somewhat fortuitous because MHT calculation was done for the solvation of an ion with the size of the eosin. Therefore, the solvation dynamics predicted by MHT is somewhat faster. We think that a major limitation of the work of Lang et al. is the neglect of the translational modes, which can be important for a charge distribution that generates higher mulitpolar moments.

In summary, according to the experimental and theoretical studies, the solvation dynamics in water involves multiple time scales of <50 fs and 1 ps. The time scales of solvent relaxation in the aqueous regions of the biomolecular systems and in the organized assemblies, however, are significantly slower. We discuss this later in this review.

III. Structure of Some Biomolecules, Organized Assemblies, and Their Hydration Zones

In this section, we briefly outline the structure of some biomolecules, organized assemblies and their hydration zones. The structure of these systems has already been discussed in a number of monographs,

reviews, and articles. Therefore, we present only a brief overview instead of giving a detailed description.

A. Amino Acid and Peptide

α-Amino acids, $RC_\alpha(H)(NH_3^+)COO^-$, are the building blocks of a protein molecule.[109] The state of ionization of an α-amino acid depends on the pH. At neutral pH, the carboxyl group dissociates to protonate the amino group to produce a zwitterion. The study of the hydration of amino acids and peptides is evidently important to understand the hydrophobic effect as well as the hydration of proteins. Hydration of amino acids and peptides has been investigated by X-ray crystallography,[110,111] dielectric relaxation,[112] neutron scattering,[113] simulation,[114,115] and several other methods.[1,116] NMR studies on the nonfreezing water in polypeptides indicate that the ionic amino acid residues contain the maximum amount of water of hydration (3−7 mol of water/mol of amino acid) while the polar and nonpolar residues contain a relatively less amount of water of hydration.[1] It should be noted that the water of hydration of peptides is sufficiently perturbed to be unable to form ice.[117] Recent simulations indicate that the energetics of hydration depends significantly on the conformation of the peptide.[114] Water molecules in the hydration shell of the amino acids and peptides form a hydrogen bond network that is relatively unstrained as compared to that in the bulk.[113] It is observed that the movement of water protons in the vicinity of the peptides is slower as compared to that in bulk water but faster than that in ice.[40,43,112] This indicates that the structure and dynamics of water in the vicinity of amino acids and peptides is different from those in bulk water.

B. Protein

Amino acids condense to form proteins having very well-defined three-dimensional structures. The function of a protein molecule crucially depends on its structure. The most common structural motifs in proteins are α-helix and β-pleated sheet.[109] The hydrogen bonds between the NH and CO units of the main chain stabilize the α-helix whereas the hydrogen bonds between the β-strands stabilize the β-sheet structure.[109] Water-soluble proteins fold into compact structures with a mostly nonpolar core. The size of the protein molecules are often fairly large. For instance, a myoglobin molecule is composed of a single polypeptide chain with 153 amino acids and has a dimension of 45 × 35 × 25 Å.[109]

The presence of water is of vital importance to preserve the structure and activity of the protein.[117−139] In the absence of water, proteins undergo denaturation and lose their ordered three-dimensional structure and biological activity. The water molecules are bound to the protein surface with one or more hydrogen bonds formed with the main chain or the side chain functional groups. The extent of hydration of different main chain and side chain functional groups has been studied in considerable detail.[118,139] The hydrogen bond energy in competition with solvent water is found to be −1.0 to −1.4 k cal mol^{-1} for the polar uncharged groups while it is −1.5 to −2.8 k cal mol^{-1} for the polar charged groups.[118] Usually about 0.3−0.7 g of bound water remains associated per gram of a "dry" protein.[50,118] The bound water constitutes a layer that contributes to the protein's effective radius of rotation.

With a gradual increase in the hydration level of a dry protein sample, at first the charged or very hydrophilic groups (e.g., COO^-, NH_3^+, NH_2, COOH) ionize with redistribution of the protons. Once the polar groups are covered by a water layer, the proteins begin to exhibit catalytic activity. This indicates that the water coverage provides the flexibility needed for the biological activity of the proteins. Further addition of water provides full monolayer coverage and enhances the enzymatic activity.[118] With a gradual increase in the hydration level, the protein dynamics changes gradually, and water helps in reducing the number of barriers in the free energy landscape.[31,32] Thus, water has a profound "loosening" or "lubricating" effect on a protein.[31,39] This effect is mutual in the sense that the structure and dynamics of water of hydration is also modified by the presence of protein and is quite different from the bulk properties. The density of the hydration shell of a protein is 10−20% higher than that of bulk water.[48,137] X-ray studies indicate that the water molecules at the protein surface are highly ordered and exist in the forms clusters and pentagons.[118] Experimental studies and theoretical calculations suggest that the translational diffusion of water in the hydration shell is much slower within the hydration shell of aqueous protein solution as compared to that in bulk water.[10,11] Recent molecular dynamics simulations on aqueous solution of protein also indicate that the translational motion within the first hydration shell is significantly modified as compared to that in the bulk.[12] Molecular dynamics simulation of the active site of lysozyme shows that the diffusion coefficient of water around atoms in charged, polar, and apolar side chains are markedly different from that in bulk water.[126] A schematic diagram of a hydrated protein molecule in aqueous solution is given in Figure 4.

C. Deoxyribonucleic Acid (DNA)

Deoxyribonucleic acids (DNAs) are polymers of deoxyribonucleotide units. A nucleotide consists of derivatives of nitrogenous bases, e.g., adenine and guanine (purines) and thymine and cytosine (pyrimidines), a sugar (which lacks an oxygen atom that is present in the parent compound, ribose), and one phosphate group.[109] Two polynucleotide chains running in the opposite direction coil around a common axis and give rise to the well-known double-helical structure.[109] The purine and pyrimidine bases remain inside the helix while the phosphate and deoxyribose units remain outside the helix. Triplex DNAs with potential use as therapeutic agents in gene regulation are also reported in the literature.[140] DNA molecules are classified according to their structural and functional characteristics. Common structural motifs are designated as A-, B-, C-, and Z-DNA. The DNA molecules have remarkable asymmetry in the sense

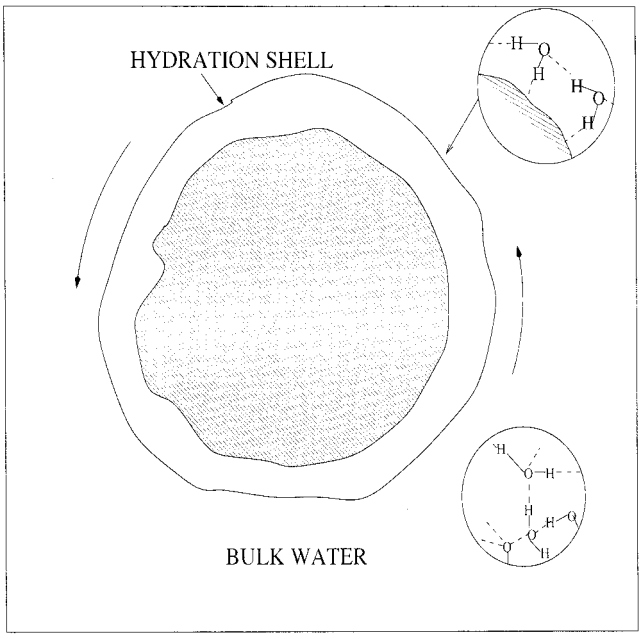

Figure 4. Schematic diagram of a hydrated protein molecule. The water molecules hydrogen-bonded with the protein molecule present in the hydration shell as well as the water molecules in the bulk hydrogen-bonded network are also shown schematically in the figure.

that their lengths are in the macroscopic scale while their diameter remains small. For example, the diameter of *Escherichia coli* DNA is only 20 Å while its length is 14×10^6 Å.[109] Many of the DNA molecules are also circular and supercoiled.[109]

The conformation and structure of the DNA molecule depend on the degree of hydration.[33,141,142] Fully hydrated DNA contains 20 water molecules per nucleotide (two water layers around the double helix).[141] The extent of hydration of the different sites of A-, B-, and Z-DNA has been studied in detail by X-ray crystallography.[141] The hydration motifs of the phosphate, sugar, or base depend on the type of DNA. The primary hydration shell of DNA does not freeze and exhibits a hydrogen-bonding pattern different from that in water.[141] Different types of DNA can be readily interconverted by changing the hydration level and the salt concentration. The structure and dynamics of DNA is profoundly influenced by its hydration shell.

D. Cyclodextrin

Cyclodextrins are cyclic oligosaccharides.[19−20,143−146] α-, *β*-, and *γ*-cyclodextrins contain 6, 7, and 8 α-amylose units, respectively. These macrocycles can act as a "host" to form inclusion complexes with "guest" molecules in solid state as well as in solution. The shape of a cyclodextrin molecule is a hollow, truncated cone (a toroid) of height 7.9 ± 0.1 Å that represents the width of the amylose unit (Figure 5).[145,146] The diameter of the cavity depends on the number of amylose units. The inner diameters are 5.0 ± 0.2, 6.2 ± 0.2, and 7.9 ± 0.4 Å, respectively, for α-, *β*-, and *γ*-cyclodextrin while the outer diameters are 14.6 ± 0.4, 15.4 ± 0.4, and 17.5 ± 0.4 Å, respectively.[143,145−146] All the hydroxyl groups of a

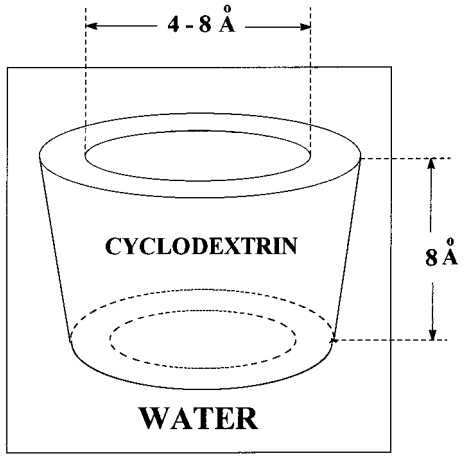

Figure 5. Schematic diagram of a cyclodextrin molecule in water. The dimensions of the cavity and the length of the toroid of *γ*-cyclodextrin are also indicated in the figure.

cyclodextrin are projected outward so that the cavity is hydrophobic and nonpolar. Thus, despite the preponderance of hydroxyl groups, the cyclodextrins offer a hydrophobic surface to which organic molecules bind in aqueous solution hydrophobically.[143−146] The primary requirement for the inclusion of a guest within the cyclodextrin cavity is that the size of the guest fits within the cavity. Along with the guest molecule, several water molecules are often trapped within the cyclodextrin cavity. If the size of the guest molecule is suitable, then the hydrogen bond network may be continued within the cavity through the open ends of the toroid and form a hydration sheath around the guest molecule. A supramolecule containing a cyclodextrin molecule as the host is perhaps the most well-defined model for an enzyme−substrate complex. Structure and dynamics of such guest−host complexes involving cyclodextrin has been studied using several experimental techniques[143−146] as well as computer simulations.[147] Most recentl,y Luzhkov and Aqvist used a free energy perturbation procedure along with molecular dynamic simulations to determine the binding energy of phenyl esters with *β*-cyclodextrin (*β*-CD) and the energy of activation for the hydrolysis of the phenyl esters bound to *β*-CD.[147] The results of this simulation[147] are in excellent agreement with the experiments. The properties of the trapped water in the cavity of cyclodextrin are very different from the bulk. The translational mobility of the encapsulated water molecules is severely restricted by the cavity wall. Consequently, the solvent relaxation is markedly slow within the cavity as compared to bulk. We discuss this in detail in section V.D.

E. Micelle

Amphiphilic surfactant molecules form spherical or nearly spherical aggregates called micelles above a certain critical concentration, known as the critical micellar concentration (cmc), and above a critical temperature, called Kraft temperature.[148] The size of the micellar aggregates is usually 1−10 nm, and the aggregation number, i.e., the number of the surfactant molecules per micelle, ranges from 20 to

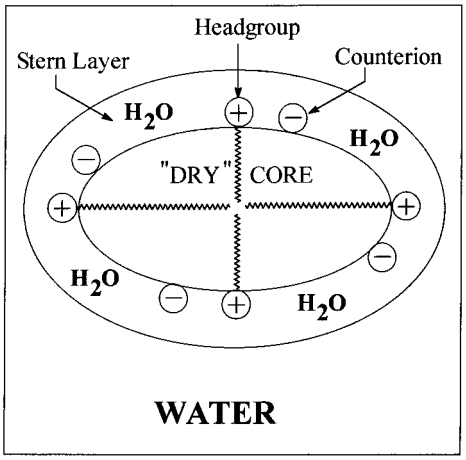

Figure 6. Schematic diagram of an aqueous micellar solution. The dry core, stern layer, headgroups, and bulk water are indicated in the figure.

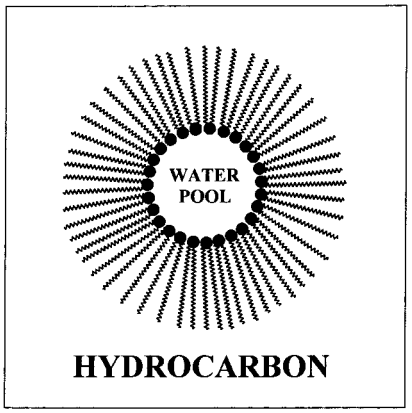

Figure 7. Schematic diagram of a reverse micelle in hydrocarbon.

200. The core of a micelle is essentially dry and consists of the hydrocarbon chains with the polar and charged headgroups projecting outward into the bulk water. The Stern layer surrounding the core comprises of the ionic or polar headgroups, bound counterions, and water molecules. Between the Stern layer and the bulk water there is a diffuse layer, termed the Guoy−Chapman (GC) layer (Figure 6).[148] The GC layer contains the free counterions and water molecules. In nonionic polyoxyethylated surfactants, the hydrocarbon core is surrounded by a palisade layer, which consists of the polyoxyethylene groups hydrogen bonded to water molecules. The structure of a micelle is metastable and involves continuous exchange of monomers between the aggregates and those in bulk solution.

Recent small-angle X-ray and neutron-scattering (SANS) studies have revealed detailed information on the structure of a variety of micelles.[149,150] According to these studies, the thickness of the Stern layer is 6−9 Å for cationic cetyl trimethylammonium bromide (CTAB) micelles and anionic sodium dodecyl sulfate (SDS) micelles, whereas the palisade layer is about 20 Å thick for neutral Triton X-100 (TX-100) micelles.[149] Radii of the dry, hydrophobic core of TX-100 are 25−27 Å, and thus the overall radius of the TX-100 micelle is about 51 Å. The overall radii of CTAB and SDS micelles are about 50 and 30 Å, respectively. The structure of more complicated micelles and their phase transitions have recently been studied using SANS.[151−154]

F. Reverse Micelle and Microemulsion

Reverse micelles refer to aggregates of surfactants (e.g., dioctyl sulfosuccinate, AOT) formed in a nonpolar solvent, in which the polar headgroups of the surfactants point inward and the hydrocarbon chains project outward into the nonpolar solvent.[156−186] Apart from liquid hydrocarbons, recently several microemulsions are reported in supercritical fluids such as ethane, propane, and carbon dioxide.[166−168]

The most important property of the reverse micelles is their ability to encapsulate fairly large amount of water to form what is known as a "microemulsion". Up to 50 water molecules per molecule of the surfactant can be incorporated inside the AOT reverse micelles. Such a surfactant-coated nanometer-sized water droplet dispersed in a nonpolar liquid is called a "water pool" (Figure 7). The radius (r_w) of the water pool varies linearly with the water to surfactant mole ratio, W_0.[158b] In *n*-heptane, r_w (in Å) is approximately equal to $2W_0$.[158b] The structural information on the microemulsions (i.e., radius of the micellar aggregates) and that of the water pool have been obtained using dynamic light scattering,[165] transient grating,[160] SANS studies,[168,175,176] small-angle X-ray scattering,[169] ultrasound velocity measurements,[163] FT-IR,[162,164] NMR, ESR, differential scanning calorimetry,[161] and dielectric relaxation.[181−183] In contrast to AOT, which does not require any cosurfactant to form reverse micelles, cationic surfactants do not form reverse micelles in the absence of cosurfactants.[177] Several nonionic or neutral surfactants (e.g., Triton X-100, etc.) have recently been reported to form reverse micelles in pure and mixed hydrocarbon solvents.[163,178] Finally, apart from water, confinement of other polar solvents such as acetonitrile, alcohol, and formamide have been reported in such microemulsions.[179]

The water molecules confined in the water pool of the microemulsions differ in a number of ways from those of bulk water. During the process of formation of a microemulsion, the first 2−4 water molecules are very tightly held by the surfactant and all the water molecules except the 6 most tightly held ones freeze at −50 °C.[161] The FT-IR[162] and the compressibility studies[163] indicate that the first three water molecules "lubricate" the dry surfactants. The compressibility of the AOT microemulsion increases steeply during this process. The next three water molecules solvate the counterion (Na^+ for Na-AOT) and start the self-organization process. At this stage, the headgroups of AOT become linked by hydrogen bonds through the water molecules, and the compressibility gradually decreases. For $W_0 > 6$, the water pool swells in size, but the compressibility reaches a plateau. Around $W_0 = 13$, the first solvation shell of AOT becomes complete, and up to this point the water structure remains severely perturbed inside the water pool. But even in the very large water pools, the compressibility of the microemulsions

remains at least 2 times higher than that of ordinary water.[163]

G. Lipid Vesicle

Lipid vesicles are the closest model of a biological cell. In a vesicle, an aqueous volume (water pool) is entirely enclosed by a membrane that is basically a bilayer of the lipid molecules.[187−197] This water is different from bulk water in a way similar to water in biological cells being different from bulk water. In the case of the unilamellar dimyristoyl phosphatidylcholine (DMPC) vesicles (radius 250 nm), there is only one such bilayer while a multilamellar vesicle (radius 1000 nm) consists of several concentric bilayers. Unilamellar vesicles can be produced by breaking the multilamellar vesicles through sonication. In such a system there are two kinds of water molecules present, those in the bulk and those entrapped within the water pool of the vesicles. The entrapped water pool of a small unilamellar DMPC vesicle is bigger (radius 250 nm) than that of the water pool of the reverse micelles (radius <10 nm). In recent years, several groups studied chain dynamics of lipids using SANS, conductivity, and electron microscopy;[187] ESR of spin-labeled lipids;[188] and fluorescence of pyrene-labeled lipids.[188] Recent molecular dynamics (MD) simulations,[189] NMR[190] crystal structure,[191] and other studies revealed detailed information about the structure of DMPC vesicles and the water molecules in its neighborhood. The most recent MD simulation[189] indicates that above a transition temperature (23 °C) each DMPC molecule is hydrogen bonded to about 4.5 water molecules, which form an inner hydration shell of the polar headgroup of the lipids, and about 70% of the DMPC molecules remain connected by the water bridges.

The vesicles undergo phase transitions at a well-defined temperature. Above the phase transition temperature, the viscosity of the lipid bilayer remains quite low, and the permeability of the bilayer wall remains high so that small molecules easily pass through the bilayer to enter the inner water pool.[192] Viscosity of the lipid bilayer becomes high, and the permeability across the bilayer membrane decreases significantly below the transition temperature. The change in the viscosity of the lipid bilayers with temperature is usually monitored by optical anisotropy studies. The transport of small organic molecules across the lipid bilayer above transition temperature is most elegantly demonstrated in a recent surface second harmonic (SSH) generation study by Srivastava and Eisenthal.[197] The SSH signal is obtained as long as the molecule stays in an inhomogeneous region, i.e., at the lipid bilayer. Above the transition temperature of the lipids, the SSH signal decays in a time scale of 100 s that denotes the residency time of the probe in the bilayer or the time taken by the probe to diffuse through the bilayer membrane from bulk water to the inner water pool. For lipids below the transition temperature, no such time dependence of the SSH signal is observed, which indicates that at a temperature below the transition temperature the bilayer membrane does not allow transport of molecules to the inner water pool.[197]

H. Polymer and Hydrogel

Water-soluble polymers have generated considerable recent interest because of their versatile applications and compatibility with biological systems.[198] The properties of aqueous polymer networks and the water molecules attached to them have been studied by various techniques such as fluorescence,[199] dielectric relaxation,[200−213] computer simulation,[214] and light scattering.[215] The microporous synthetic polymer hydrogels are those polymers that are inherently insoluble in water but can entrap a considerable amount of water within their polymer networks.[216,217] They are particularly interesting due to their diverse applications such as biomaterials (e.g., contact lenses), chromatographic packings, in devices for controlled-release of drugs, and electrophoresis gels. The polyacrylamide (PAA) hydrogel is obtained by polymerizing acrylamide in the presence of *N*,*N*-methylene bisacrylamide as a cross-linker.[218] The pore size in such a gel can be varied by change in the concentration of the monomer (acrylamide).[216] Among the various types of hydrogels, PAA is most suitable for photophysical studies as it is optically transparent over a wide range of concentrations of the monomer and the cross-linker. On absorption of water, such a hydrogel swells in size. The swelling and other properties of this interesting semirigid material have recently been studied using light scattering,[215] NMR, and calorimetry.[219] The bulk viscosity of any hydrogel is very high. However, since the hydrogels contain large pores, even very large biological macromolecules such as DNA pass through such hydrogels during gel electrophoresis. Several attempts have been made to immobilize small probe molecules (e.g., nile red)[220] or proteins[221−223] within the hydrogels. Using far field fluorescence microscopy, Dickson et al. demonstrated that, in PAA hydrogel while most nile red molecules move freely, motion of a minute fraction (2%) of them becomes severely restricted so that the Brownian motion of individual nile red molecules may be recorded.[221]

I. Zeolite

Zeolites are open structures of silica in which some of the silicon atoms in the tetrahedral sites are replaced by aluminum ions.[224−234] Counterions such as Na^+ or K^+ maintain the electroneutrality and reside freely inside certain locations in the zeolite cages. Zeolites can be represented by the empirical formula $M_2/nAl_2O_3{\cdot}xSiO_2{\cdot}yH_2O$, where M is an alkali metal or an alkaline earth metal cation of valence *n*, $x > 2$, and *y* varies from 0 to 10.[19,225] Depending on the Si/Al ratio and the cations, zeolites can have various rigid and well-defined structures that can be classified into cage and channel types. For the ZSM-5 zeolite, there are two intersecting channel systems. One system consists of straight channels with a free cross-section of 5.4−5.6 Å^2 and the other consists of sinusoidal channels with free diameter of 5.1−5.5 Å^2.[19,225] On the other hand, faujasite zeolites (Figure 8) are made up of a nearly spherical supercage of diameter 13 Å, surrounded by small sodalite cages.[19,225]

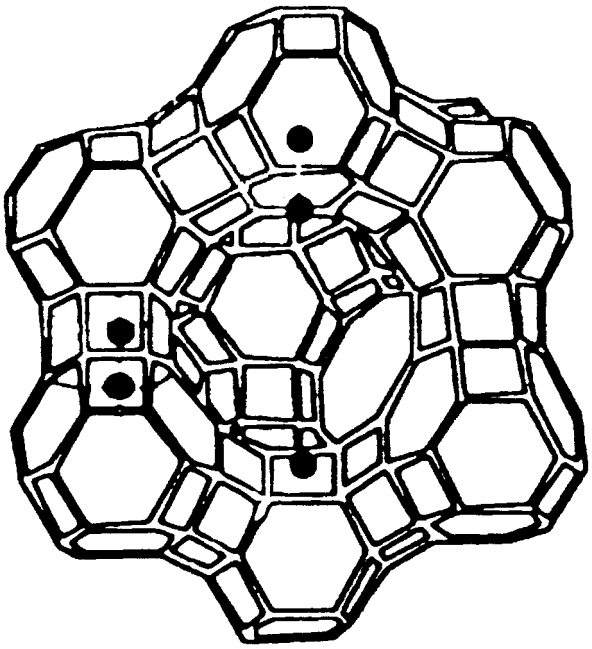

Figure 8. Schematic diagram of a faujasite zeolite.

The structure and dynamics of zeolites has been studied by molecular dynamics (MD) simulation, Monte Carlo simulation,[230,231] density functional theory, and stochastic models.[232,233] These studies indicate that the spatial locations are similar for different cations. The mechanism of electrical conduction in a zeolite has been the subject of several studies. Conduction of dehydrated potassium zeolite L has been found to involve a thermally activated process.[235,236] Dielectric properties of the zeolites depend on the degree of hydration.[237] The zeolites can act as a host for a large number of guest molecules. Neutron diffraction study suggests that in zeolite Y, cyclohexane stays in the 12-ring window site. This is in agreement with the MD simulations.[238,239] Similar results are obtained for benzene in zeolites.[238,239] NMR line width and simulation studies indicate that in the faujasite zeolites the guest aromatic molecules hop from one cage to another in the nanosecond time scale.[240] Certain positions in the inner walls of the micropores of the zeolites serve as active sites, where catalytic conversions can take place. The size of the micropores and the location of cavities can be adjusted so that only one type of molecular species can reach the active sites. Zeolites contain many acidic sites.[234] The number of different types of acidic sites in a zeolite depends on the method of activation of the zeolite. The photophysics and photochemistry of organic molecules change remarkably on encapsulation in zeolite.[225−226,229] The marked changes caused by the zeolites result partly from their rigid structure, which imposes considerable restriction on molecular motion within a zeolite. Second, the presence of cations in proximity to organic guest molecules exerts significant influences because of the strong local electric field produced by the cations and of the enhanced singlet−triplet transitions in the case of zeolites with heavy cations. The polarity and acid−base behavior of the zeolites also affect different photophysical processes.

IV. Dielectric Relaxation of Aqueous Biomolecules and Organized Assemblies

The dynamics of water near a biomolecule occurs on a time scale that ranges from femtosecond to nanosecond or even slower. Dielectric relaxation is one of the earliest methods to probe the dynamics in biological systems.[50,51] In this section, we review the dielectric relaxation studies of aqueous solutions of proteins, amino acids, and peptides; DNAs; several organized assemblies; and also the dielectric properties of liquid/liquid interfaces.

A. Dielectric Relaxation of Aqueous Protein Solutions

The dielectric spectra of aqueous protein solutions have been studied for nearly 50 years.[50−54,241−266] Cohn first pointed out that the solutions of proteins exhibit anomalous dielectric increment.[241] Oncley[51] studied the effect of orientational motions of the large protein molecules and smaller solvent molecules and proposed that the dielectric increment arises from the rotational relaxation of the protein molecules. This is however questionable because in dilute solutions the number density of the protein molecules is far below that necessary to give rise to the observed increment. The observed dielectric increment and spectra may be used to calculate the dipole moment, the degree of hydration, and the shapes of the protein.[51,242]

The dielectric relaxation spectrum of aqueous protein solutions shows several peaks, some more distinct than others. These peaks are denoted by Greek symbols, namely, β, δ, and γ. These are merely used to order relaxation frequencies from lowest to highest frequencies.

Several workers examined the role of the charged species such as counterions or protons of the proteins on the low-frequency relaxation. Kirkwood and Shumaker[243,244] proposed that the fluctuation of the dipole moment due to proton transfer may be responsible for the observed low-frequency dispersion. Lumry and Yue[245] however argued that the time constant for proton migration is much faster than the relaxation time of the protein, and the experimental pH is often unfavorable for proton transfer. Thus, the proton transfer mechanism (Kirkwood Shumaker effect) is relatively unimportant.[245]

O'Konski proposed a theoretical model according to which the excess conductivity of the protein arises from the mobility of the ions at the interface of proteins.[247,248] Schwarz suggested that the low-frequency dispersion is due to the polarization of the ionic atmosphere surrounding the protein.[249] The dielectric behavior of an aqueous protein has also been explained in terms of the dispersion behavior of a suspension of conducting particles in a nonconducting medium.[250] The major weakness of such theoretical models is the unphysical assumption of very large values of protein conductivity.[55] Jacobson[251] ascribed the low-frequency dispersion to a model of structured water molecules surrounding the macromolecule. However, there is overwhelming evidence that the orientational relaxation of perma-

Table 1. Dielectric Relaxation Times for Water Associated with Proteins[a]

solute	relaxation time and weights of relaxations
WM (0.01 M, β)[260]	74 ns (18.4 ± 1.1)[b]
WM (0.01 M, δ_1)[260]	10 ns (5.3 ± 1.5)[b]
WM (0.01 M, δ_2)[260]	40 ps (5.4 ± 0.8)[b]
WM (0.01 M, γ)[260]	8 ps (57.6 ± 0.9)[b]
EM (0.035 M, S_1)[263]	29 ns (11.0)[c]
EM (0.035 M, S_2)[263]	3 ns (0.9)[c]
EM (0.035 M, S_3)[263]	250 ps (1.3)[c]
EM (0.035 M, S_4)[263]	10 ps (68.2)[c]
EM (0.035 M, S_5)[263]	5 ps (2.7)[c]
BA (0.0015 M, 1)[256]	1 μs (8.8 ± 0.9)[b]
BA (0.0015 M, 2)[256]	204 ns (8.6 ± 0.8)[b]
BA (0.0015 M, 3)[256]	22 ns (2.11 ± 0.5)[b]
BA (0.0015 M, 4)[256]	2 ns (2.03 ± 0.5)[b]

[a] The concentration of the solution is indicated in the first column in parentheses followed by the part of the relaxation spectrum for which the time constant is given. The relaxation strengths are given in parentheses in the second column. For details of the function used to represent the relaxation processes we refer to the original literature. Symbols used are as follows: WM, whale myoglobin; EM, equine myoglobin; BA, bovine serum albumin. [b] Data at 25 °C. [c] Data at 20 °C.

nent dipole moments is responsible for the observed low-frequency dispersions. For example, freezing of albumin solution results in a drastic decrease in the dielectric constant due to the hindered rotational motion of the molecules in the frozen state.[252] Mofers et al. assumed that a protein molecule of spherical symmetry with the charged residues are placed in a medium whose dielectric constant increases continuously as a function of the distance from the center of mass.[246] The mean square dipole moment calculated using this model indicates that the fluctuation of the configurations cannot be responsible for the large dispersion in the MHz region.

The relaxation times and dielectric increments of many protein solutions have been summarized in previous reviews.[51,253−267] Time constants and relative weights of such relaxations for several proteins are reproduced in Table 1. Grant and co-workers studied quite extensively aqueous solutions of many proteins.[253−262] The high-frequency dispersions of aqueous protein solutions in the range of ∼10 MHz to ∼10 GHz are referred to as δ_1 and δ_2 dispersions. We discuss later in this review that the δ-dispersions originate from the bound water.[260]

Grant et al. attributed the rather large value of the dipole moment of myoglobin (calculated from dielectric measurements) to the permanent dipole moment (from surface groups as well as the core region) and to the charge fluctuations.[257] Dachwitz et al.[263] detected two distinct loss peaks near 10 MHz and 10 GHz, respectively. These two peaks correspond to the β and bulk water relaxations, respectively. This bimodality is much stronger and distinct from the bimodality discussed in connection with the δ-dispersion of biological water. The later dispersion occurs in the plateau region of the dielectric spectra and is relatively less prominent.[260] Dachwitz et al.[263] suggested that the δ-dispersion is due to the bound water dispersion and internal motions of myoglobin. Similar results were obtained for other proteins.[260,262] South and Grant examined different possible mechanisms for the observed β-relaxation in myoglobin solution[258] and concluded that the rotation of the permanent dipole is responsible for the observed relaxation. Further studies revealed a very interesting concentration-dependent crossover at the end of the β-relaxation.[259]

Mashimo and co-workers studied the dielectric relaxation of free and bound water molecules in several biological materials and biopolymers.[264−266] They observed two relaxation processes common to such systems. One is a low-frequency process and is characterized by a relaxation time, ∼1− 2 ns, and the other is a high-frequency process and occurs in a ∼7−20 ps time scale. Similar bimodal relaxation is reported in many other dielectric studies.[1,50] Mashimo et al.[264] assigned the low-frequency process to the relaxation of bound water and the high-frequency process to the relaxation of free water, respectively.[264] Gestblom[267] failed to detect the ∼1-ns component and argued that the 1-ns relaxation component reported by Mashimo et al.[264] is an artifact and may be due to premature truncation of the line shapes. NMR studies however suggest the presence of such a slow relaxation of the bound water molecules.[40,43,265,268]

Schlecht et al.[269] investigated the dielectric properties of unpurified, dialyzed, crystallized, and specially purified samples of horse hemoglobin and found that the results from different samples agree very well within the experimental error.[269] This indicates that the impurity and preparation procedure have no effect on the observed dielectric properties. These results and the results obtained by Lumry and Yue[245] indicate that zwitterions do not alter the dielectric parameters.

Takashima et al.[270−277] studied the effect of oxygenation and carbon monoxide addition on the dielectric properties of aqueous protein solutions. They reported two distinct maxima due to the four intermediate oxygenated species of hemoglobin. However, the so-called "Takashima effect" could not be reproduced by other workers.[278,279] This was attributed partly to the low accuracy in Takashima's original work. Another mechanism discussed by Schlecht et al.[278] was an aggregation of intermediates to a rodlike structure in a way that the dipole moments add up. However, experiments do not seem to find any indication of such aggregation.

Takashima and co-workers investigated the effect of urea on the dielectric properties of hemoglobin, bovine serum albumin, and ovalbumin.[272,276] Oxyhemoglobin exhibits a large dielectric increment at intermediate urea concentration. Takashima[272] reported anomalous temperature dependence of dielectric parameters of oxyhemoglobin and attributed this to the structural changes of oxyhemoglobin. However, no such temperature-dependent anomaly has been observed for hemoglobin.[280,281]

To understand the effect of solvent viscosity on the dielectric relaxation of proteins, dielectric spectra of several proteins have been studied in water−glycerine mixtures.[275] It is observed that the dielectric decrement decreases with a decrease in the water content. An interesting crossover was observed at intermediate concentrations similar to that of the

concentration-dependent crossover of aqueous protein solutions observed by Grant et al.[259] Hendricks et al. also reported a similar decrement in the magnitude of the dielectric function in glycerol−water and sucrose−water solutions of bovine serum albumin and transferrin.[282]

Dielectric relaxation studies of hydrated protein powders have been reviewed by several workers.[3,49,283−294] Different low-frequency relaxation processes (designated as Ω- and α-relaxations) have been studied as a function of hydration of the protein powders. To explain the relaxation process, a model-based percolation theory has been advanced.[3,294] These studies indicate that water acts as a plasticizer for the protein molecules.[49]

Until recently there have been three main objectives of the studies on the dielectric relaxation of aqueous protein solutions: (1) estimation of the degree of hydration of the protein; (2) calculation of the solvent phase dipole moment of the protein molecule; and (3) calculation of the shape or asymmetry of the protein molecule. Many anomalous phenomena observed in the dielectric spectra of aqueous protein solution have surprisingly eluded molecular explanation. They are as follow: (1) the bimodal δ-relaxation of the water of hydration of protein molecules in aqueous solution, which is generic to many other biomolecules such as DNA, etc.; (2) the significantly higher static dielectric constant of aqueous protein solutions (which can be as high as 100 for myoglobic solution) as compared to that of pure water at the low-frequency region (β-relaxation); (3) the interesting concentration-dependent crossover at the very low-frequency region where the real part of the dielectric function of the solution (ϵ') with higher concentration of protein dips suddenly and sharply to a value *lower* than that for a solution with smaller concentration; (4) the appearance of a very slow dielectric relaxation with time constant around 100 ns at moderately high concentrations. In the following subsections, we discuss the different anomalies of the dielectric spectra of aqueous protein solution and their recent molecular explanation.

A.1. Bimodality of δ-Relaxation

The almost universally observed bimodal δ-relaxation dynamics of water near a biomolecule[295] has been explained very recently in terms of an exchange model where a dynamic exchange (Figure 9) between the free and bound water states is assumed:

$$[H_2O]_{\text{free state}} \rightleftharpoons [H_2O]_{\text{bound state}} \qquad (4.1)$$

The equilibrium constant for the dynamical equilibrium between the free and bound water can be written as

$$K = \frac{k_2}{k_1} = e^{-\Delta G^*/RT} \qquad (4.2)$$

where ΔG^* is an activation energy of reaction 4.1. This is assumed to be related to the total hydrogen bonding energy per mole associated with the bound water molecules. The dynamic equilibrium between the free and bound species is shown schematically in Figure 9.

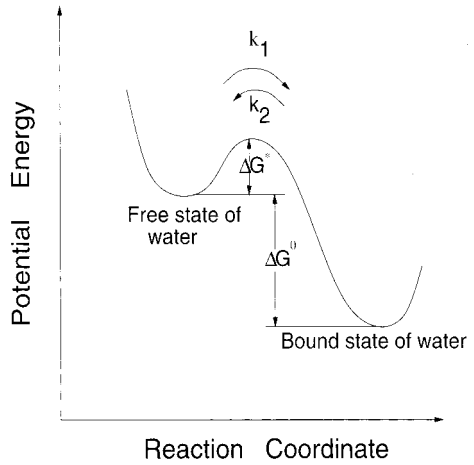

Figure 9. Schematic potential energy diagram of the bound water and free water molecules in dynamic equilibrium versus the reaction coordinate.[295] The activated complex is also shown in the figure. $\Delta G°$ is the difference in free energy of a hydrogen bond of a water molecule and a biomolecule and that of a hydrogen bond of the same water molecule with another water molecule in bulk water. ΔG^* is the energy of activation. The rate constants of the formation of bound and free species are denoted by k_1 and k_2, respectively. (Reprinted with permission from ref 295. Copyright 1997 American Chemical Society.)

The two-state model is supported by the recent molecular dynamics study,[121] which shows that among the 89 bound water molecules of carboxymyoglobin only 4 water molecules remains bound during the entire length of simulation (50 ps) while rest undergo continuous exchange between bound and free states. In the exchange model,[295] the free water molecules are assumed to be free to rotate and can contribute to the dielectric relaxation process.[295] The bound water molecules are doubly hydrogen bonded, and their rotation is coupled to the rotation of the biomolecule; hence, the hydration shell of the biomolecule rotates slowly. The energetics of the exchange depends on the strength and the number of hydrogen bond(s) of water molecule with the biomolecule. As the strength of the hydrogen bond increases, the magnitude of the rate constant, k_1, and the relative population of the bound species increase; consequently, the relative contribution and the relaxation time of the slow component also increase. At the low ΔG^* value (−1.4 kcal mol^{-1}), the relaxation time for the slow component is 44.26 ps, while at the higher ΔG^* value (−5.6 kcal mol^{-1}), the relaxation time is 28 ms.

The two-state model clearly demonstrates that the slow component observed in the dielectric measurements in biomolecule arises from the fast dynamic exchange between bound and free water molecules. The strength and the time constant of the slow component are determined by the strength of the hydrogen bonds by which the bound water molecule is attached with the biomolecule. The dipole moment correlation function from this model exhibits a strong bimodal decay.[295] The initial relaxation is very fast (∼10 ps), while the second relaxation is in the

nanosecond time scale. This is in excellent agreement with the bimodal decays reported in the literature. With the increase in the strength of the hydrogen bond, the relaxation becomes more and more slower. It is further observed that the coupling of the slow rotation of the biomolecules with the hydration shell of bound water does not affect the relaxation mechanism significantly. Halle et al.[40,43] suggested a similar dynamic exchange between the slowly rotating internal and the fast external water molecules from the NMR relaxation of ^{17}O. Fischer et al.[45] calculated the reaction path of the motion of the biological water molecules using the conjugate peak refinement method. Their calculation shows that the motion of the water molecules, buried in the proteins, involves exchange of hydrogen atoms of water and involves two successive rotations around orthogonal axes.

A.2. Anomalous Enhancement of Static Dielectric Constant and β-Relaxation

An interesting feature of aqueous protein solutions is that the value of its static dielectric constant is often found to be significantly larger than the value of pure water (78.6 at room temperature). Another anomalous behavior is that of dielectric dispersion, which leads to the decrease of the value of the dielectric constant from this high value to the value of water. The time constant of this latter dispersion is rather large indicating a slow process. This slow relaxation is known as β-relaxation. This β-relaxation is quite distinct from the δ-dispersion discussed earlier. The origin of the β-relaxation is not well understood, but it is intimately related to the enhanced value of the static dielectric constant of aqueous protein solutions.[258] In aqueous myoglobin solution, the total dielectric increment is about ~20% over the value of water. The dielectric decrement due to β-relaxation occurs in the frequency range of few megahertz to 100 GHz or so.[260]

The total time-dependent dipole moment correlation for a multicomponent system depends on the dipole moment as well as the number of dipoles present. In a typical protein solution, the number of protein molecules is nearly 1000 times smaller than the number of water molecules present. The contribution of protein molecules alone cannot give rise to the observed increment unless one makes the unphysical assumption that the dipole moment of the protein is higher than the measured value by several orders of magnitude or, consequently, cannot be explained even if one considers the relaxation of permanent dipole moment of the proteins. In the following, we briefly discuss an explanation proposed recently.[296] This explanation is based on eq 2.3 where the total dipole moment correlation function now derives contribution from all the molecules present in the system. The total dipole moment time-dependent correlation function is a sum of (1) permanent dipole moment correlation function of the protein molecules due to the permanent dipoles,[258,297] (2) the dipole moment correlation function for the water molecules in the hydration shell, and (3) the dipole moment correlation function of water in the bulk and the cross correlation between all species present in solution:

$$\langle \vec{M}(t)\cdot\vec{M}(0)\rangle \tag{4.3}$$
$$= \langle \vec{M}_p(t)\cdot\vec{M}_p(0)\rangle + \langle \vec{M}_p(t)\cdot\vec{M}_h(0)\rangle + \langle \vec{M}_p(t)\cdot\vec{M}_w(0)\rangle$$
$$+ \langle \vec{M}_h(t)\cdot\vec{M}_p(0)\rangle + \langle \vec{M}_h(t)\cdot\vec{M}_h(0)\rangle + \langle \vec{M}_h(t)\cdot\vec{M}_w(0)\rangle$$
$$+ \langle \vec{M}_w(t)\cdot\vec{M}_p(0)\rangle + \langle \vec{M}_w(t)\cdot\vec{M}_h(0)\rangle + \langle \vec{M}_w(t)\cdot\vec{M}_w(0)\rangle$$

where $\vec{M}(t)$ is the *total* dipole moment of the whole system and is given by eq 2.1. Here, p stands for a protein molecule, h stands for a water molecule in the hydration shell, and w stands for the same in the bulk.

If one considers only the dynamic exchange, then the range of the two time constants are about 30−50 ps and 10−20 ns, respectively, depending on the strength of the hydrogen bond.[295] However, a recent study on the rotation of structural water in a protein indicates that the rotational correlation time of water in bovine pancreatic trypsin inhibitor is about 45 ns.[45] The environment of hydrogen bond donors around the rotating water molecule is indicated as responsible for the slow motion of water in the protein. Previous studies indicated that the residence time of *buried* water could be even in the microsecond regime, and these molecules exchange at a slow rate with the bulk water.[43] In a recent theoretical study, it was assumed that the first time constant of the dynamics of water in the hydration shell is equal to the first component of the δ-relaxation (40 ps for myoglobin) and the second slower time constant to be 35 ns.[296] The amount of water in the hydration shell is calculated from the experimentally determined amount of hydration. Proteins usually have one or two shells of water of hydration.[44,50,260] From the known amount of protein present in solution and the amount of hydration water, the amount of bulk water present in the system may be calculated. The theoretical results are found to be rather insensitive to the choice of parameters, except for the value of the dipole moment of the bulk water molecules.[296]

In Figure 10, the theoretical and experimental plots of the ϵ' and ϵ'' of the aqueous myoglobin solution are compared. The agreement for ϵ'' in the region of absorption is not perfect, especially when the logarithmic scale of frequency is noted. Thus, the theory is only semiquantitatively successful in explaining the anomalous enhancement of the dielectric constant over the bulk value of water.[296] This increase is a result of rather delicate balance between the several terms involved in the $\langle \vec{M}(0)\cdot\vec{M}(t)\rangle$. While the contribution of the bulk water to the total dipole moment fluctuation, $\langle M(0)^2\rangle$, decreases, the cross-correlation terms, particularly those between the water molecules in the bulk and in the hydration shell surrounding the protein, increases leading to the overall increase in the value of $\langle M(0)^2\rangle$.

In summary, the heterogeneity combined with the cross-correlation is responsible for the anomalous enhancement. This theoretical result[296] is supported

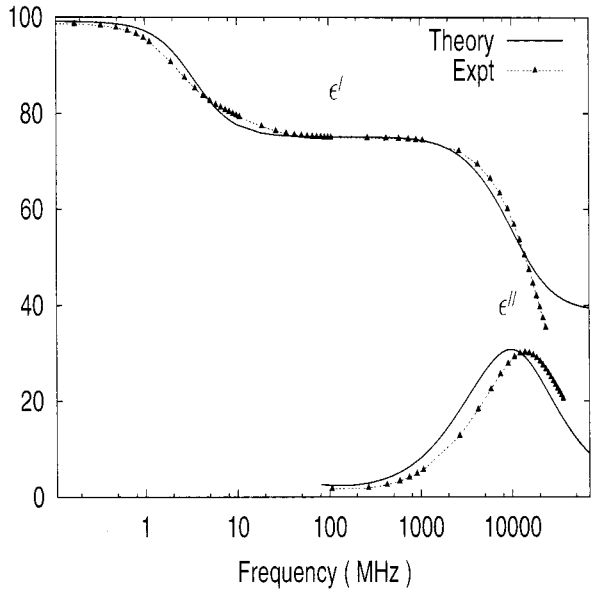

Figure 10. Real (ϵ') and imaginary (ϵ'') parts of the complex frequency-dependent dielectric function of aqueous myoglobin solution (concentration is 170 mg/mL) as determined by Grant and co-workers[260] (indicated by the dotted line with triangle) and from the theory of Nandi and Bagchi[296] (indicated by the solid line) at 298.15 K. (Reprinted with permission from ref 296. Copyright 1998 American Chemical Society.)

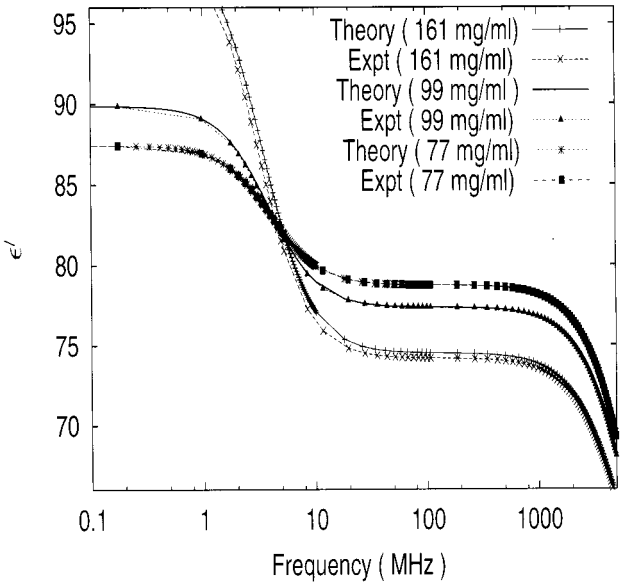

Figure 11. Concentration dependence of the real part of the complex frequency-dependent dielectric function (ϵ') of aqueous myoglobin solution (concentrations are 77, 99, and 161 mg/mL, respectively) as obtained in the experiment of Grant and co-workers[259] and from the theory of Nandi and Bagchi[296] at 293.15 K. Plots of different concentrations as obtained from the theory and experiment are indicated by different symbols as mentioned in the plot. (Reprinted with permission from ref 296. Copyright 1998 American Chemical Society.)

by the recent structural data in protein solutions which indicate that the correlations between the water molecules in the protein solution extend *beyond* the hydration shell.[137]

A.3. Concentration Dependence

The origin of the anomalous concentration dependence of dielectric relaxation of aqueous protein solution has been addressed recently.[296] Nandi and Bagchi calculated ϵ' of aqueous myoglobin solution and compared them with experimental results for three different concentrations. As indicated in Figure 11, the agreement between theory and experiment is satisfactory. With increase in the protein concentration, as the bulk water concentration decreases, the faster time scale of relaxation (due to the bulk water) is progressively replaced by the slower time scales of relaxation. Thus, the population of relaxation times shifts from the high-frequency peak to the lower frequency region. This is a manifestation of the increased population of bound water in the system. Thus, as concentration increases, faster free water gets replaced by the slower bound water.

The theoretical and the experimental results[263] for ϵ'' of aqueous myoglobin solution are shown in Figure 12. These plots clearly show the presence of a low-frequency peak in addition to the peak usually observed for water in the high-frequency region (GHz range).

The anomalies discussed above are indeed generic to protein solutions and not limited only to myoglobin solution. The theoretical results for the ϵ' of bovine serum albumin and concentration dependence of the ϵ' of equine hemoglobin compare well with those from the experiment.[254,256,280] Though hydrophobic aggregation occurs at high protein concentration, it is found to be negligible in the concentration range used in the dielectric studies. For instance, dimerization of myoglobin starts much above 150 mg/mL concentration—it becomes significant above 250 mg/mL or so.[298] Thus, protein association can be excluded as a possible reason for the crossover behavior in experiments.

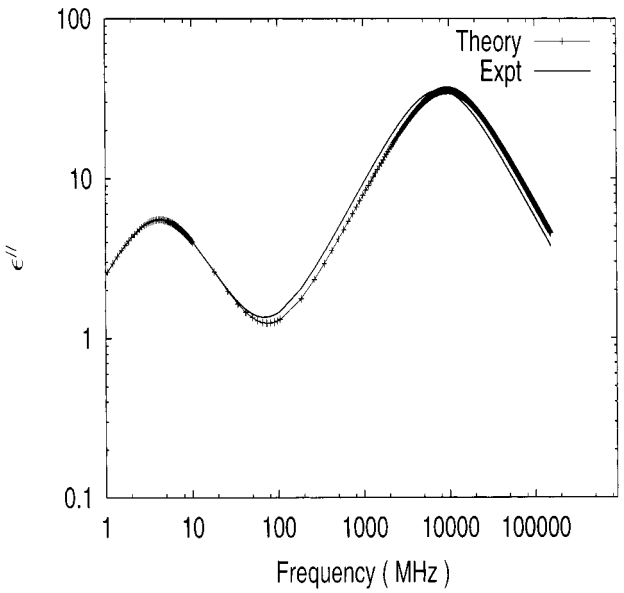

Figure 12. Imaginary part of the complex frequency-dependent dielectric function (ϵ'') of aqueous myoglobin solution (concentration is 60 mg/mL) as obtained in the experiment of Dachwitz et al.[263] (indicated by the solid line) and from the theory of Nandi and Bagchi[296] (indicated by the line with +) at 293.15 K. (Reprinted with permission from ref 296. Copyright 1998 American Chemical Society.)

A.4. Simulation Studies on Dielectric Properties of Proteins

Since electrostatic effects play a major role in the structure as well as the static and dynamic properties of aqueous protein solution, several authors have investigated the dielectric function (loosely referred to as dielectric constant) of a protein molecule.[6,353−376] However, it must be emphasized that the definition of the dielectric constant is not as straigthtforward in the case of an aqueous protein solution as it is for a homogeneous liquid. This is because the local dielectric constant varies sharply from inside a protein to the outside. Discussion in terms of a local dielectric constant is certainly ambiguous. The conventional description of a solvated protein as a uniform sphere of low dielectric surrounded by a continuum of high dielectric is incorrect due to the presence of ionized groups in the interior of proteins. Using the Poisson−Boltzmann equation, Gilson and Honig[353] predicted a homogeneous dielectric constant between 2.5 and 4 for the interior of the proteins. Fersht and Sternberg concluded that no simple relationship exists between the effective dielectric constant and the distance from the charge responsible for the interactions.[354] Gilson and Honig concluded that the distance-dependent dielectric function overestimates weak electrostatic interactions but yields relatively good results for strong ones.[353] However, Warshel et al.[355,364] pointed out that the distance-dependent dielectric function used by Gilson and Honig[353b,c] is improper because the latter did not include the solvent reaction field. Using a microscopic simulation, Warshel and co-workers demonstrated that excellent results are obtained if one assumes a high dielectric constant ($\epsilon \geq 40$) for the proteins or a dielectric constant with a sigmoidal distance dependence.[6,355,358,362] Warshel and Papazyan[363] pointed out that the value of the dielectric constant of a protein depends on what is included explicitly in the model and that small dielectric constants should not be used to describe the charge−charge interactions in continuum models. The simulation done by King et al.[356] indicates that the active sites of an enzyme possess a high dielectric constant. Thus, one should either use a large dielectric constant for charge−charge interactions and a small dielectric constant for charge-dipole interactions or consider the protein relaxation microscopically.[364]

Dimitrov and Crichton[365] considered the amino acid residues as polarizable bodies and studied the pH dependence of electrostatic interaction in proteins with a single dielectric constant. They described dielectric properties of the protein molecules in terms of the local dielectric constants determined by the space distribution of residue volume density around each ionized residue. Nakamura et al.[366] used normal-mode analysis to investigate the dielectric properties of protein and calculated the "local dielectric constant" from the electronic polarization of atoms and the orientational polarization of local dipoles. The calculated local dielectric constants ranged from 1 to 20 inside the protein. It has been pointed out that, apart from charge−charge interactions, the effect of the dipoles and the induced dipoles are important in determining the electrostatic interactions in the proteins.[362,367] Nakamura et al.[366] however did not take into account the effect of the inner and external solvent molecules.

Simonson et al. investigated the functional variation of the polarizability in a protein.[368] It is found that the contribution of the electronic degrees of freedom leads to an electronic susceptibility that is uniform throughout the molecule. The dipolar susceptibility, however, was found to vary greatly from position to position within a protein. It is suggested that this variation is related to the activity of the protein. The model is applied to model α-helices and the electron-transfer protein cytochrome *c*. The relation between the spatial variation of the susceptibility of protein to its biological function is investigated by molecular dynamics simulations.[369,370a] The dipolar susceptibility is found to be related to the structural relaxation of the α-helices.[369] The simulation further indicates that the dielectric properties determine the reorganization free energy for the electron transfer to and from protein. In cytochrome *c*, the susceptibility tensor of the heme atoms determines this energy. In aqueous solution the electronic contribution to the relaxation free energy is found to be spatially homogeneous and gives a dielectric constant of 2. The dipolar contribution is found to be less homogeneous and gives a little higher dielectric constant of magnitude 4 only. In the subsequent simulation studies on the polar fluctuations in yeast cytochrome *c*, Simonson and Perahia observed that the fluctuations follow simple probability distribution.[370b] This is consistent with the continuum models. The charged side chains are found to contribute significantly to the fluctuation. The fluctuation of water surrounding the protein is found to be similar to that in the bulk. Simonson et al.,[369] however, did not consider the charge stabilizing influence of the α-helices. Aqvist et al.[371] carried out a microscopic calculation on the charge stabilizing influence of the α-helices. They showed that the effect of helix−charge interactions is much larger than previously assumed and that the stabilizing effect of the helix is not associated with a few localized dipoles. It seems that the electron-transfer process in proteins depends on the local dielectric constant or local solvation as suggested by Warshel et al.[359,371] rather than the overall dielectric constant of the protein as proposed by Simonsen et al.[369b]

More recently, the reorganization energy of cytochrome *c* is studied by Muegee et al. from linear response theory.[372] They showed that the dielectric constant of a protein is model-dependent and that the dielectric function which reproduces the protein reorganization energy may not correspond to the macroscopic dielectric function of cytochrome *c* derived from simulations.[369] In a recent study, Simonson et al. extended their previous studies on the dielectric properties of cytochrome *c* where the cutoff used in previous simulation is removed.[373a] This theoretical study suggests that the interior of cytochrome *c* may have a low dielectric constant of 3 ± 1 while the overall dielectric constant is 25 ± 10. Charged side chains are found to contribute mostly

to the overall dielectric constant. It is argued that even if the water fluctuations are affected by the use of cutoff in simulation, the protein dipolar fluctuations are insensitive to it.[373a]

Krishtalik and co-workers[375] theoretically studied the formation and motion of charge within a protein and suggested that two dielectric constants are necessary for the calculation of the total free energy. The first one is related to the interaction of the newly created charge and the preexisting intraprotein field while the second is related to the polarization of the solvent by the new charge. The optical (electronic) dielectric constant is operative in the intraprotein interaction, and the static dielectric constant is relevant for the charging process of the newly created ion. More recently, Voges and Karshikoff[376] calculated local dielectric constants of protein molecules using classical electrostatics and considering the protein as being composed of polarizable sites and point dipoles at fixed positions. They estimated the dielectric constants of amino acid residues using the Onsager and Kirkwood equations. The Onsager equation leads to the lowest dielectric constant of 2.3 for Phe and the highest dielectric constant of 72.0 for Asn, whereas, the Kirkwood equation predicts 2.5 and 55.7 for the same residues, respectively. These calculations seem to verify the low dielectric constant of proteins with no or little polar groups. The Kirkwood equation, which includes local orientational correlations, might provide a somewhat better estimate.

The hydrophobic effect, i.e., the tendency of organic molecules to minimize water−organic interfacial area, leads to aggregation and complex surfaces for the biomolecules. Many biomolecules are characterized by surfaces containing extended nonpolar regions. Such surfaces contain convex patches, concave grooves, and nearly flat surfaces. Very recently Cheng and Rossky[8] studied the effect of surface topography on protein (mellitin)−water interactions. They demonstrated the existence of two different hydration structures—one clathrate-like and another fluctuating between clathrate-like and less ordered structure. The two structures differ in water−water interaction, and their relative contributions depend strongly on the topography of the surface. Lum et al.[15] have recently developed an elegant theory of solvation of small and large dipolar solutes in water. The theory can explain the hydrophobicty observed at both small and large length scales. In particular, the interesting experimental observation of the attraction between two hydrophobic surfaces can be explained by the theory.

The biological function of a protein depends crucially on its specific three-dimensional (3D) structure. The formation of a specific 3D structure is known as the "protein-folding" process.[109] Recently, several groups applied extensive molecular dynamics simulation to understand the thermodynamics and mechanism of the folding/unfolding process.[34,35]

Many recent simulation studies focused on the dielectric relaxation in aqueous protein solutions such as trypsin inhibitor and lysozyme.[299] In most of these simulations, the protein molecules are assumed to be spherical and placed in a dielectric continuum. Long time runs (nanosecond scale) are necessary to achieve convergence in the calculated dielectric constant. For this reason, neglect of the polarization contribution and rotation of the protein molecule are common in these simulations. Periodic boundary conditions with a twin cutoff (a smaller cutoff distance for short-range nonbonded interactions and another larger cutoff distance for the long-range interaction) have been employed frequently. The use of such cutoff methods enhances the speed of computation at the expense of reduction of the solvent contribution to the calculated properties. This is reflected in the calculated real and imaginary dielectric functions. They do not exhibit the typical anomalous behavior common for protein solutions. For example, the enhancement of the static dielectric constant over the bulk value, the bimodal δ-dispersion, and the bimodal shape of the imaginary part of the dielectric function are not observed in the results from simulations.[299] From extensive simulation studies, Loncharich and Brooks concluded that the use of long-range cutoff also affects the simulated dynamic properties of the protein itself.[300] Simulations of the dielectric properties of protein solutions in many cases further suffer from the non-inclusion of the cross correlation terms in the dipole moment correlation function, and consequently, the estimates of the static and dynamic dielectric properties should be considered incomplete.[296]

B. Dielectric Relaxation of Aqueous Solutions of Amino Acid and Peptide

Not only proteins but also solutions of small amino acids exhibit large dielectric increments and broad relaxation spectrum.[241,301−302] The broad relaxation observed has been assigned to the rotation of amino acid and of bound and bulk water. The magnitude of the dielectric increment of the polypeptides consisting of only one kind of amino acid increases with the increase in chain length.[301] The dielectric increment of the polyglycine chains (up to heptapeptide) is given by the following empirical relation:[53]

$$\Delta\epsilon' - \Delta\epsilon_\infty = c(14.51n - 5.87) \qquad (4.4)$$

where, ϵ' is the real part of dielectric permittivity, ϵ_∞ is the high-frequency dielectric constant, n is the number of chemical bonds between terminal amino and carboxyl groups, and c is the molar concentration. Values of relaxation times and dielectric increment of a few amino acid solutions are presented in Table 2.

Aqueous solution of glycine (1 M) gives rise to a static dielectric constant of about 100 at low frequency, and the imaginary part of the permittivity shows a bimodal peak.[52,54] Since the dipole moment of glycine is quite low (15−20 D), it is unlikely that the low-frequency increment is due to the permanent dipole relaxation of glycine.

Mashimo and co-workers studied the dielectric relaxation of polyglutamic acid and observed a peak around 70 MHz.[303] Bordi et al. studied the high-frequency dispersion (1−1000 MHz) of aqueous solution of sodium salt of poly-L-glutamic acid.[304] The

Table 2. Low-Frequency Dielectric Relaxation Times for Water Associated with Amino Acids and Their Derivatives[a]

solute	relaxation time and dielectric increment
glycine[54]	49 ps[b]
glycine[301]	62 ps (24.3 ± 1.2)
glycine[241]	(22.6)
diglycine[301]	156 ps (76.8 ± 3.8)[b]
diglycine[241]	(70.6)
triglycine[54]	200+ ps[b]
triglycine[301]	228 ps (126.8 ± 6.3)
triglycine[241]	(113.3)
tetraglycine[241]	(159.2)
pentaglycine[241]	(214.5)
hexaglycine[241]	(234.2)
heptaglycine[241]	(290.0)
lysylglutamic acid[241]	(345.0)
α-alanine[301]	88 ps (26.3 ± 1.3)[b]
α-alanine[54]	92 ps[b]
β-alanine[301]	88 ps (34.6 ± 1.7)[b]
β-alanine[54]	87 ps[b]
glycylalanine[301]	156 ps (79.9± 3.9)[b]
glycylalanine[54]	170 ps[b]

[a] The increment of the dielectric constant per mole of the solute is given within parentheses.[241] For details, we refer to the original literature. [b] Data at 20 °C.

dispersion is analyzed in terms of the Williams−Watts relaxation function in the time domain as well as the Cole−Davidson relaxation function in the frequency domain. They modeled the peptide as made up of dipole domains with opposing orientations and applied Skinner's kinetic Ising model[305,306] to study the diffusive process among these dielectric domains. The extracted dipole correlation function exhibits marked nonexponetial behavior.

Urry and co-workers[307] studied the temperature dependence of dielectric relaxation of protein-based polymers. These polymers exhibit a marked increase in intensity in the imaginary part of the dielectric dispersion (i.e., in dielectric loss) on dilution at low temperatures that depends on the hydrophobicity of the residues of the polymers. They characterized the water of hydration associated with the hydrophobic polymer and indicated that there are possibilities of the existence of an extended shell of water of hydration around the amino acid residues as suggested by others.[308]

The dielectric spectra of lower amino acid solutions are characterized by the following features: (1) the low-frequency peak of ϵ'' between 0.5 and 4 GHz; (2) the absence of a very low-frequency (MHz) peak of ϵ'' observed in protein solutions; (3) the magnitude of the dielectric increment increases with the increase in amino acid units in the peptide molecule; and (4) the absence of the broad plateau region of the δ-relaxation regime. The above features could make further study of amino acids solution worthwhile.

Recently, Loffler et al.[309] carried out a simulation of 18-residue zinc finger HIV peptides[308] using a nonpolarizable water model with a twin range cutoff and calculated the dielectric properties of each component (water and peptide) from a linear response formalism. They showed that for the correct description of the dielectric relaxation of peptide solutions it is essential to include the coupling term between the dipole moment of the peptide and the dipole moment of the water component. They demonstrated that neglect of the cross correlation terms significantly underestimates the static dielectric constant. These conclusions are in close agreement with theory.[296]

Table 3. Dielectric Relaxation Times of DNA Samples[a]

DNA	time constant and dielectric increment
calf thymus[313]	18 ms (4800)[b]
	2.3 ms (600)[b]
E. coli[313]	1.6 ms (220)[c]
calf thymus[315]	42 ms (830)[d]
salmon testis[315]	2.6 ms (320)[e]
sodium salt of salmon DNAs[317]	170 ms (240)[f]

[a] The dielectric increments are given in parentheses in the second column. For details, we refer to the original literature. [b] Sample 1 in ref 313. [c] Sample 5 in ref 313. [d] Sample AE in ref 315. [e] Sample B in ref 315. [f] Temperature is 22.5 °C in ref 317.

Despite the zwitterionic nature of lower amino acids, the increase in fluctuation dipole moment due to proton jump is expected to be small in the case of lower amino acids due to the small size of the molecules, as pointed out by Lumry and Yue.[245] The observed substantial dielectric increment of glycine and its homologues may be due to the inhomogeneous nature of the solution.

C. Dielectric Relaxation of Aqueous DNA Solutions

Dielectric relaxation studies on aqueous DNA solutions indicate the presence of large dielectric increments in the low-frequency region (10−1000 Hz).[52,310] For example, the increment is about 1000 or more for a $\sim 10^{-4}$ M solution of DNA of molecular weight 2×10^{-6}. Values of the time constants and dielectric increments observed in some DNA solutions are given in Table 3. The relaxation typically shows a positive temperature coefficient in contrast to the $1/T$ temperature dependence characteristic for permanent dipole polarization. As the two helices of a DNA point in opposite direction, there is no net dipole moment of the molecule. However, DNA bears a net negative charge in neutral aqueous solution and is surrounded by an ionic environment. In the presence of an externally applied field, these counterions move and give rise to an induced dipole. This induced dipole could be responsible for the dielectric increment observed in DNA solution.[310−328]

Takashima and co-workers[311] studied the dielectric relaxation of DNA samples and identified two dispersions, one between 1 MHz and 1 GHz and the second one above 1 GHz. It is observed that the relaxation of unbound water is only slightly affected at low DNA concentration. Several monovalent and divalent ions were shown to have a noticeable effect on the dielectric increment via counterion fluctuation while the large tetramethylammonium bromide ion has been reported to have negligible influence.[311a] Takashima[311a] considered DNA as a one-dimensional array of potential wells that represents the charged sites and neglected the electrostatic interaction be-

tween the counterions. This model is similar to the surface conductivity theories of O'Konski, Schwarz, Schwan, and Mandel.[247−249,312]

Hanss and Bernengo suggested that the dielectric relaxation of DNA at very low frequencies (1−100 Hz) is due to the orientational polarization of the permanent dipoles or the quasi-permanent dipoles due to the counterion fluctuation.[313] Sakamoto et al. reported similar results.[314−316] They found that protein contamination has little effect on the measured dielectric properties. Goswami and Dasgupta studied the temperature dependence of the dielectric relaxation of DNA samples.[317] They found that, with rise in temperature, the dielectric increment in the frequency range of 100 Hz−100 kHz increases while the relaxation time decreases. This observation goes against the counterion polarization theory.[317] The dipole moment of DNA has been estimated from Kirkwood theory and is found to be fairly large even at 0 °C. Mandel and co-workers[318] detected two dielectric dispersions for calf thymus DNA, one in a few kilohertz and the other in the 100 MHz region the amplitude of later decreases with concentration. The role of counterions in the dielectric dispersion of DNA samples is also emphasized in other studies.[319] Bone and Small suggested that the counterion fluctuation along the subunits of DNA chain contributes to the relaxation.[320,321]

Mashimo and co-workers[322] studied the dielectric spectroscopy of A-, B-, and Z-DNA samples and assigned the peaks at around 100 MHz to bound water and suggested that the structural transition from B- to Z-DNA is caused by the removal of bound water molecules preferentially from the phosphate groups. They proposed that the B-DNA to A-DNA transition takes place if the water molecules are removed to equal extent from phosphate groups as well as the grooves. The minimum number of water molecules necessary to maintain the structure of B-DNA is found to be 19 per nucleotide while 13 water molecules are bound to the A-form and 9 molecules to the Z-form. Several groups suggested the possibility of resonance absorptions by DNA in the GHz range and discussed its biological implications.[52,323−326]

The complex dielectric constants of arginine and protamine from herring sperm (clupeine) and their complexes with herring sperm DNA are measured at 10 GHz in the temperature range of −20 to 45 °C by a microwave cavity perturbation method.[327] The experimental results were analyzed in terms of the three components present in the system (solute molecules, interfacial water, and bulk water). The fractional volume of modified water and, hence, the specific hydration of the samples are calculated. The 4-fold reduction of the specific hydration for the clupeine molecule as compared to the free monomers has been attributed to the folded conformation of the protein in the solution.[327] It is suggested that, because of the intimate contact between the clupeine and DNA, the water molecules are excluded and the nucleoprotamines remain in a highly condensed form as they exist in vivo.

Recently Baker-Jarvis et al.[328] reviewed the dielectric properties of solvated DNA molecules and the theoretical models available so far and studied the dielectric relaxation of double- and single-stranded DNA from herring sperm in protamine solution. The low-frequency relaxation is found to be consistent with the counterion sheath relaxation models while the relaxation at MHz frequency region is explained in terms of the site-bound counterion models.

Yang et al. carried out 1.155-ns molecular dynamics simulation of a triple-helical DNA, $d(CG{\cdot}G)_7$, with 37 Na^+, 16 Cl^{-1}, and 837 water molecules with periodic boundary condition at 300 K.[329] The dielectric constant of DNA is found to be around 16, whereas that for the bases and sugars combined is only 3. The dielectric constant of water is underestimated to be 41. The decrement of the water dielectric constant is ascribed to the strong hindrance imposed on water molecules by the presence of DNA and ions. The mean square deviation of the dipole moment of each species and their cross correlations are presented. The cross terms are found to be always much smaller than the larger of the self-terms of the two species under consideration. The dipole relaxation time of water in the triplex system is found to be 9.7 ps. It is suggested that the presence of DNA and ions makes the water relaxation slower as compared to the bulk value.

Young et al. performed a 14-ns molecular dynamics simulation for ionic solutions of B-DNA.[330] The overall dielectric profile around DNA is observed to be a steep sigmoidal function that goes to the bulk value beyond 5 Å. The relative permittivities in the first shell decrease as phosphate backbone > major groove > minor groove. It is suggested that the decrement may be caused by the opposing influence of the solute and solvent molecules on any given reference water molecules.[330] This study raises the important question about the validity of the dielectric constant estimated from the finite length simulations and the use of spheres of finite radii carved out in solvent. This question pertains to the simulation studies on dielectric relaxation of protein solutions or other biomolecules also as discussed in subsection IV.A.4.

D. Dielectric Relaxation of Micelle, Reverse Micelle, and Microemulsion

Telgmann and Kaatze studied the structure and dynamics of micelles using ultrasonic absorption in the 100 kHz−2 GHz frequency range.[155] They detected several relaxation times in the long (μs), intermediate (10 ns), and fast (0.1−0.3 ns) time scale. The longest relaxation time is attributed to the exchange of monomer between bulk and micelles while the fastest is to the rotation of the alkyl chains of the surfactants in the core of the micelle. The intermediate relaxation time has not been assigned to any particular motion. We discuss later that the intermediate relaxation times in the 10-ns time scale may well be due to the solvent relaxation in the Stern layer.

Recent dielectric relaxation studies of bound water in reverse micelles provide information on the mobil-

Table 4. Dielectric Relaxation Times for Water Associated with Microemulsions and Micellar Solutions[a]

microemulsion	time constant and weight of relaxation
water/oil/SDS/1-butanol[185]	0.44 ns (0.48)[a]
	0.05 ns (1.0)[a]
water/oil/SDS/1-butanol[185]	0.23 ns (2.1)[b]
	0.02 ns (1.6)[b]
water/oil/SDS/1-butanol[185]	0.15 ns (14)[c]
lysolecithin[338]	1.54 ± 0.1 ns (21.7 ± 1.2)[d]

[a] The weights of relaxation are given in parentheses in the second column. [b] A1 solution as given in ref 185; temperature is 25 °C. [c] A9-B1 solution as given in ref 185; temperature is 25 °C. [d] C1 solution as given in ref 185; temperature is 25 °C. [e] 0.4 M solution in D_2O, ref 338; temperature is 20 °C.

ity of the water molecules in the nanometer-sized pools.[181−183] THz spectroscopic studies in the frequency range of 0.2−2 THz show that the amplitude of the dielectric relaxation in the water pool is substantially smaller than that in bulk water.[181] It is suggested that confinement, rather than local structure of the hydrogen bonded network, is responsible for the suppression of the relaxation amplitude and that, within the water pool, the "free" water is not structurally equivalent to the bulk water.[181] They observed weak high-frequency mode and ascribed it to the disrupted hydrogen bond network structure. The time constants and the corresponding weight of relaxation for a few microemulsions are given in Table 4. Note that the weights are *not* normalized.

D'Angelo et al.[182] studied dielectric relaxation of AOT−water−carbon tetrachloride (CCl_4) microemulsion in the 0.02−3 GHz frequency range as a function of the water to AOT molar ratio ($0.2 < W_0 < 10$). They detected a single relaxation time (about 7 ns at the lowest water content, $W_0 = 0.2$) that becomes shorter with an increase in W_0. It is proposed that the relaxation time represents the reorientational time of the micelle itself. The polar headgroups progressively become more hydrated with increasing W_0 and their mobilities gradually increase. The relaxation at the highest W_0 value is interpreted in terms of the rotational relaxation of the completely hydrated AOT ion pairs at the headgroup region.[182] In a subsequent study, D'Angelo et al.[183] extended the frequency range up to 20 GHz and used *n*-heptane as well as CCl_4 as a solvent and concluded that the relaxation at low water content represents that of the dehydrated micelle and that observed at the higher water content arises from the motion of the hydrated headgroups.

The quaternary microemulsion containing water, oil, SDS, and 1-butanol exhibits two relaxation processes.[184,185] The amplitude of the low-frequency relaxation increases with increase in the water content whereas the high-frequency process is found to be independent of hydration. The low-frequency relaxation shifts to the high-frequency range with an increase in the water content and is faster than the relaxation time of neat alcohol. Consequently, the low-frequency relaxation is attributed to the dipolar reorientation of water−alcohol mixture at the interfacial layer. The second relaxation at about 5 GHz is independent of water content and is attributed to the secondary relaxation of alcohol. Peyrelasse and Boned[186] studied the AOT−water−dodecane system at $W_0 < 10$ by time domain reflectometry and reported an apparent increase in the asymmetry of the micellar shape with increasing hydration.

E. Dielectric Relaxation of Lipid Vesicle

The amphiphilar assemblies such as the phospholipid bilayers mimic biological membranes. The dielectric studies of lipids and biological tissues provide valuable information about the electrical properties and the structure of the membranes as well as conductance of the intercellular fluids and cytoplasms.[52] Phospholipid vesicles show two dispersions, called α- and β-dispersions, in the 1−100 MHz frequency regime. The α-dispersion is ascribed to the relaxation of ionic atmosphere surrounding the vesicle while the β-dispersion is due to the relaxation of the vesicles that are dielectric shells with bound water inside.[331] Significant dielectric increment over the bulk value is observed in the low-frequency region in such systems.

Kaatze and co-workers investigated the dielectric relaxation of different analogues of phosphatidylcholine (lecithin analogues) and other phospholipids up to the gigahertz frequency range.[332−337] Two pronounced dispersions are commonly observed in lecithin solutions. One of them is at around 0.1 GHz while the other is above or near 10 GHz. It is pointed out that the higher frequency dispersion is due to solvent relaxation and that the low-frequency dispersion is due to the thermal orientational relaxation of the zwitterionic dipoles.[332] The relaxation time of the bound water is indicated as being slow as compared to pure water.[333] This scenario is qualitatively similar to that observed in the water pools of reverse micelles.[181]

The temperature variations of the real and imaginary parts of the frequency-dependent dielectric function (ϵ' and ϵ'') show distinct step-like changes at the lipid phase transition temperature. The experimental results were interpreted in terms of two types of water: bound (adjacent to lipid molecules) and free water. Thus, the frequency-dependent dielectric function can be expressed as follows:

$$\epsilon(\omega) = S(\omega) + L(\omega) - i\frac{2\sigma}{\omega} \qquad (4.5)$$

where $S(\omega)$ is the solvent contribution, $L(\omega)$ is the lipid contribution, and the last term represents the decrement due to conductivity. However, only lysolecithin fits well to this function. A multilamellar model seems to better fit the experimental result. The effect of cooperative orientational motions of the zwitterionic headgroups was also considered in subsequent studies.[335−337]

The detailed dielectric spectrum of lecithin solution shows the presence of three distinct relaxation regions.[337] The low-frequency dispersion (less than 40 MHz) is suggested to be due to ionic contributions. Phospholipid samples show no dispersion below 20−10 MHz, but a dispersion appears in this range when fatty acid or its salt is added in the sample. The

Table 5. Dielectric Relaxation for Water Associated with Hydrogels[a]

solute	relaxation time and dielectric increment
TSK gel SP-2SW[213]	2.97 ns (5.50)[b]
	0.06 ns (0.77)[b]
TSK gel G-2000SW[213]	1.44 ns (0.32)[c]
	0.05 ns (0.55)[c]

[a] The dielectric increments are given in parentheses in the second column. For details, we refer to the original literature. [b] Data at 23 °C. [c] Data at 22 °C.

presence of a fatty acid or its salt induces the growth of phospholipid aggregates by dissolving the phospholipid. This irreversible growth of the aggregates causes the observed dielectric increment. The intermediate dispersion (20−300 MHz) is suggested to be due to the rotational motion of the charged lipid molecules and their counterions (zwitterionic relaxation). The high-frequency dispersion (6−80 GHz) is due to bulk water dispersion. However, the relaxation frequency of the bulk water relaxation is slightly higher than the corresponding pure water relaxation frequency.

The important biological process of incorporation of gramicidin in lipid has been studied by dielectric method.[338] The pure lipid (lysolecithin) solution and the gramicidin-incorporated lipid solution exhibit different types of temperature-dependent dielectric spectra. Incorporation of the gramicidin causes a change in the hydration of the assembly, which leads to a change in the shape of the plateau region of the dielectric spectrum.

F. Dielectric Relaxation of Polymer and Hydrogel

Dielectric relaxation of aqueous solutions of polymers are studied extensively with the aim to understand the complex interaction between polymer chain and water molecules. Kaatze and co-workers studied relaxation in aqueous solutions of poly(ethylene oxide) (PEO), poly(vinyl alcohol) (PVA), and polyvinyl methyl ether (PVME).[203] It is observed that the relaxation strength ($\Delta\epsilon = \epsilon_0 - \epsilon_\infty$) as well as the frequency of relaxation decreases with an increase in the polymer concentration. It is assumed that the water molecules in the hydration layer surrounding the polymer molecules have a different relaxation time as compared to the bulk. Also the polar groups of the solute molecules contribute to the relaxation process. The relaxation time of the water of hydration is found to be in the range of few tens of picoseconds. It is suggested that apart from the chemical composition of the polymer the following factors influence the relaxation of hydration water: (1) the total size of the polymer molecule; (2) the overall shape of the polymer molecule with respect to the water arrangement around it: and (3) the flexibility of the linear polymer chains versus the inflexibility of the tightly packed cyclic groups.[203] Time constants and the corresponding weight of relaxations of several hydrogels and polymers are given in Tables 5 and 6, respectively.

Mashimo and co-workers investigated the dynamics of water in poly(ethylene glycol) (PEG) and poly(vinylpyrrolidone) (PVP).[204,205] PVP shows two relaxation peaks, and PEG shows only one relaxation peak in the 1 MHz−10 GHz frequency range. The high-frequency peak in the PEG solution is explained to be due to the rotational diffusion of water clusters, and the concentration dependence of the relaxation time is explained in terms of the free volume theory. The peak shifts to high frequency as the polymer concentration decreases and that extrapolated to zero concentration coincides with that of water. This indicates that the relaxation is due to reorientational motion of water, which is hindered by the polymer. The low-frequency relaxation is suggested to be due to the water molecules bound to polymer. The single relaxation observed in PEG is suggested to be due to orientational motions of water clusters. The possibility of existence of a low-frequency peak due to segmental motion is indicated in the PEG solution. It is indicated that if the segmental motion is faster than the bound water reorientation then only the peak due to segmental motion can be measured. This may cause the absence of the low-frequency bound water peak in PEG. The segmental motion of the PVP chain was extensively studied in a subsequent work.[205] The temperature variation of dielectric relaxation of aqueous PVME was also measured.[206] The above experimental results were analyzed by using the theory of Roland and Ngai.[339]

Table 6. Dielectric Relaxation Times for Water Associated with Polymers[a]

polymer	time constant and weight of relaxation
PEG[201]	32.36 ps (48.61)[b]
PVP[205]	56.23 ns (37.64)[c]
	24 ps (39.39)[c]
PVP[260]	25.26 ns (28.6 ± 0.5)[d]
	18.09 ps(50.0 ± 0.3)[d]
PVME[206]	2.51 ns (6.6)[c]
	35.48 ps (28.2)[c]
Na polyacrylate[208]	1.2 ± 0.2 μs (13.9 ± 0.5)[e]
	41 ± 2 ns (7.4 ± 1.1)[e]
	0.28 ± 0.05 ns (0.58 ± 0.02)[e]

[a] The relative weights of relaxation are given in parentheses in the second column. [b] 50.69% solution; temperature is 25 °C. [c] 50% solution; temperature is 25 °C. [d] 3 M solution; temperature is 25 °C. [e] pH is 7.12, and temperature is 24 °C.

Sato et al.[207] studied dielectric relaxation of aqueous oligo ethylene glycol 200 and 400 (degree of polymerization, $N = 4$ and 9) in the 300 MHz−20 GHz frequency range. A single relaxation process is observed and is found to be critically dependent on the concentration. It is concluded that the ether oxygen atoms are inserted into the water structure by replacing the water oxygen atom. The solvation of ethylene glycol does not perturb the water structure, and the hydration mechanism makes stable structures in solution.

Dielectric relaxation studies are carried out for polyelectrolyte solutions.[208,209] Attempts are made to characterize the conductive contribution to the high- and low-frequency relaxation processes. However, the role of hydration water in the relaxation process of polyelectrolyte solutions is yet to be investigated in detail.

Polymer hydrogels exhibit very slow dielectric relaxation (in the millisecond time scale). Dielectric

relaxation measurement in lecithin/isooctane/water gel shows a single low-frequency dispersion with high dielectric increment.[210] The entangled micelles form a cage in the hydrogel, and the water molecules within the micelle are dynamically frozen. The water molecules diffuse when the lecithin molecule reorients and breaks the hydrogen bonds. The gel becomes more swollen with an increase in temperature, and the width of the distribution of relaxation times tends to increase. This indicates that the faster diffusive motion of water within the micelle influences the slower lecithin dipole reorientation. Hill et al.[211,212] studied the large dielectric increment observed in the very low-frequency region ($10^{-3}-10^{4}$ Hz) of the dielectric spectra of heterogeneous gels. The relaxation is interpreted in terms of the electrode interface effect combined with slow micellar motions present in such systems.[211,212] The higher frequency dispersion was found to be dominated by aqueous dynamics. Partially hydrated silica gels are studied by time domain reflectometry, and two relaxation time constants of 1.5 ns and 50−100 ps are observed.[213] The former is ascribed to the rigidly bound water while the faster time constant is ascribed to the secondary hydration layer.[213]

G. Dielectric Properties of Liquid/Liquid Interface

In recent years there has been a growing interest in investigating the static dielectric properties of liquid/liquid interfaces by different experimental techniques as well as by simulation.[29,342−346] Visible attenuated total internal reflectance spectroscopy (ATR) has been employed to study the polarity of various oil water interfaces.[344] The effective interfacial dielectric constants for the *n*-alkane/water and the *n*-alkane/aqueous micelle (SDS, CTAB) interfaces are found to be as small as 8 whereas those for different micellar and water/oil microemulsions are found to be higher, e.g., the water/oil interface in AOT/hexane/water microemulsion has effective interfacial dielectric constant of 47.

Recently, Eisenthal et al.[345] employed second harmonic generation spectroscopy to estimate the polarity of various interfaces such as air/water, 1,2-dichloroethane/water, and chlorobenzene/water interfaces. They found that the polarity of the interface is equal to the *arithmetic average* of the polarity of the adjoining bulk phases. The authors suggested that this simple result points to the importance of the long-range nature of the solute solvent interaction at the interface rather than the local interaction at the interface (first shell solute solvent interaction). No first principle theory of this interesting problem is yet available.

Benjamin reviewed the structure, dynamics, and electrical properties of liquid/liquid interfaces as well as the solvation and reactions there.[29] He pointed out that a steep change in polarity can occur at the liquid/liquid interface where, within a narrow range, the polarity must change from that of one phase to the other. The orientation of the molecules at the interface also contributes to the modified polarity. In the absence of direct experimental or theoretical knowledge about the dielectric profile, at an interface usually two types of models are adopted. The first model assumes that the two bulk dielectrics are separated by a sharp interface where the dielectric function is discontinuous. The second model assumes that the interface region is a separate homogeneous phase with a dielectric constant that has some intermediate value between those of the two bulk liquids. It is also pointed out that the effective pair potential description, which is suitable to describe the individual bulk properties of the two immiscible liquids, may fail to describe their common interfacial properties and care must be taken to use these effective potentials in molecular dynamics simulations. The importance of the proper inclusion of the many body effects has also been emphasized by Benjamin.

Benjamin also carried out a molecular dynamics study of the solvent dynamical response to the charge-transfer reaction at the interface between a model diatomic polar and nonpolar solvents. The response of the solvent to the charge-transfer reaction at the interface is found to be slow as compared to that in the bulk.[342] The large structural change of the surface dipoles needed for the solvation of the newly created ion pair is suggested to be responsible for the observed interfacial effects on the solvent relaxation. This is clearly a feature not present in any of the pure bulk phases. Michael and Benjamin showed that the solvent dynamical response at the water/octanol interface was different as compared to those of the two bulk solvents.[343]

The main obstacle for developing a molecular theory for the interfaces is the difficulty of calculating the pair correlation function in an inhomogeneous medium. As an alternative, one can use continuum models where the detailed dielectric information is provided as an input. The molecular dynamics simulations of Benjamin of solvation in a liquid/vapor interface showed that static continuum models can predict qualitative features of the energetics of adsorption at such interfaces.[346] The choice of the distance-dependent dielectric function, $\epsilon_{int}(r)$, of the interfacial region is not easy. In the absence of any microscopic information about the distance dependence of the dielectric function, different smoothly varying functions can be used to mimic the gradual change of dielectric function from one phase to the other.[351] Recent simulation study indicates that the distance-dependent dielectric function of the solvent in the vicinity of a DNA molecule can be described by a sigmoidal function.[330] Such sigmoidal functions have been used earlier to represent the distance-dependent dielectric properties of proteins and helical peptides.[6,352,355]

V. Solvation Dynamics in Biomolecules and Organized Assemblies

In this section, we review how the photodynamics of solvents are affected near or inside biological macromolecules and organized assemblies and what information about the biomolecules and organized assemblies can be inferred from the solvation dy-

namics studies. It should be noted that, because of molecular diffusion, a probe molecule undergoes an excursion over a region of radius of a few nanometers within its excited state lifetime of several nanoseconds. Thus, a fluorescent probe actually reports the property of a microenvironment with a radius of a few nanometers.[340,341] For a homogeneous fluid, the slight uncertainty about the position of the fluorophore does not cause any serious problem. However, since an organized medium is a few nanometers in size, it is necessary to ensure that the fluorescent probe resides within the microenvironment under study. Fortunately, the position of the maximum, the intensity, and the temporal decay of the emission often change drastically on incorporation in a complex biomolecular system and, thus, exhibit an unmistakable signature that the probe is really confined in the organized medium.

Among all the solvents, the study of relaxation properties of water in organized media is of special importance because the water molecules present in the confined environments control the structure, dynamics, and reactivity of biological systems. The results of the dielectric relaxation experiments, discussed in section IV, suggest that the water molecules present in biological environments are substantially slower as compared to ordinary water. We show now that the solvation dynamics studies indicate similar trends and reveal many other finer details. As mentioned before, in many biologically relevant systems the probe molecule is located in an interface that separates two immiscible liquids of different polarity. Thus, solvation dynamics at the liquid/liquid interface is of considerable current interest. This is the subject of the first subsection. In the following subsections, we discuss the solvation dynamics in proteins, DNA, cyclodextrin, micelles, microemulsions, and other complex systems.

A. Solvation Dynamics at Water/Biomolecule Interfaces

Electron and proton transfer reactions in biological systems often involve solvation of charged species at an interface. The properties of water in the interfacial region are drastically modified due to local heterogeneity. Eisenthal et al.[347] studied excited-state solvation dynamics of coumarin 314 dye at the air/water interface using femtosecond time-resolved second harmonic generation (TRSHG) spectroscopy. The solvation time at the air/water interface has been found to be 790 $\pm$ 30 fs. The time scale is close to that observed for the later part of solvation in the bulk water solvation dynamics and may be due to the fact that at the air/water interface the solvation dynamics is solely due to the water and air does not participate in the solvation dynamics. It has been suggested that the progress of solvation at the liquid/liquid interface could exhibit more complex dynamics. Unlike bulk water, no ultrafast, intertial component was observed at the air/water interface, which may be due to the inadequate time resolution used in the experiment.

Eisenthal et al.[345] pointed out that for many liquid/liquid interfaces, the polarity of the interface is the arithmetic mean of the individual bulk liquids. It is not clear what effects such a rule may have on the dynamical processes at the interface. More experimental and theoretical studies are required to understand the issue fully.

B. Solvation Dynamics in Protein

One of the longstanding goals of biology is to unravel the dynamics in complex biomolecules such as proteins and DNA.[377−383] The dynamics is enormously complex for several reasons. The systems are often spatially inhomogeneous, and there are many correlated motions of the different species of the multicomponent system. As mentioned before, in a pure liquid the position of the probe is unimportant due to the isotropic nature of the solvent, which is not the case for proteins and their solutions. Note that in an aqueous protein solution the probe can be located in different regions, depending on the probe−chromophor interactions. It can remain at the protein/water interface, completely buried within the protein matrix, or in the bulk solvent away from any protein molecule. In each case, the probe is surrounded by an inhomogeneous dielectric environment.

Several groups reported that the solvation dynamics of protein bound fluorophores is significantly slower as compared to bulk water. Pierce and Boxer[379] and Bashkin et al.[380] reported that the solvation dynamics in the protein environments is nonexponential with a long component with a time constant of 10 ns. It is interesting to note that this time scale is very close to the nanosecond component of dielectric relaxation observed earlier for the aqueous protein solutions.[50,260,295,296] More recently, Joo et al.[381a] and Beck et al.[382,383] used two third-order spectroscopic methods, namely, the three-photon echo shift (3PEPS) measurement and transient-grating (TG) spectroscopy, to study the early events of solvation dynamics in proteins as well as in homogeneous solutions and polymer matrixes. The 3PEPS technique permits separation of the inertial solvation response from the typically faster part of the dynamic Stokes shift, which involves the displacement of the intra-chromophoric vibrational modes. The 3PEPS results indicate the presence of an inertial solvation component that arises from the protein−matrix surroundings of an embedded probe molecule.[381−383] The TG signal appears to be more sensitive to the slower dynamical response as compared to 3PEPS.[381−383] The time constants characterizing the photodynamics in various proteins are listed in Table 7. In addition, Fleming et al.[381b] have very recently reported a nonlinear spectroscopic study of solvation dynamics in aqueous protein solution (eosin in lysozyme). They observed an ultrafast component of the same type as observed in pure water. However, they also observed a very slow component with a decay time about 530 ps that contributed about 8.

A multishell continuum model[348,351] can be used to analyze the solvation dynamics when the probe is deeply buried within the protein core. It is assumed that the protein matrix consists of two concentric shells: a spherical protein core surrounded by the

Table 7. Time Constants Characterizing the Photodynamics in Protein Solutions[a]

system and probe	time constant and weight of relaxation
C-phycocyanin[382] (phycocyanobilin)	<100 fs (0.9)[b] >10 ps (0.1)[c]
C-phycocyanin[383] (phycocyanobilin)	17 ± 7.8 fs (6.7 ± 0.91)[d] 97 ± 27 fs (3.0 ± 0.44)[b] 5.5 ± 4.6 ps (2.8 ± 0.19)[c] (0.91 ± 0.18)[e]
allophycocyanin[383] (phycocyanobilin)	16 ± 4.8 fs (6.3 ± 0.95)[d] 56 ± 34 fs (1.7 ± 0.63)[f] 81 ± 32 fs (2.6 ± 0.33)[b] 220 ± 81 fs (2.4 ± 0.22)[f] >10 ps (0.70 ± 0.19)[c,e]

[a] The probe is indicated in parentheses in the first column. The relative weights of relaxations are given in parentheses in the second column. Note that these time constants have different dynamical origin in many cases, and we refer to the original literature for details. [b] Assigned to the inertial response of the protein matrix. [c] Assigned to the diffusive response of the protein matrix. [d] Assigned to intrachromophore vibrational modes. [e] Assigned to long-lived inhomogeneity. [f] Assigned to interexciton state radiationless decay.

surface region, which contains the side chains of the proteins. Each shell is characterized by a homogeneous dielectric function. Poisson's equation and the usual boundary conditions at each discrete shell boundary are employed to calculate the static reaction potential. The time scale of the relaxation of the protein residues can be obtained from the molecular dynamics simulations.[36,377] While the relaxation process of the core residues mostly involves the rigid body motions because they are highly constrained, the residues at the surface of protein matrix have more flexibility.[36,377] The dielectric behavior of the hydration shell of the protein is bimodal (section IV.A.1). The last shell is the solvent water that contains protein molecules whose dielectric behavior is given by the dielectric function of an aqueous protein solution (discussed in section IV.A). The results indicate that the solvation dynamics in the protein matrix is markedly slower than that in the bulk water and the decay of the solvation time correlation function is nonexponential in nature.[348] It is suggested that the slow component could arise because the probe within the matrix is sensitive to the slow, diffusive dynamics present within the protein core as well as the slow relaxation processes present in the hydration shell and the solvent region surrounding the protein.

When the probe is deeply buried within the protein matrix, then the solvation dynamics results provide information about the dynamics of the matrix. As mentioned before, different ultrafast techniques are applied to study the protein matrix solvation dynamics. Two relaxation processes are observed. The fast femtosecond component is ascribed to the inertial response of the protein matrix, whereas the slower picosecond component arises from the diffusive response from the matrix.[382−383] It may be recalled that the simulation studies of Warshel et al.[374] indicate femtosecond dynamics in the interior of the proteins. Bright and co-workers pointed out that the environment surrounding the probe is responsible for most of the time-dependent response observed in BSA.[384]

C. Solvation Dynamics in DNA

The static and dynamic properties of DNA have been studied by the temperature-dependent Stokes shift of an intercalated dye, acridine orange,[385] and by molecular dynamic simulation.[386] A large part of the Stokes shift of the intercalated dye in DNA is found to be frozen out at low temperature, as in the solution.[385] Thus, the interior of DNA is found to have the diffusive and viscous dynamic characteristics of a fluid rather than the purely vibrational characteristics of a crystal. The results suggest that the probe dye molecule senses the movement of DNA and at high viscosity, the DNA motion is limited by the solvent motion.[385]

D. Solvation Dynamics in Cyclodextrin

Vajda et al.[387] first studied solvation dynamics of two laser dyes, coumarin 480 (C480) and coumarin 460 (C460) in γ-cyclodextrin (γ-CD) cavity using time-dependent Stokes shift (TDSS). The marked blue shift of the emission spectra and the increase in fluorescence lifetimes of the two probes on addition of γ-CD to their aqueous solutions indicate that the probes are located inside the γ-CD cavity.[388,389] The initial component of solvation in γ-CD is found to be similar to that in bulk water.[387] However, at longer times the solvent response in γ-CD is at least 3 orders of magnitude slower compared to bulk water. In γ-CD, the slow relaxation reveals three components of 13, 109, and 1200 ps for C480. Molecular dynamics simulations indicate that in the γ-CD cavity there are 13 water molecules for C480/γ-CD complexes and 16 in the case of C460. These numbers resemble the number of water molecules present in the first solvent shell of the dye molecules in the aqueous solutions. If the first solvent shell dominates the response at short times, the response at short times for the C480/γ-CD complexes should have been different from that of the C460/γ-CD complex due to the presence of fewer water molecules for the former. However, since the initial Gaussian component is the same for the two dye molecules in γ-CD, it seems that it is incorrect to assume that the first solvent shell dominates the solvent response.[387]

The multishell continuum model (MSCM) discussed in the subsection V.B has been used to study solvation dynamics in cyclodextrin.[390] The geometry of the solvent region is represented by two concentric shells: an aqueous region enclosed by the cyclodextrin cavity and the bulk water. Nandi and Bagchi further presented a molecular theory of solvation dynamics in cyclodextrin based on molecular hydrodynamic theory (MHT).[390] In the MHT formulation, the major static and dynamic ingredients necessary to obtain the time-dependent polarization are usually described in the wavevector space ($\vec{k}$ space)[69,100] where the description of the heterogeneous γ-cyclodextrin/water system is difficult. However, this nontrivial problem can be avoided if the contributions of the different wavevector modes (small to intermediate to large) to the dynamics of ion solvation are explicitly analyzed. At small distances from the probe, which corresponds approximately to the in-

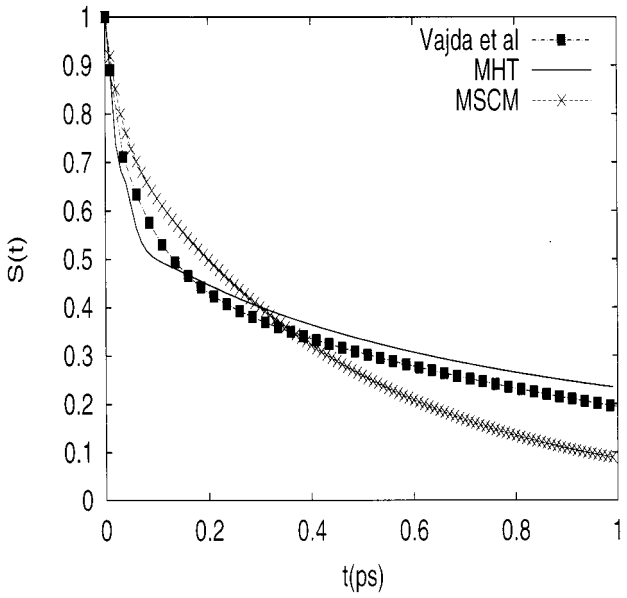

Figure 13. Solvation time correlation function for the solvation of coumarin 480 dye in the water enclosed within the cavity of γ-cyclodextrin cavity as obtained from the experiment of Vajda et al.[387] (indicated by the lines with solid squares). The theoretical results for the solvation of an ionic solute of the same size of coumarin 480 dye in the water enclosed within the cavity of γ-cyclodextrin as obtained from the MHT and MSCM are also shown in the same figure by solid line and line with *x*, respectively.

termediate wavevectors, the orientational relaxation is relatively slow, and so in that region only the translational contribution can be significant. Within the cyclodextrin cavity, the solvent molecules are likely to lose their translational degrees of freedom and can relax only by orientational motions. Thus, in this region, the translational modes have negligible contribution. On the other hand, for small wavevectors ($k \rightarrow 0$ limit), the orientational relaxation is fast, and thus the translational contribution is always unimportant. In summary, within the γ-cyclodextrin/water system, the translational contribution might be negligible for the whole heterogeneous system, and the polarization relaxation should be controlled only by the orientational mechanism. The solvation time correlation function calculated from both MSCM and MHT theory are in good agreement with the experimental result[387] as shown in Figure 13.

The agreement between the theory and the experiment at an ultrashort time scale is due to inclusion of the intermolecular vibrational mode in the dielectric scheme. The theory also suggests that the slower long time decay may partly be due to the freezing of the solvent translational modes. Comparison of the results of the MSCM and MHT calculations shows that the molecular approach give somewhat better agreement. MSCM does not reproduce the experimental results very well. This might be due to the absence of a good dielectric function at different solvent zones. On the other hand, there is a sharp break in the solvation time correlation function predcited by MHT that is absent in the experimental result. This could be a limitation of the frequency-dependent dielectric function used in MHT or a fundamental defect of the theoretical approach.

E. Solvation Dynamics in Reverse Micelle and Microemuslion

As noted in section III.F, the surfactant-coated water droplets in water-in-oil microemulsions provide an elegant model for water molecules in confined environments. For a microemulsion, the emission spectrum of the probe changes markedly when it is transferred from bulk hydrocarbon to the water pool. For example, the absorption maxima of coumarin 480 (C480) in *n*-heptane and water are at 360 and 395 nm, respectively while the emission maxima are at 410 and 490 nm, respectively.[391] On addition of AOT and subsequently water to a *n*-heptane solution of C-480, a very prominent shoulder appears at 480 nm.[392] The 480-nm band is assigned to the C480 molecules in the water pool of the microemulsion since the position and excitation peak (at 390 nm) of this band are very different from those of the C480 molecules in bulk *n*-heptane. The position of the 480-nm band indicates that the polarity of the water pool resembles that of alcohol.[392] Sarkar et al. studied the solvation dynamics of C480 in AOT/*n*-heptane/water microemulsions.[392] They observed a distinct rise time in the range of nanoseconds at the red end of the emission spectra. This indicates nanosecond solvation dynamics in the microemulsions. They observed that in a small water pool ($W_0 = 4$, $r_w = 8$ Å) the solvation time is 8 ns while for a very large water pool ($W_0 = 32$, $r_w = 64$ Å) the response is bimodal with a fast component of 1.7 ns and a slower component of 12 ns. Bright et al. studied the solvation dynamics of acrylodan-labeled human serum albumin in AOT microemulsion by phase fluorimetry.[393] They reported that the solvation time is about 8 ns for a small water pool ($W_0 = 2$) and 2 ns for a large water pool ($W_0 = 8$). For 4-aminophthalimide (4-AP), in a large water pool, the solvation dynamics is biexponential with an average solvation time of 1.9 ns.[394] In AOT microemulsions, the solvation time of 4-AP increases from 1.9 ns in H_2O to 2.3 ns in D_2O, which displays a 20% deuterium isotope effect. The appearance of a nearly 2-ns component in the large water pools indicates that even in the large water pools of the microemulsions the water molecules are about 6000 times slower as compared to bulk water.

A semiquantitative explanation of the 2-ns component may be as follows. The static polarity or the dielectric constant of the water pool of the AOT microemulsions can be obtained from the position of the emission maximum of the probes (C480 and 4-AP).[392−394] For both probes, the water pool resembles an alcohol-like environment with an effective dielectric constant of 30−40. If one makes a reasonable assumption that the infinite frequency dielectric constant of water in the water pool of the microemulsions is same as that of ordinary water, then using the experimentally determined dielectric relaxation time of the microemulsion of about 10 ns,[182,183] the solvent relaxation time should be about 1.67 ns, which is close to the observed solvation time in AOT microemulsions.

One might argue that the nanosecond dynamics observed in the water pool is not due to the slower water molecules but is because of the solvation by

the Na^+ counterions present in the water pool for the AOT microemulsions. Nanosecond solvation dynamics due to ions, in solutions as well as molten salts, is well documented in the literature.[395−397] Mandal et al.[398] studied the solvation dynamics of 4-AP in a microemulsion containing neutral surfactant Triton X-100 where no ions are present in the water pool. The Triton X-100 microemulsion also exhibits nanosecond solvation dynamics, which suggests that the ionic solvation dynamics has little or no role in the solvation dynamics observed in the water pool.

Levinger et al. studied the solvation dynamics of a charged dye coumarin 343 (C343) in lecithin and AOT microemulsions using femtosecond upconversion.[399−402] For lecthin microemulsions,[399] the solvent relaxation displays a very long component that does not become complete within 477 ps. This observation is similar to the nanosecond dynamics reported by Bright et al. and Sarkar et al. For C343 in AOT, Levinger et al. observed that the decay characteristics of the emission intensity at different wavelengths display considerable differences for sodium and ammonium counterions.[400] They however did not present a complete analysis of this result in terms of dynamic Stokes shift and the decay of the solvent response function $C(t)$. For Na-AOT, the solvation dynamics reported by Levinger et al.[401] for the charged probe C343 is faster than that reported by Bright et al. and Sarkar et al.[392] It is obvious that due to its inherent negative charge, AOT repels the negatively charged C343 probe from its vicinity. Thus, the C343 anion is expected to reside in the central region of the water pool. Neutral probes such as C480 and 4-AP may stay both in the central region of the pool as well as in the peripheral region close to the AOT molecules. The discrepancy in the results in the case of AOT microemulsions, reported by Levinger et al.[401] and those of Sarkar et al.[392] and Bright et al.,[393] however, is too large to be explained in terms of different locations of the probes and merits further careful investigation.

Marzola and Gratton[403] studied the solvation dynamics of different proteins such as lysozyme, human serum albumin, and liver alcohol dehydrogenase in the water pool of AOT in isooctane by exciting the tryptophanyl residues of the proteins using frequency domain fluorescence techniques. It is observed that the correlation time of the overall rotation and the internal motion of the proteins are different in the water pool as compared to those in the bulk water. It is found that when the water content of the pool is increased, the width and the center of the lifetime distribution increases, indicating a faster interconversion rate between the substrates. In all the cases, the relaxation is fitted to a multiple exponential decay with time constants in the nanosecond to subnanosecond time scale. The anisotropy decay indicates that the longer correlation time is related to the tumbling of the whole protein and that shorter correlation time corresponds to that of tryptophan residue with respect to the protein molecule. The rotational relaxation time of the proteins are found to become faster with an increase in the water content of the pool.

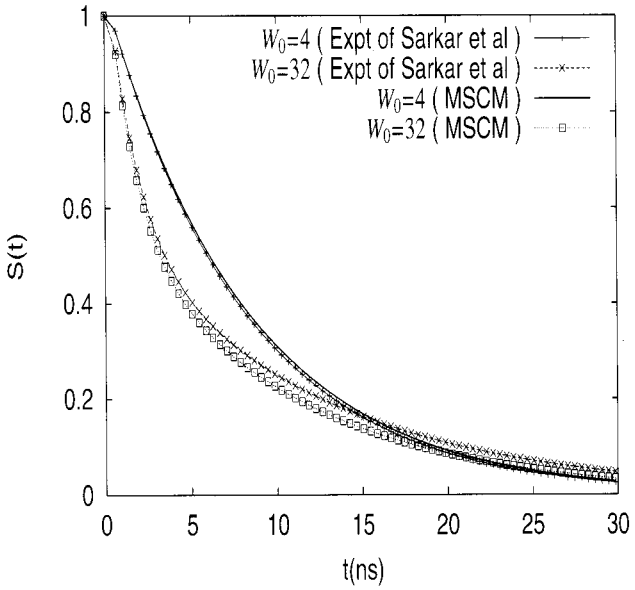

Figure 14. Solvation time correlation function for the solvation of coumarin 480 dye in the water pool of reverse micelle AOT/*n*-heptane at water contents $W_0 = 4$ and 32 as obtained from the experiment of Sarkar et al.[392] (indicated by the lines with + for $W_0 = 4$ and with *x* for $W_0 = 32$, respectively). The theoretical results for the solvation of an ionic solute of the same size of coumarin 480 dye in the water pool of AOT/*n*- heptane reverse micelle as obtained from the MSCM[404] are shown in the same figure for $W_0 = 4$ by the solid line and for $W_0 = 32$ by line with empty squares, respectively.

The MCM model has been used to study solvation dynamics in the water pool of the reverse micelle.[404] The solvation dynamics in both low water content and high water content of the pool are studied by the use of the appropriate frequency-dependent dielectric function of the water pool for each cases. At the low water content state, most of the water molecules are hydrogen bonded to the headgroups of the surfactant molecules and are rigidly bound. The corresponding relaxation time of the water molecules in the pool is expected to be slower. When the water content (W_0) is high, the water molecules in the central region of the pool are away from the headgroup region and exhibit faster dynamics as compared to the water molecules at the peripheral region of the pool. The theoretical results show that in the low water content state the solvation time correlation function should decay at a slower rate as compared to the bulk water. At high W_0, the decay of the solvation time correlation function is faster as compared to the low water content state but still slower as compared to the bulk water relaxation. The relatively faster dynamics in the high water content can be ascribed to the faster dynamics of the water molecules in the central region of the pool. These results are in reasonable agreement with the available experimental results as shown in Figure 14.[404] In the calculations reported in Figure 14, it has been assumed that, for the low water content case ($W_0 = 4$), dielectric relaxation consists of two Debye terms with time constants equal to the experimentally observed values of 10 ns and 10 ps, respectively. With the former carrying 90, this strength parameter is not fully available from experiments, and this should be considered only as

a fit parameter. However, given the low water content, this estimate seems reasonable. For the high water content case ($W_0 = 32$), the water is divided into two shells. The first shell starts from the center and extends to one layer from the surface. This layer contains the same dielectric relaxation properties as in bulk water. The second shell again has the two time constants with values of 5.5 ns and 10 ps, with the former carrying most of the strength. The time constant of the slow time has been used to obtain the best agreement with the experimental results.

Most recently, several groups studied solvation dynamics of nonaqueous solvents, such as formamide,[402] acetonitrile,[405] and methanol[405] in AOT microemulsions. Using a picosecond setup, Shirota and Horie[405] demonstrated that in the AOT microemulsions the solvation dynamics of acetonitrile and methanol are nonexponential and 1000 times slower as compared to those in the pure solvents. They attributed the nonexponential decay to the inherent inhomogeneous nature of the solvent pools. Evidently, the static polarity and relaxation properties of the entrapped polar solvents vary quite strongly as a function of the distance from the ionic headgroup of the AOT surfactants. As noted earlier within its nanosecond excited lifetime, the probe passes through different layers of solvents of different relaxation properties within the pool. This quite reasonably may give rise to a nonexponential decay.

F. Solvation Dynamics in Micelle

In the case of the micelles, there are three possible locations of the probe, namely, the bulk water, the dry micellar core, and the Stern layer. If the probe stays in the bulk water, obviously the solvation time will be in the subpicosecond time scale. Since the core of the micelle resembles aliphatic hydrocarbons, the probe is not expected to exhibit dynamic Stokes shift in the core. However, if the probe stays in the Stern layer, its solvation dynamics may be quite different from that in the bulk water because the mobility of the water molecules may be considerably constrained in the Stern layer. Solvation dynamics in micelles has been studied using C480 and 4-AP as probes.[406,407] Emission properties of the probes in the micelles are very different from those in water and in hydrocarbon.[406,407] This shows that the probes reside neither in bulk water nor in core of the micelles and, hence, are located in the Stern layer of the micelles. Sarkar et al.[406] and Datta et al.[407] studied solvation dynamics of C480 and 4-AP, respectively, in neutral (TX-100), cationic (CTAB), and anionic (SDS) micelles. It is observed that for SDS, CTAB, and TX-100 the average solvation times are respectively 180, 470, and 1450 ps for C480[406] and 80, 270, and 720 ps for 4-AP.[407] The solvation times in micelles differ only by a factor of 2 for the two probes. Thus, although the solvation times do depend on the probe (whose origin has not been analyzed in detail), this dependence seems to be weak. It is readily seen that the solvation dynamics in the Stern layer of the micelles is 3 orders of magnitude slower than that in bulk water, about 10 times faster than that in the water pool of the microemulsions,[406,407] and is slightly faster than the longest component of solvation dynamics in γ-CD.[387] The main candidates causing solvation in the Stern layer of the micelles are the polar or ionic headgroups of the surfactants, the counterions (for SDS and CTAB), and the water molecules. Since the headgroups are tethered to the long alkyl chains, their mobility is considerably restricted. The dynamics of such long alkyl chains occurs in the 100-ns time scale[188] and, hence, is too slow to account for the subnanosecond solvation dynamics observed in the micelles. The role of ionic solvation by the counterions also appears to be minor because of the very similar time scale of the ionic (CTAB) and the neutral (TX-100) micelles.

For both the probes, it is observed that the solvation times are in the order TX > CTAB > SDS. Qualitatively, the differences in the solvation times in the three micelles may be ascribed to the differences in their structures.[149] As mentioned earlier, the thickness of the hydrated shell for TX-100 (25 Å) is larger than that for SDS and CTAB (6−9 Å). Thus, for SDS and CTAB, the probe remains close or partially exposed to the bulk water while for TX it remains well shielded from bulk water and hence exhibits slower solvation dynamics. The SANS studies indicate that CTAB micelles are drier than SDS micelles.[149] Thus the faster solvation dynamics in SDS as compared to CTAB may be due to the more water-like environment in SDS. It is interesting to note that the time scale of solvation is similar to the intermediate range of dielectric relaxation times reported by Telgmann and Kaatze.[155]

G. Solvation Dynamics in Lipid Vesicle

The state of solvation of a fluorescent probe, in the ground state, in the unilamellar and multilamellar vesicles is usually studied by red edge excitation spectroscopy (REES).[195] The idea behind REES is that in such an inhomogeneous medium the probe molecules in different regions remain in different states of solvation and, as a result, exhibit different absorption and emission characteristics. This is reflected in the gradual shift in the emission maximum as the wavelength of excitation is varied. The REES gives information on the state of solvation in the ground state of the molecules and gives no dynamic information on the relaxation properties inside the vesicles. The dynamics of the surfactant chain in the lipid bilayer is investigated using ESR.[195] However, the interesting issue of the dynamics of the water molecules inside the water pool of vesicles has been addressed only recently.[408] Datta et al. studied C480 in sonicated unilamellar DMPC vesicles.[408] The position of the emission maximum of C480 in DMPC vesicles is once again different from that in bulk water and in hydrocarbon. This indicates the probe stays in the inner water pool of the vesicle. Datta et al. observed that the solvation dynamics of C480 in DMPC vesicles is highly nonexponential with two components of 0.6 (40%) and 11 ns (60%).[408] This result is very similar to the solvation dynamics of the same probe in the large water pools of AOT microemulsions.[392,393] The nanosecond solvation dynamics in lipids cannot be due to the chain dynamics of

Table 8. Relaxation Times in Reverse Micelles and Vesicles Obtained from Time-Resolved Emission Spectroscopy[a]

system and probe	time constant and weight of relaxation
AOT ($W_0 = 4$)[392] (C-480)	8.0 ns (1.0)
AOT ($W_0 = 32$)[392] (C-480)	1.7 ns (0.5) 12.0 ns (0.5)
DMPC[408] (C-480)	600 ps (0.4) 11000 ps (0.6)

[a] The probe dye used is given in parentheses in the first column. The relative weights of relaxations are given in parentheses in the second column.

DMPC, which occurs in the 1000ns time scale.[188] Since in the bulk water the solvation dynamics is faster, the results reported by Datta et al.[408] demonstrate restricted motion of the water molecules in the inner water pool of the vesicles. The time constants of relaxation in reverse micelles and vesicles are given in Table 8.

H. Solvation Dynamics in Polymer and Hydrogel

The bulk viscosity of most polymers and particularly the semi-rigid hydrogels are very high. Thus, at first sight one expects very slow relaxation of the water molecules in polymer matrixes and polymer hydrogels. Contrary to this expectation, in the orthosilicate[409] and polyacrylamide[410] hydrogels, both solvation dynamics and rotational relaxation are found to occur in <50-ps time scale. The surprisingly fast solvation and rotational dynamics of small probe molecules in hydrogels may be attributed to the porous structure of the hydrogels, through which even large biomolecules pass through easily. Datta et al.[410] demonstrated that the microenvironment of 4-AP in polyacrylamide (PAA) hydrogel is quite heterogeneous. In the PAA hydrogel there are broadly two kinds of environments. One of them is water-like in which the 4-AP molecules exhibit an emission maximum at 550 nm with a lifetime of 1.3 ns and the other is quite aprotic in which 4-AP emits at 470 nm with a 7.2-ns lifetime. The recent steady-state anisotropy measurements by Claudia-Marchi et al.[411] for titania gels at the sol−gel transition point when the bulk viscosity increases abruptly shows that the emission anisotropy does not change perceptibly. Thus the microviscosity of the gel is very low despite the very high bulk viscosity. The NMR[412] and simulation[413] studies indicate that the diffusion coefficient of water molecules in polymer hydrogels is not appreciably slower as compared to ordinary water and is smaller at most by a factor of 2 than that in ordinary water. Argaman and Huppert[414] studied solvation dynamics of coumarin 153 in polyethers and found very fast solvation times ranging from 50 fs to 100 ps. The fast solvation dynamics in polymer matrixes is consistent with the dielectric relaxation studies,[200,201] which shows that except for the highly water-soluble polymer, polyvinyl pyrolidone, the dielectric relaxation times of most aqueous polymer solutions are faster than the 100-ps time scale. In Table 2, we have summarized the solvation dynamics of water in different environments. Examples of experimentally obtained time constants of relaxation in polymers and hydrogels are given in Table 9.

Table 9. Relaxation Times in Hydrogels Obtained from Time-Resolved Emission Spectroscopy[a]

system and probe	time constant and weight of relaxation
polyacrylamide gel[410] (4-AP)	<50 ps

[a] The probe dye used is given in parentheses in the first column. For details, we refer to the original literature.

I. Solvation Dynamics in Liquid Crystal

It is observed that, in the nematic phase of a liquid crystal, solvation dynamics of coumarin 503 is biexponential.[415] The slowest time constant decreases from 1670 ps at 311.5 K to 230 ps at 373 K. The solvation time is not affected by the nematic−isotropic phase transition. Thus, it appears that the local environment and not the long range order controls the time-dependent Stokes shift. A theoretical model[415] has been developed to explain the experimental findings. This model takes into account the reorientation of the probe as well as the fluctuation of the local solvent polarization. Similar results are also obtained for rhodamine 700 in the isotropic phase of octylcyanobiphenyl.[416]

J. Solvation Dynamics in Zeolite and Nanoparticle

The solvation dynamics in microporous solids has been the subject of several recent studies. Sarkar et al.[417] showed that C480 exhibits wavelength-dependent decays and time-dependent Stokes shift in a solid host, faujasite zeolite 13X. They observed a highly nonexponential decay with an average solvation time of 8 ns. Interestingly the 8-ns time constant is very close to the nanosecond solvation dynamics (4.1 ns) observed in molten salts.[395] In a faujasite zeolite there are two mobile components: the sodium ions and the probe dye molecule itself. Since in a faujasite zeolite the encapsulated guest molecules hop from one cage to another in the nanosecond time scale,[240] the 8-ns relaxation time observed in zeolite may also arise as result of the self-motion of the probe from one cage to another. The role of self-motion of solutes on the solvation dynamics has been discussed recently.[418] However, it is difficult to establish unequivocally whether the nanosecond dynamics observed in zeolite is due to ionic solvation or self-motion of the probe.

Pant and Levinger[419] studied solvation dynamics of C343 in a suspension of nanodimensional zirconia particles of radius 2 nm in a water−acetone mixture (95:5, v/v). They observed two subpicosecond components similar to those in bulk but with different amplitudes resulting in a relaxation time faster than that in bulk solution. They also showed that the maximum Stokes shift is 3 times smaller for the dye molecules adsorbed on the zirconia particles as compared to those in bulk solution.

VI. Concluding Remarks and Future Problems

The present review attempts to survey the current status of the theoretical, experimental, and simula-

tion studies on the dynamics of the water molecules in complex chemical and biological systems. These complex systems include biomolecules such as proteins, amino acids, and peptides as well as organized molecular assemblies such as host−guest complexes involving cyclodextrin, assemblies of different amphiphiles, etc. The experimental results demonstrate that the dynamics of water present either in the vicinity or entrapped within the structure of these complex systems is significantly different from bulk water. The dielectric spectra or the decay of solvent relaxation function of the solution are often drastically different from those of the bulk solvent and often dramatically slower by 3−4 orders of magnitude. According to the recent molecular theories and simulations, the observed differences from the bulk behavior arise from the correlation present among the different species in these systems and their inherent heterogeneous nature. The presence of an extended correlation in the system emphasizes the complementary biological role of the water and the biomolecules. While a microscopic understanding of biomolecular dynamics in the solution state has begun to emerge, there are a large number of issues that remain to be addressed and unravelled soon. A few of these issues are as follows:

Both bulk water and proteins individually involve complicated energy landscape.[7,420−424] It will be important to construct and understand the global potential energy surface of a solvated biomolecule. This will reveal the nature of the reaction coordinates and energy barriers for the solvated systems and provide very useful information about the reactions taking place in the biological system. The relation between glass transition behavior in proteins and their hydration is a subject of vigorous recent interest.[117] Several recent works discussed the fragile nature of bulk water.[423,424] It will be interesting to find out how the structure and dynamics of the glassy state of protein is influenced by the fragility of surrounding solvent molecules and its biophysical significance.

Simulation studies on the dielectric relaxation and solvation dynamics in pure liquids provided very valuable information that complemented the theoretical and experimental studies. Similar studies on solvated biomolecular systems that include full solvent contribution are yet to be carried out. With the increasing availability of supercomputers, it is hoped that very large scale simulations will be carried out soon. Recent molecular dynamics simulation of the dielectric spectra of solvated peptides showed the important role of cross correlations of different species in the system, which is complementary to the theoretical studies.[296,308] Such information is often unavailable from experiments. More such simulation studies are necessary to improve our understanding of the water/biomolecule interactions.

Relaxation processes at slow and fast time scales are involved in many fundamental chemical and biological processes.[425] Photophysical methods have been used to probe these diverse time scales.[426,427] Because of the heterogeneity of the biomolecular solution, the observed time-dependent response should depend on the position of the probe. This can provide information about the local dynamics of the system that is often unavailable from other methods. Recently axially-dependent laser fields have been used to excite individual fluorescent molecules and individual labeled proteins to image a single molecule in three dimensions.[220,221] Such studies have the advantage of studying spatially resolved dynamics of local environments of different parts of the biomolecular system unobscured by the dynamics of the other molecules present in the ensemble.[220,221] Single molecule dynamics can now be studied in a local environment with a wide time resolution[222] using fluorescence spectroscopy. Very recently population dynamics of green fluorescent protein is studied using chirped pulses.[428] The observed fluorescence is found to be different for positively and negatively chirped pulses. The rate of photobleaching as a function of chirp indicates that the bleaching of the protein is a thermal process rather than excited-state photoreaction. This study demonstrates the possibility of quantum control of the biological processes.

Valuable information at the molecular level about blood and its constituents can be obtained from dielectric studies.[429,430] Dielectric studies on tissues and cells provide important information regarding the development of cancers and other types of tumors.[52] Time domain dielectric spectroscopic studies on the hydration of isomers of vitamin C show that hydration could possibly influence the biological activity of vitamin.[431] The studies on the concentration dependence of dielectric relaxation spectra may help to elucidate the forces responsible for protein association. The latter process competes with protein folding and is responsible for many diseases such as prion disease, cataracts, etc.[432] Thus, dielectric studies have promising future biomedical implications.

Many biological processes involve electron-transfer process. The study of the dielectric properties of protein solutions is helpful in understanding the electron-transfer reactions in protein solutions.[433] The simulation studies discussed in this review have revealed how the dielectric properties of the proteins control protein dynamics and enzyme action.[6a,365,375] Electron paramagnetic resonance and simulation studies on the dynamics of α-chymotrypsin in solvents with dielectric constants ranging from 72 to 1.9 suggest that solvent dielectric properties have profound influence on protein dynamics and play an important role in modified stereoselectivities of enzymes in nearly dry organic solvents.[434] More studies are required in this direction for a better understanding of the effect of dielectric environment on the enzyme action. Recent molecular dynamics simulation of ion solvation and transport through the model peptide ionophore, gramicidin A, shows that dynamic properties of the water molecules in the channel differ markedly from those in bulk.[435] Strongly correlated motions are observed over a long distance and are suggested to cause the allosteric effect of enzymes.[435] It is proposed that water acts as a molecular chaperon, accompanying the reactants in their search for each other in all biological associations.[436] In summary, water drives many molecular processes

in nature, and future studies are expected to unveil further the fascinating role of water in complex biological systems.

VII. Acknowledgments

We thank Prof. G. R. Fleming and Prof. I. Ohmine for helpful discussions and for their interest in this work. We thank Mr. Rajesh Murarka for a critical reading of the manuscript. We deeply appreciate the critical comments of two reviewers that have led to extensive revision of an earlier version of the manuscript. A part of this work was done when B.B. was visiting the Department of Chemistry, University of Wisconsin, and he thanks the faculty of UW for the hospitality. We thankfully acknowledge the partial support by the Japan Society for the Promotion of Science and the Department of Science and Technology, Government of India, and Council of Scientific and Industrial Research.

VIII. References

(1) Kuntz, I. D., Jr.; Kauzmann, W. *Adv. Protein Chem.* **1974**, *28*, 239.
(2) Gregory, R. B., Ed. *Protein Solvent Interactions*; Marcel Dekker: New York, 1995.
(3) Rupley, J. A.; Careri, G. *Adv. Protein Chem.* **1991**, *41*, 37.
(4) Pethig, R. *Annu. Rev. Phys. Chem.* **1992**, *43*, 177.
(5) Robinson, G. W., Zhu, S.-B., Singh, S., Evans, M. W., Eds. *Water in Biology, Chemistry and Physics*; World Scientific: Singapore, 1996; Chapter 7.
(6) (a) Warshel, A. *Computer Modelling of Chemical Reactions in Enzymes and in Solution*; Wiley: New York, 1991. (b) Aqvist, A.; Warshel, A. *Chem. Rev.* **1993**, *93*, 2423.
(7) Ohmine, I.; Tanaka, H. *Chem. Rev.* **1993**, *93*, 2545.
(8) Cheng, Y.-K.; Rossky, P. J. *Nature* **1998**, *392*, 696.
(9) Teeter, M. M. *Annu. Rev. Biophys. Chem.* **1991**, *20*, 577.
(10) Wang, J. H.; Anfinsen, C. B.; Polestra, F. M. *J. Am. Chem. Soc.* **1954**, *76*, 4763.
(11) Wang, J. H. *J. Am. Chem. Soc.* **1954**, *76*, 4755.
(12) Makarov, V. A.; Feig, M.; Andrews, B. K.; Pettitt, B. M. *Biophys. J.* **1998**, *75*, 150.
(13) Bryant, R. G. *Annu. Rev. Phys. Chem.* **1978**, *29*, 167.
(14) (a) Breslow, R. *Chem. Rev.* **1998**, *98*, 1997. (b) Breslow, R. *Acc. Chem. Res.* **1991**, *24*, 159.
(15) Lum, K.; Chandler, D.; Weeks, J. D. *J. Phys. Chem. B* **1999**, *103*, 4570.
(16) Blokzijl, W.; Engberts, J. B. F. N. *Angew. Chem., Int. Ed. Engl.* **1993**, *32*, 1545.
(17) Pindur, U.; Lutz, G.; Oho, C. *Chem. Rev.* **1993**, *93*, 741.
(18) Cramer, C. J.; Truhler, D. G. *Science* **1992**, *256*, 213.
(19) Ramamurthy, V., Ed. *Photochemistry in Organized and Constrained media*; VCH: New York, 1991.
(20) D'Souza, V. T., Lipkowitz, K. B., Eds. Special issue on Cyclodextrins. *Chem. Rev.* **1998**, *98*, 1741−2076.
(21) Bortulos, P.; Monti, S. *Adv. Photochem.* **1995**, *21*, 1.
(22) Konnors, K. A. *Chem. Rev.* **1997**, *97*, 1325.
(23) Wenz, G. *Angew. Chem., Int. Ed. Engl.* **1994**, *33*, 741.
(24) Warner, I. M. *Anal. Chem.* **1998**, *70*, 477.
(25) Eisenthal, K. B. *Chem. Rev.* **1996**, *96*, 1343.
(26) Zhu, S.-B.; Singh, S.; Robinson, G. W. *Adv. Chem. Phys.* **1994**, *85*, 627.
(27) Bittner, E. R.; Rossky, P. J. *J. Chem. Phys.* **1995**, *103*, 8130.
(28) Benjamin, I. *Acc. Chem. Res.* **1995**, *28*, 233.
(29) Benjamin, I. *Annu. Rev. Phys. Chem.* **1997**, *48*, 407.
(30) Sokhan, V. P.; Tildesky, P. J. *Mol. Phys.* **1997**, *92*, 625.
(31) Barron, L. D.; Hecht, L.; Wilson, G. *Biochemistry* **1997**, *36*, 13143.
(32) Sundaralingham, M.; Sekharudu, Y. C. *Science* **1989**, *244*, 1333.
(33) Jeffrey, G. A.; Saenger, W. *Hydrogen bonding in biological systems*; Springer-Verlag: Berlin, 1991.
(34) Tirado-Rives, J.; Jorgensen, W. L. *Biochemistry* **1991**, *30*, 3864.
(35) Tobias, D. J.; Brooks, C. L., III. *Biochemistry* **1991**, *30*, 6059.
(36) Brooks, C. L.; Karplus, M.; Pettitt, B. M. *Proteins, A theoretical perspective of dynamics, structure and thermodynamics*; Wiley: New York, 1988.
(37) Karplus, M.; Petsko, G. A. *Nature* **1990**, *347*, 631.
(38) Israelachvili, J.; Wennerstrom, H. *Nature* **1996**, *379*, 219.
(39) Phillips G. N., Jr.; Pettitt, B. M. *Protein Sci.* **1995**, *4*, 149.
(40) Denisov, V. P.; Halle, B. *Faraday Discuss.* **1996**, *103*, 227.
(41) Wuthrich, K.; Billeter, M.; Guntert, P.; Lunginbuhl, P.; Riek, R.; Wider, G. *Faraday Discuss.* **1996**, *103*, 245.
(42) Bellissent-Funel, M.-C.; Zanotti, J.-M.; Chen, S. H. *Faraday Discuss.* **1996**, *103*, 281.
(43) Denisov, V.; Halle, B.; Peters, J.; Horlein, H. D. *Biochemistry* **1995**, *34*, 9046.
(44) Kashpur, V. A.; Maleev, V.; Shchegoleva, T. *Mol. Biol.* (*Moscow*) **1976**, *10*, 568.
(45) Fischer, S.; Verma, C. S.; Hubbard, R. E. *J. Phys. Chem. B* **1998**, *102*, 1797.
(46) Hummer, G.; Garde, S.; Garcia, A. E.; Pohorille, A.; Pratt, L. R. *Proc. Natl. Acad. Sci. U.S.A.* **1996**, *93*, 8951.
(47) Richards, F. M. *Annu. Rev. Biophys. Bioeng.* **1977**, *6*, 151.
(48) Gerstein, M.; Chothia, C. *Proc. Natl. Acad. Sci. U.S.A.* **1996**, *93*, 10167.
(49) Pethig, R. Chapter 4 in ref 2.
(50) Oncley, J. L. *Proteins, Amino Acids and Peptides*; John, E. J., Edsall, J. T., Eds.; Reinhold: New York, 1943' Chapter 22, p 543.
(51) Oncley, J. L. *Chem. Rev.* **1942**, *30*, 433.
(52) Pethig, R.; Kell, D. B. *Phys. Med. Biol.* **1987**, *32*, 933.
(53) Pethig, R. *Dielectric and electronic properties of biological materials*; Wiley: Chichester, 1979.
(54) Grant, E. H.; Sheppard, R. J.; South, G. P. *Dielectric behavior of biological molecules in solution*; Clarendon: Oxford, 1978.
(55) Hasted, J. B. *Aqueous Dielectrics*; Chapman and Hall: London, 1973.
(56) Hasted, J. B. In *Water: A Comprehensive Treatise*; Franks, F., Ed.; Plenum: New York, 1982; Vol. 1, Chapter 7.
(57) Kirkwood, J. G. *J. Chem. Phys.* **1939**, *7*, 911.
(58) Debye, P. *Polar Molecules*; Dover: New York, 1945.
(59) Hill, N. E.; Vaughan, W. E.; Price, A. H.; Davies, M. *Dielectric properties and molecular behavior*; Von Nostrand: New York, 1970.
(60) Frohlich, H. *Theory of Dielectrics*; Oxford: London, 1950.
(61) Böttcher, C. J. F. *Theory of electric polarization*; Elsevier: Amsterdam, 1973.
(62) McConnell, J. *Rotational Brownian Motion and Dielectric Theory*; Academic: London, 1980.
(63) Barthel, J.; Buchner, R. *Pure. Appl. Chem.* **1991**, *63*, 1473.
(64) Kindt, J. T.; Schmuttenmaer, C. A. *J. Phys. Chem.* **1996**, *100*, 10373.
(65) Bertolini, D.; Tani, A. *Mol. Phys.* **1992**, *75*, 1047.
(66) Guillot, B. *J. Chem. Phys.* **1991**, *95*, 1543.
(67) Neuman, M. *J. Chem. Phys.* **1985**, *82*, 5663.
(68) Neuman, M. *J. Chem. Phys.* **1988**, *85*, 1567.
(69) Bagchi, B.; Chandra, A. *Adv. Chem. Phys.* **1991**, *80*, 1.
(70) Pollack, E. L.; Alder, B. J. *Annu. Rev. Phys. Chem.* **1981**, *32*, 311.
(71) Williams, G. *Chem. Rev.* **1972**, *72*, 55.
(72) Zwanzig, R. *Annu. Rev. Phys. Chem.* **1965**, *16*, 67.
(73) Titulaer, U. M.; Deutch, J. M. *J. Chem. Phys.* **1974**, *60*, 1502.
(74) Franks, F., Ed. *Water: A Comprehensive Treatise*; Plenum: New York, 1982; Vol. 4.
(75) Hasted, J. B.; Hussain, S. K.; Frescura, F. A. M.; Birch, J. R. *Infrared Phys.* **1987**, *27*, 11.
(76) Afsar, M. N.; Hasted, J. B. *Infrared Phys.* **1978**, *18*, 835.
(77) Hale, G. M.; Querry, M. R. *Appl. Opt.* **1973**, *12*, 555.
(78) Bertie, J. E.; Ahmed, K. M.; Eysel, H. H. *J. Phys. Chem.* **1989**, *93*, 2210.
(79) Nandi, N.; Roy, S.; Bagchi, B. *J. Chem. Phys.* **1995**, *102*, 1390.
(80) Nandi, N.; Bagchi, B. *J. Phys. Chem.* (submitted for publication).
(81) Maroncelli, M. *J. Mol. Liq.* **1993**, *57*, 1.
(82) Maroncelli, M.; Fleming, G. R. *J. Chem. Phys.* **1988**, *89*, 5044.
(83) Jimenez, R.; Fleming, G. R.; Kumar, P. V.; Maroncelii, M. *Nature* **1994**, *369*, 471.
(84) Lang, M. J.; Jordanides, X. J.; Song, X.; Fleming, G. R. *J. Chem. Phys.* **1999**, *110*, 5884.
(85) Hsu, C. P.; Song, X.; Marcus, R. A. *J. Phys. Chem. B* **1997**, *101*, 2546.
(86) Warshel, A.; Hwang, J.-K. *J. Chem. Phys.* **1986**, *84*, 4938.
(87) (a) Silva, C.; Walhout, P. K.; Yokoyama, K.; Barbara, P. *Phys. Rev. Lett.* **1998**, *80*, 1086. (b) Alfano, J. C.; Walhout, P. K.; Kimura, Y.; Barbara, P. F. *J. Chem. Phys.* **1993**, *98*, 5996. (c) Kummrow, A.; Emde, M. F.; Baltuska, A.; Pshenichnikov, M. S.; Wiersma, D. A. *J. Phys. Chem. A* **1998**, *102*, 4172. (d) Bratos, S.; Leickman, J.-Cl. *Chem. Phys. Lett.* **1998**, *261*, 117.
(88) Kimura, Y.; Alfano, J. C.; Walhout, P. K.; Barbara, P. F. *J. Phys. Chem.* **1994**, *98*, 3450.
(89) (a) Jarzeba, W.; Walker, G. C.; Johnson, A. E.; Kahlow, M. A.; Barbara, P. F. *J. Phys. Chem.* **1988**, *92*, 7039. (b) Barbara, P. F.; Jarzeba, W. *Adv. Photochem.* **1990**, *15*, 1.
(90) Zolotov, B.; Gan, A.; Fainberg, B. D.; Huppert, D. *Chem. Phys. Lett.* **1997**, *265*, 418.
(91) Schwatrz, B.; Rossky, P. J. *J. Chem. Phys.* **1994**, *101*, 6902.
(92) Schwatrz, B.; Rossky, P. J. *J. Chem. Phys.* **1994**, *101*, 6917.
(93) Schwatrz, B.; Rossky, P. J. *Phys. Rev. Lett.* **1991**, *72*, 3283.
(94) Barnett, R. B.; Landman, U.; Nitzan, A. *J. Chem. Phys.* **1989**, *90*, 4413.

(95) Neria, E.; Nitzan, A.; Barnett, R. B.; Landman, U. *Phys. Rev. Lett.* **1991**, *67*, 1011.
(96) Neria, E.; Nitzan, A. *J. Chem. Phys.* **1989**, *90*, 4413.
(97) Staib, A.; Borgis, D. *J. Chem. Phys.* **1995**, *103*, 2642.
(98) Muino, P. L.; Callis, P. R. *J. Chem. Phys.* **1994**, *100*, 4093.
(99) Roy, S.; Bagchi, B. *J. Chem. Phys.* **1993**, *99*, 9938.
(100) Bagchi, B. *Annu. Rev. Phys. Chem.* **1989**, *40*, 115.
(101) Roy, S.; Komath, S.; Bagchi, B. *J. Chem. Phys.* **1993**, *99*, 3139.
(102) Roy, S.; Bagchi, B. *J. Chem. Phys.* **1993**, *99*, 1310.
(103) Komath, S.; Bagchi, B. *J. Chem. Phys.* **1993**, *98*, 8987.
(104) Biswas, R.; Bagchi, B. *J. Phys. Chem.* **1996**, *100*, 1238.
(105) Biswas, R.; Nandi, N.; Bagchi, B. *J. Phys. Chem. B* **1997**, *101*, 2968.
(106) Resat, H.; Raineri, F. O.; Perng, B. W.; Friedman, H. L. *Hydrogen Bond Networks*; NATO ASI Series 435; Bellissent Funel, M. C., Dore, J. C., Eds.; Kluwer Academic: Boston, 1994.
(107) Resat, H.; Raineri, F. O.; Friedman, H. L. *J. Chem. Phys.* **1992**, *97*, 2618.
(108) Raineri, F. O.; Resat, H.; Friedman, H. L. *J. Chem. Phys.* **1992**, *96*, 3068.
(109) Stryer, L. *Biochemistry*, 4th ed.; W. H. Freeman: New York, 1998.
(110) Jeffrey, G. A.; Saenger, W. *Hydrogen bonding in biological systems*; Springer-Verlag: Berlin, 1991; Chapter 14.
(111) Jeffrey, G. A.; Maluszynska, H. *Int. J. Biol. Macromol.* **1982**, *4*, 173.
(112) Edsall, J. T. In *Proteins, Amino acids and Peptides*; John, E. J., Edsall, J. T., Eds.; Reinhold: New York, 1943; Chapter 6.
(113) (a) Pertsemlidis, A.; Saxena, A. M.; Soper, A. K.; Head-Gordon, T.; Glaeser, R. M. *Proc. Natl. Acad. Sci. U.S.A.* **1996**, *93*, 10769. (b) Pertsemlidis, A.; Soper, A. K.; Sorensen, J. M.; Head-Gordon, T. *Proc. Natl. Acad. Sci. U.S.A.* **1999**, *96*, 481.
(114) Kinoshita, M.; Okamoto, Y.; Hirata, F. *J. Chem. Phys.* **1997**, *107*, 1586.
(115) Olatunji, O. L.; Premilat, S. *Biochem. Biophys. Res. Commun.* **1985**, *126*, 247.
(116) Eagland, D. In *Water: A Comprehensive Treatise*; Franks, F., Ed.; Plenum: New York, 1982; Vol. 4, Chapter 4.
(117) Gregory, R. B., Ed. *Protein Solvent Interactions*; Marcel Dekker: New York, 1995; Chapter 3.
(118) Jeffrey, G. A.; Saenger, W. *Hydrogen bonding in biological systems*; Springer-Verlag: Berlin, 1991; Chapter 23.
(119) Baker, E. W. In *Hydrogen bonding in biological systems*; Jeffrey, G. A.; Saenger, W., Eds.; Springer-Verlag: Berlin, 1991; Chapter 2.
(120) Goldaskii, V. I.; Krupyanskii, Y. F. In *Protein Solvent Interactions*; Gregory, R. B., Ed.; Marcel Dekker: New York, 1995; Chapter 5.
(121) Gu, W.; Schoenborn, B. P. *Proteins* **1995**, *22*, 20.
(122) Abseher, R.; Schreiber, H.; Steinhauser, O. *Proteins* **1996**, *25*, 366.
(123) Lounnas, V.; Pettitt, B. M.; Phillips, G. N., Jr. *Biophys. J.* **1994**, *66*, 601.
(124) (a) Lounnas, V.; Pettitt, B. M. *Proteins* **1994**, *18*, 148. (b) Lounnas, V.; Pettitt, B. M. *Proteins* **1994**, *18*, 133.
(125) York, D. M.; Darden, T. A.; Pedersen, L. G.; Anderson, M. W. *Biochemistry* **1993**, *32*, 1443.
(126) Brooks, C. L., III; Karplus, M. *J. Mol. Biol.* **1989**, *208*, 159.
(127) *Biophysics of water*; Franks, F., Mathias, S., Eds.; Wiley: Chichester, 1982.
(128) Kovacs, H.; Mark, A. E.; van Gunsteren, W. F. *Proteins* **1997**, *27*, 395.
(129) Fox, T.; Kollman, P. A. *Proteins* **1996**, *25*, 315.
(130) Fraternali, F.; Van Gunsteren, W. F. *J. Mol. Biol.* **1996**, *256*, 939.
(131) Banks, J.; Brower, R. C.; Ma, J. *Biopolymers* **1995**, *35*, 331.
(132) Kumosinski, T. F.; King, G.; Farrell, H. M., Jr. *J. Protein Chem.* **1994**, *13*, 701.
(133) Kitchen, D. B.; Reed, L. H.; Levy, R. M. *Biochemistry* **1992**, *31*, 10083.
(134) Williams, R. L.; Vila, J.; Perrot, G.; Scheraga, H. A. *Proteins* **1992**, *14*, 110.
(135) Schiffer, C. A.; Caldwell, J. W.; Stroud, R. M.; Kollman, P. A. *Protein Sci.* **1992**, *1*, 396.
(136) (a) Gerstein, M.; Chothia, C. *Proc. Natl. Acad. Sci. U.S.A.* **1999**, *93*, 10167. (b) Yu, B.; et al. *Proc. Natl. Acad. Sci.* **1999**, *96*, 103.
(137) Svergun, D. I.; Richard, S.; Koch, M. H. J.; Sayers, Z.; Kuprin, S.; Zaccai, G. *Proc. Natl. Acad. Sci. U.S.A.* **1998**, *95*, 2267.
(138) Baker, E. N.; Hubbard, R. E. *Prog. Biophys. Mol. Biol.* **1984**, *44*, 97.
(139) Thanki, N.; Thornton, J. M.; Goodfellow, J. M. *J. Mol. Biol.* **1988**, *202*, 637.
(140) Cheng, Y. K.; Pettitt, B. M. *Prog. Biophys. Mol. Biol.* **1992**, *58*, 225.
(141) Jeffrey, G. A.; Saenger, W. *Hydrogen bonding in biological systems*; Springer-Verlag: Berlin, 1991; Chapter 24.
(142) (a) Perahia, D.; Jhon, M. S.; Pullman, B. *Biochim. Biophys. Acta* **1977**, *474*, 349. (b) Sokolov, A. P.; Grimm, H.; Kahm, R. *J. Chem. Phys.* **1999**, *110*, 7053.
(143) (a) Bender, M. L.; Komiyama, M. *Cyclodextrin Chemistry*; Springer: New York, 1978. (b) Szejtli, J. *Cyclodextrins and their inclusion complexes*; Akademiai Kidao: Budapest, 1982.
(144) Ramamurthy, V.; Eaton, D. F. *Acc. Chem. Res.* **1988**, *21*, 300.
(145) (a) Saenger, W. *Ang. Chem. Int. Ed. Eng.* **1980**, *19*, 344. (b) Saenger, W. In *Inclusion compounds*; Atwood, J. L., Davis, J. E. D., MacNicol, D. D., Eds.; Academic: New York, 1984; Vol. 2, p 231.
(146) Jeffrey, G. A.; Saenger, W. *Hydrogen bonding in biological systems*; Springer-Verlag: Berlin, 1991; Chapter 18.
(147) Luzhkov, V.; Aqvist, J. *Chem. Phys. Lett.* **1999**, *302*, 267.
(148) (a) Attwood, D.; Florence, A. T. *Surfactant Systems*; Chapman Hall: London, 1983. (b) *Surfactant solution. New Methods of Investigation*; Zana, R., Ed.; Marcel Dekker: New York, 1987. (c) Almgren, M. *Adv. Colloid Interface Sci.* **1992**, *41*, 9. (d) Gehlan, M.; DeSchryver, F. C. *Chem. Rev.* **1993**, *93*, 199. (e) Kalyansundaram, K. *Microheterogeneous systems*; Academic: New York, 1987.
(149) (a) Paradies, H. H. *J. Phys. Chem.* **1980**, *84*, 599. (b) Berr, S. S. *J. Phys. Chem.* **1987**, *91*, 4760. (c) Berr, S. S.; Coleman, M. J.; Jones, R. R. M.; Johnson, J. S. *J. Phys. Chem.* **1986**, *90*, 5766. (d) Berr, S. S.; Caponetti, E.; Jones, R. R. M.; Johnson, J. S.; Magid, L. J. *J. Phys. Chem.* **1986**, *90*, 5766.
(150) (a) Phillies, G. D. J.; Yambert, J. E. *Langmuir* **1996**, *12*, 3431. (b) Phillies, G. D. J.; Hunt, R. H.; Strang, K.; Sushkin, N. *Langmuir* **1995**, *11*, 3408.
(151) Magid, L. J. *J. Phys. Chem. B* **1998**, *102*, 4064.
(152) Aswal, V. K.; Goyal, P. S.; Thiyagarajan, P. *J. Phys. Chem. B* **1998**, *102*, 2469.
(153) De, S. K.; Aswal, V. K.; Goyal, P. S.; Bhattacharyya, S. *J. Phys. Chem. B* **1998**, *102*, 6152.
(154) De, S. K.; Aswal, V. K.; Goyal, P. S.; Bhattacharya, S. *J. Phys. Chem.* **1996**, *100*, 11664.
(155) Telgmann, T.; Kaatze, U. *J. Phys. Chem. A* **1998**, *102*, 7758 and 7766.
(156) Moulik, S. P.; Pal, B. K. *Adv. Colloid Interface Sci.* **1998**, *78*, 99.
(157) De, T.; Maitra, A. *Adv. Colloid Interface Sci.* **1995**, *59*, 95.
(158) (a) Eastoe, J. *Langmuir* **1992**, *8*, 1503. (b) Eastoe, J.; Young, W. K.; Robinson, B. H. *J. Chem. Soc., Faraday Trans.* **1990**, *86*, 2883.
(159) Jean, Y. C.; Ache, J. H. *J. Am. Chem. Soc.* **1978**, *100*, 984, 6320.
(160) Cao, Y. N.; Chen, H. X.; Diebold, G. J.; Sun, T.; Zimmt, M. B. *J. Phys. Chem. B* **1997**, *101*, 3005.
(161) Hausier, H.; Haering, G.; Pande, A.; Luisi, P. L. *J. Phys. Chem.* **1989**, *93*, 7869.
(162) Christopher, D.; Yarwood, J.; Belton, P. S.; Hills, B. P. *J. Colloid Interface Sci.* **1992**, *152*, 465.
(163) Amararene, A.; Gindre, M.; Le Huerou, J.-Y.; Nicot, C.; Urbach, W.; Waks, M. *J. Phys. Chem. B* **1997**, *101*, 10751.
(164) (a) Temsamani, M. B.; Maeck, M.; El-Hassani, I.; Hurwitz, H. D. *J. Phys. Chem. B* **1998**, *102*, 3335. (b) Jain, T. K.; Varshney, M.; Maitra, A. *J. Phys. Chem.* **1989**, *93*, 7409.
(165) Mukherjee, K.; Mukherjee, D. C.; Moulik, S. P. *Langmuir* **1993**, *9*, 1727.
(166) (a) Niemeyer, E. D.; Bright, F. V. *J. Phys. Chem. B* **1998**, *102*, 1474. (b) Heitz, M. P.; Carlier, C.; deGrazia, J.; Harrison, K. L.; Johnston, K. P.; Randolph, T. W.; Bright, F. V. *J. Phys. Chem. B* **1997**, *101*, 6707.
(167) Johnston, K. P.; Harrison, K. L.; Clarke, M. J.; Howdla, S.; Heitz, M. P.; Bright, F. V.; Carlier, C.; Randolph, T. N. *Science* **1996**, *271*, 624.
(168) Zielinsky, R. G.; Kline, S. R.; Kalev, E. W.; Rosov, N. *Langmuir* **1997**, *13*, 3934.
(169) Fulton, J. L.; Pfund, D. M.; McClain, J. B.; Romack, T. J.; Maury, E. E.; Combes, J. R.; Samulski, E. T.; De Simone, J. M.; Capel, M. *Langmuir* **1995**, *11*, 4241.
(170) (a) Cassin, G.; Duda, Y.; Holovko, M.; Badiali, J. P.; Pileni, M. P. *J. Chem. Phys.* **1997**, *107*, 2683. (b) Kotlarchyk, M.; Huang, J. S.; Chen, H. *J. Phys. Chem.* **1985**, *89*, 4382.
(171) Kalev, E. W.; Billman, J. F.; Fulton, J. L.; Smith, R. D. *J. Phys. Chem.* **1991**, *95*, 458.
(172) Lipgens, S.; Schubel, D.; Schlicht, L.; Spilgies, J.-H.; Ilgenfritz, G. *Langmuir* **1998**, *14*, 1041.
(173) Cassini, G.; Badiali, J. P.; Pileni, M. P. *J. Phys. Chem.* **1995**, *99*, 12941.
(174) Quist, P. O.; Halle, B. *J. Chem. Soc., Faraday Trans. 1* **1988**, *84*, 1033.
(175) Bardez, E.; Vy, N. C.; Zemb, T. *Langmuir* **1995**, *11*, 3374.
(176) (a) Capuzzi, S.; Pini, F.; Gambi, C. M. L.; Monduzzi, M.; Baglioni, P. *Langmuir* **1997**, *13*, 6927. (b) Khan, A.; Fonhill, K.; Lindman, B. *J. Colloid Interface Sci.* **1984**, *101*, 193.
(177) (a) Lang, J.; Lalem, N.; Zana, R. *J. Phys. Chem.* **1991**, *95*, 9533. (b) Verbeck, A.; Voortmans, G.; Jachers, C.; De Schryver, F. C. *Langmuir* **1989**, *5*, 766.
(178) (a) Zhu, D.-M.; Wu, X.; Schelly, Z. A. *Langmuir* **1992**, *8*, 1538, 48. (b) Zhu, D.-M.; Wu, W.; Schelly, Z. A. *J. Phys. Chem.* **1992**, *96*, 2382, 712. (c) Caldaru, H.; Caragheorgheopal, A.; Dimonie,

M.; Donescu, D.; Dragutan, I.; Marinescu, N. *J. Phys. Chem.* **1992**, *96*, 7109.
(179) (a) Samii, A. A.-Z.; de Savignac, A.; Rico, I.; Lattes, A. *Tetrahedron* **1985**, *41*, 3683. (b) Riter, R. E.; Kimmel, J. R.; Undiks, E. P.; Levinger, N. E. *J. Phys. Chem. B* **1997**, *101*, 8292.
(180) (a) Perez-Casa, S.; Castillo, R.; Costas, M. *J. Phys. Chem. B* **1997**, *101*, 7043. (b) Compere, A. L.; Griffith, W. L.; Johnson, J. J.; Caponetti, E.; Chillura-Martino, D.; Triolo, R. *J. Phys. Chem. B* **1997**, *101*, 7139.
(181) Mittleman, D. M.; Nuss, M. C.; Colvin, V. L. *Chem. Phys. Lett.* **1997**, *275*, 332.
(182) D'Angelo, M.; Fioretto, D.; Onori, G.; Palmieri, L.; Santucci, A. *Phys. Rev. E* **1996**, *54*, 993.
(183) D'Angelo, M.; Fioretto, D.; Onori, G.; Palmieri, L.; Santucci, A. *Phys. Rev. E* **1995**, *52*, 4620.
(184) Cole, R. H.; Delbos, G.; Winsor, P., IV; Bose, T. K.; Moreau, J. M. *J. Phys. Chem.* **1985**, *89*, 3339.
(185) Bose, T. K.; Delbos, G.; Merabet, M. *J. Phys. Chem.* **1989**, *93*, 867.
(186) Peyrelasse, J.; Boned, C. *J. Phys. Chem.* **1985**, *89*, 370.
(187) Bergmeir, M.; Gradzielski, M.; Hoffman, H.; Mortensen, K. *J. Phys. Chem. B* **1998**, *102*, 2837.
(188) (a) Cassol, R.; Ge, M.-T.; Ferrarini, A.; Freed, J. H. *J. Phys. Chem. B* **1997**, *101*, 8782. (b) Sung-Suh, M. M.; Kevan, L. *J. Phys. Chem. A* **1997**, *101*, 1414. (c) Jutila, A.; Kinnunen, P. K. J. *J. Phys. Chem. B* **1997**, *101*, 7635.
(189) (a) Pasenkiewicz-Gierula, M.; Takaoka, V.; Miyagawa, H.; Kitamura, K.; Kusumi, A. *J. Phys. Chem. A* **1997**, *101*, 3677. (b) Lopez Cascales, J.; Berendsen, H. J. C.; Dela Tome, J. G. *J. Phys. Chem.* **1996**, *100*, 862. (c) Alper, H. E.; Bassolino-Klimar, D.; Stouch, T. R. *J. Chem. Phys.* **1993**, *99*, 5547.
(190) (a) Nagle, J. F. *Biophys. J.* **1993**, *64*, 1476. (b) Vanderkooi, G. *Biochemistry* **1991**, *30*, 10760.
(191) (a) Pearson, R. M.; Pascher, I. *Nature* **1979**, *81*, 499. (b) Borle, F.; Seelig, J. *Biochim. Biophys. Acta* **1983**, *735*, 131.
(192) See, for example. *Liposomes: A practical approach*; New, R. R. C., Ed.; Oxford University Press: Oxford, 1990.
(193) (a) Dhami, S.; Philips, D. *J. Photochem. Photobiol. A* **1996**, *100*, 77. (b) Song, X.; Geiger, C.; Vadas, S.; Perlstein, J.; Whitten, D. G. *J. Photochem. Photobiol. A* **1996**, *102*, 39.
(194) Lakowicz, J. R.; Keating-Nakamoto, S. *Biochemistry* **1984**, *23*, 3013.
(195) (a) Demchenko, A. P.; Ladokhin, A. S. *Eur. Biophys. J.* **1988**, *15*, 569. (b) Chattopadhyay, A.; Mukherjee, S. *Biochemistry* **1993**, *32*, 3804.
(196) de Haas, K. H.; Blom, C.; van den Ende, D.; Devits, M. H. G.; Haveman, B.; Mellema, J. *Langmuir* **1997**, *13*, 6658.
(197) Srivastava, A.; Eisenthal, K. B. *Chem. Phys. Lett.* **1998**, *292*, 345.
(198) (a) *Water Soluble Polymers*; Shalaby, S., McCormick, C., Butler, G., Eds.; ACS Symposium Series 467; American Chemical Society: Washington, DC, 1991. (b) Jenkins, R. D.; Delong, L.; Bassett, D. R. In *Hydrophilic Polymer*; Glass, J. E., Ed.; ACS Advances in Chemistry 248; American Chemical Society: Washington, DC, 1996; p 425.
(199) (a) Kumacheva, E.; Rharbi, Y.; Mitchel, R.; Winnik, M. A.; Guo, L.; Tam, K. C.; Jenkins, R. D. *Langmuir* **1997**, *13*, 182. (b) Eckert, A. R.; Martin, T. J.; Webber, S. E. *J. Phys. Chem. A* **1997**, *101*, 1646. (c) Yekta, A.; Xu, B.; Duhamel, J.; Brochard, P.; Adiwidjaja, H.; Winnik, M. A. *Macromolecules* **1995**, *28*, 956.
(200) Shiyanishiki, N.; Yagihara, S.; Arita, I.; Mashimo, S. *J. Phys. Chem. B* **1998**, *102*, 3249.
(201) Shinyashiki, N.; Asaka, N.; Mashimo, S.; Yagihara, S. *J. Chem. Phys.* **1990**, *93*, 760.
(202) Menzel, K.; Rupprecht, A.; Kaatze, U. *J. Phys. Chem. B* **1997**, *101*, 1255.
(203) Kaatze, U.; Gottmann, O.; Podbielski, R.; Pottel, R.; Terveer, U. *J. Phys. Chem.* **1978**, *82*, 112.
(204) Shinyashiki, N.; Asaka, N.; Mashimo, S.; Yagihara, S. *J. Chem. Phys.* **1990**, *93*, 760.
(205) Miura, N.; Shinyashiki, N.; Mashimo, S. *J. Chem. Phys.* **1992**, *97*, 8722.
(206) Shinyashiki, N.; Matsumura, Y.; Mashimo, S.; Yagihara, S. *J. Chem. Phys.* **1996**, *104*, 6877.
(207) Sato, T.; Niwa, H.; Chiba, A.; Nozaki, R. *J. Chem. Phys.* **1998**, *108*, 4138.
(208) Penafiel, L. M.; Litovitz, T. A. *J. Chem. Phys.* **1992**, *97*, 559.
(209) Diaz-Calleja, R.; Riande, E.; Roman, J. S. *J. Phys. Chem.* **1993**, *97*, 4848.
(210) Aliotta, F.; Fontanella, M. E.; Galli, G.; Lanza, M.; Migliardo, P.; Salvato, G. *J. Phys. Chem.* **1993**, *97*, 733.
(211) Hill, R. M.; Beckford, E. S.; Rowe, R. C.; Jones, C. B.; Dissado, L. A. *J. Colloid Interface Sci.* **1990**, *138*, 521.
(212) Dissado, L. A.; Rowe, R. C.; Haidar, A.; Hill, R. C. *J. Colloid Interface Sci.* **1987**, *117*, 310.
(213) Sakamoto, T.; Nakamura, H.; Uedaira, H.; Wada, A. *J. Phys. Chem.* **1989**, *93*, 357.
(214) Olender, R.; Nitzan, A. *J. Chem. Phys.* **1995**, *102*, 7180.
(215) (a) Bromberg, L.; Grossberg, A. Yu.; Suzuki, Y.; Tanaka, T. *J. Chem. Phys.* **1997**, *106*, 2906. (b) Ohmine, I.; Tanaka, T. *J. Chem. Phys.* **1982**, *77*, 8725. (c) Ohmine, I.; Tanaka, T. *Phys. Rev. Lett.* **1978**, *40*, 820. (d) Ohmine, I.; Tanaka, T. *Phys. Rev. A* **1978**, *17*, 8725. (e) Zhang, Y. B.; Zhang, Y. X. *Macromolecules* **1996**, *29*, 2494.
(216) (a) Rodbard, D. *Methods of Protein Separation*; Catsimpoolas, N., Ed.; Plenum: New York, 1976; Vol. 2, p 145. (b) Chrambach, A.; Rodbard, D. *Science* **1971**, *172*, 440. (c) Raymond S.; Nakamichi, M. *Anal. Biochem.* **1962**, *3*, 23. (d) White, M. L. *J. Phys. Chem.* **1960**, *664*, 1563.
(217) Mathur, A. M.; Moorjani, S. K.; Scranton, A. B. *J. Macromol. Sci.—Rev. Macromol. Chem. Phys.* **1996**, *C36*, 405.
(218) Janas, V. F.; Rodriguez, F.; Cohen, C. *Macromolecules* **1980**, *13*, 977.
(219) (a) Walderhans, H.; Nystrom, B. *J. Phys. Chem. B* **1997**, *101*, 1524. (b) Uemura, Y.; McNulty, J.; Macdonald P. *Macromolecules* **1995**, *28*, 4150. (c) Inomata, H.; Goto, S.; Ohtake, K.; Saito, S. *Langmuir* **1993**, *8*, 687. (d) Park, T. G.; Hoffman, A. S. *Macromolecules* **1993**, *26*, 5045. (e) Lele, A. K.; Hirve, M. M.; Badiger, M. V.; Mashelkar, R. A. *Macromolecules* **1997**, *30*, 157.
(220) Dickson, R. M.; Norris, D. J.; Tzeng, Y.-L.; Moerner, W. E. *Science* **1996**, *274*, 966.
(221) Dickson, R. M.; Cubitt, A. M.; Tsien, R. Y.; Moerner, W. E. *Nature* **1997**, *388*, 355.
(222) Xie, X. S. *Acc. Chem. Res.* **1996**, *29*, 598.
(223) Ellerby, L. M.; Nishida, C. R.; Nishida, F.; Yamanaka, S. A.; Dunn, B.; Valentine, J. S.; Zink, I. *Science* **1992**, *255*, 1113.
(224) *Introduction to zeolite science and practice*; van Beklum, H., Flanigen E. M., Jansen, J. C., Eds.; Elsevier: Amsterdam, 1991.
(225) (a) Ramamurthy, V.; Eaton, D. F.; Casper, J. V. *Acc. Chem. Res.* **1992**, *25*, 299. (b) Ramamurthy, V. *J. Phys. Chem. B* **1999**, *103*, 303.
(226) Ramamurthy, V.; Lakshminarasimhan, P. H.; Grey, C. P.; Johnston, L. J. *J. Chem. Soc. Chem. Commun.* **1998**, 2411.
(227) Leibovitch, M.; Olovsson, G.; Sundrababu, G.; Ramamurthy, V.; Scheffer, J. R.; Trottler, J. *J. Am. Chem. Soc.* **1996**, *118*, 1219.
(228) Branalean, L.; Brousmiche, D.; Jayatirtha Rao, V.; Johnston, L. J.; Ramamurthy, V. *J. Am. Chem. Soc.* **1998**, *120*, 4926.
(229) Ramamurthy, V.; Robbins, R. J.; Thomas, K. J.; Lakshminarasimhan, P. H. *Organized Molecular Assemblies in the Solid State*; Marcel Dekker, New York: 1999; pp 63−140.
(230) (a) Lachet, V.; Boutin, A.; Tavitian, B.; Fuchs, A. H. *J. Phys. Chem. B* **1998**, *102*, 9224. (b) Demontis, P.; Suffriti, G. B. *Chem. Rev.* **1997**, *97*, 2845. (c) Higgins, F. M.; Watson, G. W.; Parker, S. C. *J. Phys. Chem. B* **1997**, *101*, 9964.
(231) (a) Smit, B.; Maesen, T. L. M. *Nature* **1995**, *374*, 42. (b) van Tassel, R. P.; Davis, H. T.; McCornick, A. V. *J. Phys. Chem.* **1993**, *98*, 8919.
(232) Campana, L.; Selloni, A.; Goursot, A. *J. Phys. Chem. B* **1997**, *101*, 9932.
(233) Tsekov, R.; Smirniotis, Y. S. *J. Phys. Chem. B* **1998**, *102*, 9305.
(234) Farneth, W. E.; Gorte, R. J. *Chem. Rev.* **1995**, *95*, 615.
(235) Mongensen, N. H.; Shore, E. *Solid State Ionics* **1995**, *77*, 51.
(236) Anderson, P. A.; Armstrong, A. R.; Porch, A.; Edwards, P. P.; Woodball, L. J. *J. Phys. Chem. B* **1997**, *101*, 9892.
(237) Abdoulaye, A.; Chabanis, G.; Giuntini, J. C.; Vanderschcuren, J.; Zanchetta, J. V.; Di Ranzo, F. *J. Phys. Chem. B* **1997**, *101*, 1831.
(238) Vitale, G.; Mellot, C. F.; Bull, M.; Cheetham, A. K. *J. Phys. Chem. B* **1997**, *101*, 4559.
(239) Bull, L. M.; Cheetham, A. K.; Powell, B. M.; Ripmeester, J. A.; Ratcliffe, C. I. *J. Am. Chem. Soc.* **1995**, *117*, 4328.
(240) Schrimp, G.; Tavitian, B.; Espinat, D. *J. Phys. Chem.* **1995**, *99*, 10932.
(241) Cohn, E. J. *Annu. Rev. Biochem.* **1935**, *4*, 93.
(242) Buchanan, T. J.; Haggis, G. H.; Hasted, J. B.; Robinson, B. G. *Proc. R. Soc., London* **1952**, *213A*, 379.
(243) Kirkwood, J. G.; Shumaker, J. B. *Proc. Natl. Acad. Sci. U.S.A.* **1952**, *38*, 855.
(244) Kirkwood, J. G.; Shumaker, J. B. *Proc. Natl. Acad. Sci. U.S.A.* **1952**, *38*, 863.
(245) Lumry, R.; Yue, H.-S. R. *J. Phys. Chem.* **1965**, *69*, 1162.
(246) Mofers, F. J.; Casteleijn, G.; Levine, Y. K. *Biophys. Chem.* **1982**, *16*, 9.
(247) O'Konski, C. T. *J. Chem. Phys.* **1955**, *23*, 1559.
(248) O'Konski, C. T. *J. Phys. Chem.* **1960**, *64*, 605.
(249) Schwarz, G. *J. Phys. Chem.* **1962**, *66*, 2636.
(250) Schwan, H. P. *Advances in Biological and Medical Physics*; Lawrence, J. H., Tobias, C. A., Eds.; Academic: New York, 1957; Vol. 5.
(251) Jacobson, B. *J. Am. Chem. Soc.* **1955**, *77*, 2919.
(252) Takashima, S. *J. Am. Chem. Soc.* **1958**, *80*, 4478.
(253) Grant, E. H. *Nature* **1962**, *196*, 1194.
(254) Grant, E. H. *J. Mol. Biol.* **1966**, *19*, 133.
(255) Grant, E. H.; Keefe, S. E.; Takashima, S. *J. Phys. Chem.* **1968**, *72*, 4373.

(256) Essex, C. G.; Symonds, M. S.; Sheppard, R. J.; Grant, E. H.; Lamote, R.; Soetewey, F.; Rosseneu, M. Y.; Peeters, H. *Phys. Med. Biol.* **1977**, *22*, 1160.
(257) Grant, E. H.; South, G. P.; Walker, I. O. *Biochem. J.* **1971**, *122*, 765.
(258) South, G. P.; Grant, E. H. *Proc. R. Soc., London* **1972**, *328A*, 371.
(259) Grant, E. H.; Mitton, B. G. R.; South, G. P.; Sheppard, R. J. *Biochem. J.* **1974**, *139*, 375.
(260) Grant, E. H.; McClean, V. E. R.; Nightingale, N. R. V.; Sheppard, R. J.; Chapman, M. J. *Bioelectromagnetics* **1986**, *7*, 151.
(261) Grant, E. H.; South, G. P.; Takashima, S.; Ichimura, H. *Biochem. J.* **1971**, *122*, 691.
(262) Essex, C. G.; Grant, E. H.; Sheppard, R. J.; South, G. P.; Symonds, M. S.; Mills, G. L.; Slack, J. *Ann. N.Y. Acad. Sci.* **1977**, *303*, 142.
(263) Dachwitz, E.; Parak, F.; Stockhausen, M. *Ber. Bunsen-Ges. Phys. Chem.* **1989**, *93*, 1454.
(264) Mashimo, S.; Kuwabara, S.; Yagihara, S.; Higasi, K. *J. Phys. Chem.* **1987**, *91*, 6337.
(265) Fukuzaki, M.; Miura, N.; Shinyashiki, N.; Kurita, D.; Shioya, S.; Haida, M.; Mashimo, S. *J. Phys. Chem.* **1995**, *99*, 431.
(266) Mashimo, S.; Umehara, T.; Kuwabara, S.; Yagihara, S. *J. Phys. Chem.* **1989**, *93*, 4963.
(267) (a) Gestblom, B. *J. Phys. Chem.* **1991**, *95*, 6064. (b) Gestblom, B.; Noreland, E. *J. Phys. Chem.* **1984**, *88*, 664.
(268) Belton, P. S. *J. Phys. Chem.* **1995**, *99*, 17061.
(269) Schlecht, P.; Mayer, A.; Hettner, G.; Vogel, H. *Biopolymers* **1969**, *7*, 963.
(270) Delalic, Z.; Takashima, S.; Adachi, K.; Asakura, T. *J. Mol. Biol.* **1983**, *168*, 659.
(271) Takashima, S. *J. Am. Chem. Soc.* **1956**, *78*, 541.
(272) Takashima, S. *Arch. Biochem. Biophys.* **1958**, *77*, 454.
(273) Takashima, S.; Lumry, R. *J. Am. Chem. Soc.* **1958**, *80*, 4238.
(274) Takashima, S.; Lumry, R. *J. Am. Chem. Soc.* **1958**, *80*, 4244.
(275) Takashima, S. *J. Polym. Sci.* **1962**, *56*, 257.
(276) Takashima, S. *Biochim. Biophys. Acta* **1964**, *79*, 531.
(277) Takashima, S. *Biophys. J.* **1963**, *64*, 1550.
(278) Schlecht, P.; Vogel, H.; Mayer, A. *Biopolymers* **1968**, *6*, 1717.
(279) Hanss, M.; Banerjee, R. *Biopolymers* **1967**, *5*, 879.
(280) Pennock, B. E.; Schwan, H. P. *J. Phys. Chem.* **1969**, *73*, 2600.
(281) Steinhoff, H.-J.; Kramm, B.; Hess, G.; Owerdieck, C.; Redhardt, A. *Biophys. J.* **1993**, *65*, 1486.
(282) Hendrickx, H.; Verbruggen, R.; Rosseneu-Motreff, M. Y.; Blaton, V.; Peeters, H. *Biochem. J.* **1968**, *110*, 419.
(283) Bone, S.; Pethig, R. *J. Mol. Biol.* **1982**, *157*, 571.
(284) Bone, S.; Pethig, R. *J. Mol. Biol.* **1985**, *181*, 323.
(285) Bone, S.; Pethig, R. *Int. J. Quantum Chem., Quantum Biol. Symp.* **1981**, *8*, 307.
(286) Bone, S.; Gascoyne, P. R.; Pethig, R. *J. Chem. Soc., Faraday Trans. 1* **1977**, *73*, 1605.
(287) Eden, J.; Gascoyne, P. R. C.; Pethig, R. *J. Chem. Soc., Faraday Trans. 1* **1980**, *76*, 426.
(288) Hawkes, J. J.; Pethig, R. *Biochim. Biophys. Acta* **1988**, *952*, 27.
(289) Grigera, J. R.; Vericat, F.; Hallenga, K.; Berendsen, H. J. C. *Biopolymers* **1979**, *18*, 35.
(290) Takashima, S.; Schwan, H. P. *J. Phys. Chem.* **1965**, *69*, 4176.
(291) Rosen, D. *Trans. Faraday Soc.* **1963**, *59*, 2178.
(292) Eley, D. D.; Lockhart, N. C.; Richardson, C. N. *J. Chem. Soc., Faraday Trans. 1* **1979**, *75*, 323.
(293) Careri, G. *Prog. Biophys. Mol. Biol.* **1998**, *70*, 223.
(294) Careri, G.; Giansanti, A.; Rupley, J. A. *Proc. Natl. Acad. Sci. U.S.A.* **1986**, *83*, 6810.
(295) Nandi, N.; Bagchi, B. *J. Phys. Chem. B* **1997**, *101*, 10954.
(296) Nandi, N.; Bagchi, B. *J. Phys. Chem. A* **1998**, *102*, 8217.
(297) Barlow, D. J.; Thornton, J. M. *Biopolymers* **1986**, *25*, 1717.
(298) Minton, A. P.; Lewis, M. S. *Biophys. Chem.* **1981**, *14*, 317.
(299) Smith, P. E.; Brunne, R. M.; Mark, A. E.; van Gunsteren, W. F. *J. Phys. Chem.* **1993**, *97*, 2009.
(300) Loncharich, R. J.; Brooks, B. R. *Proteins* **1989**, *6*, 32.
(301) Grant, E. H. *Ann. N.Y. Acad. Sci.* **1965**, *125*, 418.
(302) Hasted, J. B. *Aqueous Dielectrics*; Chapman and Hall: London, 1973; Chapter 7.
(303) Mashimo, S.; Ota, T.; Shinyashiki, N.; Tanaka, S.; Yagihara, S. *Macromolecules* **1989**, *22*, 1285.
(304) Bordi, F.; Cametti, C.; Paradossi, G. *Biopolymers* **1995**, *36*, 539.
(305) (a) Skinner, J. L. *J. Chem. Phys.* **1983**, *79*, 1955. (b) Budimir, J.; Skinner, J. L. *J. Chem. Phys.* **1985**, *82*, 5232.
(306) Urry, D. W.; Peng, S.; Xu, J.; McPherson, D. T. *J. Am. Chem. Soc.* **1997**, *119*, 1161.
(307) Swaminathon, S.; Harrison, S. W.; Beveridge, D. L. *J. Am. Chem. Soc.* **1978**, *100*, 5705.
(308) Loffler, G.; Schreiber, H.; Steinhauser, O. *J. Mol. Biol.* **1997**, *270*, 520.
(309) Nandi, N.; Bagchi, B. Manuscript in preparation.
(310) Cole, R. H. *Ann. N.Y. Acad. Sci.* **1977**, *303*, 59.
(311) (a) Takashima, S. *Biopolymers* **1967**, *5*, 899. (b) Takashima, S.; Gabriel, C.; Sheppard, R. J.; Grant, E. H. *Biophys. J.* **1984**, *46*, 29.
(312) Mandel, M. *Mol. Phys.* **1961**, *4*, 489.
(313) Hanss, M.; Bernengo, J. C. *Biopolymers* **1973**, *12*, 2151.
(314) Sakamoto, M.; Kanda, H.; Hyakawa, R.; Wada, Y. *Biopolymers* **1976**, *15*, 879.
(315) Sakamoto, M.; Hayakawa, R.; Wada, Y. *Biopolymers* **1979**, *18*, 2769.
(316) Sakamoto, M.; Fujikado, T.; Hyakawa, R.; Wada, Y. *Biophys. Chem.* **1980**, *11*, 309.
(317) Goswami, D. N.; Dasgupta, N. N. *Biopolymers* **1974**, *13*, 1549.
(318) Vreugdenhil, T.; van der Touw, F.; Mandel, M. *Biophys. Chem.* **1979**, *10*, 67.
(319) Saif, B.; Mohr, R. K.; Montrose, C. J.; Litovitz, T. A. *Biopolymers* **1991**, *31*, 1171.
(320) Bone, S.; Small, C. A. *Biochim. Biophys. Acta* **1995**, *1260*, 85.
(321) Flock, S.; Labarbe, R.; Houssier, C. *Biophys. J.* **1996**, *71*, 1519.
(322) Umehara, T.; Kuwabara, S.; Mashimo, S.; Yagihara, S. *Biopolymers* **1990**, *30*, 649.
(323) Swicord, M. L.; Davis, C. C. *Biopolymers* **1982**, *21*, 2453.
(324) Edwards, G. S.; Davis, C. C.; Saffer, J. D.; Swicord, M. L. *Phys. Rev. Lett.* **1984**, *53*, 1284.
(325) Edwards, G. S.; Davis, C. C.; Saffer, J. D.; Swicord, M. L. *Biophys. J.* **1985**, *47*, 799.
(326) Swicord, M. L.; Davis, C. C. *Bioelectromagnetics* **1986**, *4*, 21.
(327) Bonincontro, A.; Caneva, R.; Pedone, F.; Romano, T. F. *Phys. Med. Biol.* **1989**, *34*, 609.
(328) Baker-Jarvis, J.; Jones, C. A.; Riddle, B. National Institute of Standards and Technology Technical Note 1509; NIST: Gaithersburg, MD, 1998.
(329) Yang, L.; Weerasinghe, S.; Smith, P. E.; Pettitt, B. M. *Biophys. J.* **1995**, *69*, 1519.
(330) Young, M. A.; Jayaram, B.; Beveridge, D. L. *J. Phys. Chem. B* **1998**, *102*, 7666.
(331) Redwood, W. R.; Takashima, S.; Schwan, H. P.; Thompson, T. E. *Biochim. Biophys. Acta* **1972**, *255*, 557.
(332) Kaatze, U.; Henze, R.; Seegers, A.; Pottel, R. *Ber. Bunsen-Ges. Phys. Chem.* **1975**, *79*, 42.
(333) Kaatze, U.; Limberg, C. H.; Pottel, R. *Ber. Bunsen-Ges. Phys. Chem.* **1974**, *78*, 561.
(334) Kaatze, U.; Henze, R.; Eibl, H. *Biophys. Chem.* **1979**, *10*, 351.
(335) Kaatze, U.; Henze, R. *Ber. Bunsen-Ges. Phys. Chem.* **1980**, *84*, 1102.
(336) (a) Kaatze, U. *Phys. Med. Biol.* **1990**, *35*, 1663. (b) Kaatze, U. *Prog. Colloid Polym. Sci.* **1980**, *67*, 117.
(337) Pottel, R.; Gopel, K.-D.; Henze, R.; Kaatze, U.; Uhelendorf, V. *Biophys. Chem.* **1984**, *19*, 233.
(338) Buchet, R.; Luan, C. H. *Biophys. Chem.* **1988**, *32*, 199.
(339) Roland, C. M.; Ngai, K. L. *J. Chem. Phys.* **1995**, *103*, 1152.
(340) Toptygin, D.; Svodva, J.; Konopasek, I.; Brand, L. *J. Chem. Phys.* **1992**, *96*, 7919.
(341) (a) Ware, W. R. *J. Phys. Chem. B* **1999**, *103*, 563. (b) James, D. R.; Ware, W. R. *Chem. Phys. Lett.* **1985**, *120*, 485.
(342) Benjamin, I. *Chem. Phys.* **1994**, *180*, 287.
(343) Michael, D.; Benjamin, I. *J. Phys. Chem.* **1995**, *99*, 1530.
(344) Perera, J. M.; Stevens, G. W.; Grieser, F. *Colloids Surf.* **1995**, *95*, 185.
(345) Wang, H.; Borguet, E.; Eisenthal, K. B. *J. Phys. Chem. B* **1998**, *102*, 4927.
(346) Benjamin, I. *J. Chem. Phys.* **1991**, *95*, 3698.
(347) Zimdars, D.; Dadap, J. I.; Eisenthal, K. B.; Heinz, T. F. *Chem. Phys. Lett.* **1999**, 112.
(348) Nandi, N.; Bagchi, B. Manuscript in preparation.
(349) Jackson, J. D. *Classical electrodynamics*; John Wiley: New York, 1975.
(350) (a) Wolynes, P. G. *J. Chem. Phys.* **1987**, *86*, 5133. (b) Rips, I.; Klafter, J.; Jortner, J. *J. Chem. Phys.* **1988**, *88*, 3246.
(351) Castner, E. W., Jr.; Fleming, G. R.; Bagchi, B.; Maroncelli, M. *J. Chem. Phys.* **1988**, *89*, 3519.
(352) Okamoto, Y. *Biopolymers* **1994**, *34*, 529.
(353) (a) Gilson, M. K.; Honig, B. H. *Biopolymers* **1986**, *25*, 2097. (b) Gilson, M. K.; Honig, B. H. *Proteins* **1988**, *3*, 32. (c) Gilson, M. K.; Honig, B. H. *J. Mol. Biol.* **1985**, *184*, 503. (d) Honig, B. H.; Nicholls, A. *Science* **1995**, *268*, 1144.
(354) Fersht A. R.; Sternberg, M. J. *Protein Eng.* **1989**, *2*, 527.
(355) Warshel, A. *Nature* **1987**, *330*, 15.
(356) King, G.; Lee, F. S.; Warshel, A. *J. Chem. Phys.* **1991**, *95*, 4366.
(357) Warshel, A.; Aqvist, J. *Annu. Rev. Biophys. Biophys. Chem.* **1991**, *20*, 267.
(358) Warshel, A.; Russell, S. T. *Q. Rev. Biophys.* **1984**, *17*, 283.
(359) Warshel, A.; Chu, Z. T.; Parson, W. W. *Science* **1989**, *246*, 112.
(360) Churg, A. K.; Warshel, A. *Biochemistry* **1986**, *25*, 1675.
(361) Russell, S. T.; Warshel, A. *J. Mol. Biol.* **1985**, *185*, 389.
(362) Warshel, A.; Russell, S. T.; Churg, A. K. *Proc. Natl. Acad. Sci. U.S.A.* **1984**, *81*, 4785.
(363) Warshel, A.; Papazyan, A. *Curr. Opin. Struct. Biol.* **1998**, *8*, 211.
(364) Sham, Y. Y.; Muegge, I.; Warshel, A. *Biophys. J.* **1998**, *74*, 1744.
(365) Dimitrov, R. A.; Crichton, R. R. *Proteins* **1997**, *27*, 576.
(366) Nakamura, H.; Sakamoto, T.; Wada, A. *Protein. Eng.* **1988**, *2*, 177.

(367) Van Belle, D.; Couplet, I.; Prevost, M.; Wodak, S. J. *J. Mol. Biol.* **1987**, *198*, 721.
(368) Simonson, T.; Perahia, D.; Bricogne, G. *J. Mol. Biol.* **1991**, *218*, 859.
(369) Simonson, T.; Perahia, D.; Brunger, A. T. *Biophys. J.* **1991**, *59*, 670.
(370) (a) Simonson, T.; Perahia, D. *J. Am. Chem. Soc.* **1995**, *117*, 7987. (b) Simonson, T.; Perahia, D. *Faraday Discuss.* **1996**, *103*, 71.
(371) Aqvist, J.; Luecke, F. A.; Quochio, F. A.; Warshel, A. *Proc. Natl. Acad. Sci., U.S.A.* **1991**, *88*, 2026.
(372) Muegge, I.; Qi, P. X.; Wand, A. J.; Chu, Z. T.; Warshel, A. *J. Phys. Chem. B* **1997**, *101*, 825.
(373) (a) Simonson, T. *J. Am. Chem. Soc.* **1998**, *120*, 4875. (b) Simonson, T.; Perahia, D. *Proc. Natl. Acad. Sci. U.S.A.* **1995**, *92*, 1082.
(374) Warshel, A.; Sussman, F.; Hwang, J.-K. *J. Mol. Biol.* **1988**, *201*, 139.
(375) Krishtalik, L. I.; Kuznetsov, A. M.; Mertz, E. L. *Proteins: Struct., Funct., Genet.* **1997**, *28*, 174.
(376) Voges, D.; Karshikoff, A. *J. Chem. Phys.* **1998**, *108*, 2219.
(377) Furois-Corbin, S.; Smith, J. C.; Kneller, G. R. *Proteins* **1993**, *16*, 141.
(378) (a) McGregor, R. B.; Weber, G. *Nature* **1986**, *319*, 70. (b) DeToma, R. P.; Easter, T. H.; Brand, L. *J. Am. Chem. Soc.* **1976**, *98*, 5001. (c) Lakowicz, R. In *Principles of Fluorescence Spectroscopy*; Plenum Press: New York, 1983; Chapter 8.
(379) Pierce, D. W.; Boxer, S. G. *J. Phys. Chem.* **1992**, *96*, 5560.
(380) Baskhin, J. S.; McLendon, G.; Mukamel, S.; Marohn, J. *J. Phys. Chem.* **1990**, *94*, 4757.
(381) (a) Joo, T.; Jai, Y.; Yu, J.-Y.; Jonas, D. M.; Fleming, G. R. *J. Phys. Chem.* **1996**, *100*, 2399. (b) Jordanides, X. J.; Lang, M. J.; Song, X.; Fleming, G. R. *J. Phys. Chem.* **1999**, *103*, 7995.
(382) Riter, R. R.; Edington, M. D.; Beck, W. F. *J. Phys. Chem.* **1996**, *100*, 14198.
(383) Homoelle, B. J.; Edington, M. D.; Diffey, W. M.; Beck, W. F. *J. Phys. Chem. B* **1998**, *102*, 3044.
(384) Wang, R.; Sun, S.; Bekos, E. J.; Bright, F. V. *Anal. Chem.* **1995**, *67*, 149.
(385) Brauns, E. B.; Murphy, C. J.; Berg, M. *J. Am. Chem. Soc.* **1998**, *120*, 2449.
(386) Mazur, A. K. *J. Am. Chem. Soc.* **1998**, *120*, 10298.
(387) Vajda, S.; Jimenez, R.; Rosenthal, S. J.; Fidler, V., Fleming, G. R.; Castner, E. W., Jr. *J. Chem. Soc., Faraday Trans.* **1995**, *91*, 867.
(388) Nag, A.; Chakrabarty, T.; Bhattacharyya, K. *J. Phys. Chem.* **1990**, *94*, 4203.
(389) Bergmark, W. R.; Davies, A.; York, C.; Jones, G., II. *J. Phys. Chem.* **1990**, *94*, 5020.
(390) Nandi, N.; Bagchi, B. *J. Phys. Chem.* **1996**, *100*, 13914.
(391) Jones, G., II; Jackson, W. P.; Choi, C. Y. *J. Phys. Chem.* **1985**, *89*, 294.
(392) Sarkar, N.; Das, K.; Datta, A.; Das, S.; Bhattacharyya, K. *J. Phys. Chem.* **1996**, *100*, 10523.
(393) Lundgren, J. S.; Heitz, M. P.; Bright, F. V. *Anal. Chem.* **1995**, *67*, 3775.
(394) Das, S.; Datta, A.; Bhattacharyya, K. *J. Phys. Chem. A* **1997**, *101*, 3299.
(395) Bart, E.; Melstein, A.; Huppert, D. *J. Phys. Chem.* **1995**, *99*, 9253.
(396) Neria, E.; Nitzan, A. *J. Chem. Phys.* **1994**, *100*, 3855.
(397) Chandra, A.; Wei, D.; Pattey, G. N. *J. Chem. Phys.* **1993**, *98*, 4959.
(398) Mandal, D.; Datta, A.; Pal, S. K.; Bhattacharyya, K. *J. Phys. Chem. B* **1998**, *102*, 9070.
(399) Willard, D. M.; Riter, R. E.; Levinger, N. E. *J. Am. Chem. Soc.* **1998**, *120*, 4151.
(400) Riter, R. E.; Undiks, E. P.; Levinger, N. E. *J. Am. Chem. Soc.* **1998**, *120*, 6062.
(401) Riter, R. E.; Willard, D. M.; Levinger, N. E. *J. Phys. Chem. B* **1998**, *102*, 2705.
(402) Riter, R. E.; Undiks, E. P.; Kimmel, J. R.; Pant, D. D.; Levinger, N. E. *J. Phys. Chem. B* **1998**, *102*, 7931.
(403) Marzola, P.; Gratton, E. *J. Phys. Chem.* **1991**, *95*, 9488.
(404) Nandi, N.; Bagchi, B. (Unpublished work).
(405) Shirota, H.; Horie, K. *J. Phys. Chem. B* **1999**, *103*, 1437.
(406) Sarkar, N.; Datta, A.; Das, S.; Bhattacharyya, K. *J. Phys. Chem.* **1996**, *100*, 15483.
(407) Datta, A.; Mandal, D.; Pal, S. K.; Bhattacharyya, K. *J. Mol. Liq.* **1998**, *77*, 121.
(408) Datta, A.; Pal, S. K.; Mandal, D.; Bhattacharyya, K. *J. Phys. Chem. B* **1998**, *102*, 6114.
(409) Jordan, J. D.; Dunbar, R. A.; Bright, F. V. *Anal. Chem.* **1995**, *67*, 2436.
(410) Datta, A.; Das, S.; Mandal, D.; Pal, S. K.; Bhattacharyya, K. *Langmuir* **1997**, *13*, 6922.
(411) Claudia-Marchi, M.; Bilmes, S. A.; Negri, R. *Langmuir* **1997**, *13*, 3655.
(412) Hsu, T.-P.; Ma, D. S.; Cohen, C. *Polymer* **1983**, *24*, 1273.
(413) Netz, P. A.; Dorfmuller, T. *J. Phys. Chem. B* **1998**, *102*, 4875.
(414) Argaman, R.; Huppert, D. *J. Phys. Chem. A* **1998**, *102*, 6215.
(415) Saielli, G.; Polomeno, A.; Nordio, P. L.; Bertolini, P.; Ricci, M.; Righini, R. *J. Chem. Soc., Faraday Trans.* **1998**, *94*, 121.
(416) (a) Ferrante, C.; Rau, J.; Deeg, F. W.; Brauchle, C. *J. Lumin.* **1998**, *76*, *77*, 64. (b) Ferrante, C.; Rau, J.; Deeg, F. W.; Brauchle, C. *J. Phys. Chem.* **1999**, *B103*, 931.
(417) Das, K.; Sarkar, N.; Das, S.; Datta, A.; Bhattacharyya, K. *Chem. Phys. Lett.* **1996**, *249*, 323.
(418) Bagchi, B.; Biswas, R. *Acc. Chem. Res.* **1998**, *31*, 181.
(419) (a) Pant, D.; Levinger, N. E. *Chem. Phys. Lett.* **1996**, *292*, 200. (b) Pant, D.; Levinger, N. E. *J. Phys. Chem.* **1999**, *B103*, 7846.
(420) Ohmine, I. *J. Phys. Chem.* **1995**, *99*, 6767.
(421) Stillinger, F. H. *Philos. Trans. R. Soc., London* **1977**, *278B*, 97.
(422) (a) Mountain, R. D.; Thirumalai, D. *Proc. Natl. Acad. Sci. U.S.A.* **1998**, *95*, 8436. (b) Mohanty, D.; Elber, R.; Thirumalai, D.; Beglov, D.; Roux, B. *J. Mol. Biol.* **1997**, *272*, 423. (c) Straub, J. E.; Thirumalai, D. *Proc. Natl. Acad. Sci. U.S.A.* **1993**, *90*, 809
(423) (a) Angell, C. A. *Annu. Rev. Phys. Chem.* **1983**, *34*, 539. (b) Angell, C. A. *Science* **1995**, *267*, 1924.
(424) Frauenfelder, H.; Stephen, G. S.; Wolynes, P. G. *Science* **1991**, *254*, 1598.
(425) Fleming, G. R.; Martin, J. L.; Breton, J. *Nature* **1988**, *333*, 190.
(426) Fleming, G. R. *Chemical applications of Ultrafast spectroscopy*; Oxford University Press: New York, 1986.
(427) Fleming, G. R.; Cho, M. *Annu. Rev. Phys. Chem.* **1996**, *47*, 109.
(428) Bardeen, C. J.; Yakovlev, V. V.; Squier, J. A.; Wilson, K. R. *J. Am. Chem. Soc.* **1998**, *120*, 13023.
(429) Schwan, H. P. *Blut* **1983**, *46*, 185.
(430) Laogun, A. A.; Ajayi, N. O.; Okafor, L. O.; Osamo, N. O. *Phys. Med. Biol.* **1983**, *28*, 341.
(431) Umehara, T.; Tominaga, Y.; Hikida, A.; Mashimo, S. *J. Chem. Phys.* **1995**, *102*, 9474.
(432) Uversky, V. N.; Segel, D. J.; Doniach, S.; Fink, A. L. *Proc. Natl. Acad. Sci. U.S.A.* **1998**, *95*, 5480.
(433) Marcus, R. A. *Protein Electron Transfer*; Bendall, D. S., Ed.; Bios Scientific: Oxford, 1996; Chapter 10.
(434) Affleck, R.; Haynes, C. A.; Clark, D. S. *Proc. Natl. Acad. Sci. U.S.A.* **1992**, *89*, 5167.
(435) Mackay, D. H.; Wilson, K. R. *J. Biomol. Struct. Dyn.* **1986**, *4*, 491.
(436) Lemieux, R. U. *Acc. Chem. Res.* **1996**, *29*, 373.

CR980127V